TRACER/TIME-LAPSE RADAR IMAGING TEST; DESIGN, OPERATION, AND PRELIMINARY RESULTS

Warren Barrash[1], Tom Clemo[1], David Hyndman[2], Edward Reboulet[1], and Elisabeth Hausrath[1,3]

[1] Center for Geophysical Investigation of the Shallow Subsurface (CGISS) and
Department of Geosciences, Boise State University
[2] Department of Geological Sciences, Michigan State University
[3] Department of Geosciences, Pennsylvania State University

Technical Report BSU CGISS 02-02

June 30, 2002

Report Documentation Page

Form Approved
OMB No. 0704-0188

1. REPORT DATE	2. REPORT TYPE	3. DATES COVERED
30 JUN 2002		**00-00-2002 to 00-00-2002**

4. TITLE AND SUBTITLE	5a. CONTRACT NUMBER
Tracer/Time-Lapse Radar Imaging Test: Design, Operation, And Preliminary Results	5b. GRANT NUMBER
	5c. PROGRAM ELEMENT NUMBER
6. AUTHOR(S)	5d. PROJECT NUMBER
	5e. TASK NUMBER
	5f. WORK UNIT NUMBER
7. PERFORMING ORGANIZATION NAME(S) AND ADDRESS(ES) **Boise State University,Department of Geosciences,Boise,ID,83725**	8. PERFORMING ORGANIZATION REPORT NUMBER
9. SPONSORING/MONITORING AGENCY NAME(S) AND ADDRESS(ES)	10. SPONSOR/MONITOR'S ACRONYM(S)
	11. SPONSOR/MONITOR'S REPORT NUMBER(S)

12. DISTRIBUTION/AVAILABILITY STATEMENT
Approved for public release; distribution unlimited

13. SUPPLEMENTARY NOTES

14. ABSTRACT

15. SUBJECT TERMS

16. SECURITY CLASSIFICATION OF:			17. LIMITATION OF ABSTRACT	18. NUMBER OF PAGES	19a. NAME OF RESPONSIBLE PERSON
a. REPORT **unclassified**	b. ABSTRACT **unclassified**	c. THIS PAGE **unclassified**	**Same as Report (SAR)**	**121**	

TABLE OF CONTENTS

LIST OF TABLES

LIST OF FIGURES

LIST OF APPENDICES

SUMMARY

1. This report describes a tracer/time-lapse radar imaging test (TTLT) that was conducted in a heterogeneous fluvial aquifer at the Boise Hydrogeophysical Research Site (BHRS) between August 1-18, 2001 to demonstrate, evaluate, and improve the capability to image temporal and spatial changes in an electrically conductive plume during a tracer test, and to provide quantitative results for geophysical, hydrologic, and combined hydrologic and geophysical modeling of plume detection, plume evolution, and permeability heterogeneity.

2. Custom in-well equipment was designed with and manufactured by collaborators at Michigan State University to allow: (a) simultaneous logging with radar instruments for cross-hole imaging and collection of water samples and head-change measurements from isolated zones in the same wells; and (b) collection of high-resolution water chemistry samples and head-change data in the middle region of two tomographic planes for quantitative calibration of attenuation differences detected by radar tomography.

3. Pre-test flow and transport modeling with generalized aquifer parameter estimates, and better-known topography on hydrostratigraphic contacts, was run to help select a pumping rate at withdrawal well B6 that would assure passage of the tracer plume through A1 with limited distortion of the plume up-gradient of well A1, and with complete breakthrough at A1 within two weeks. The modeling indicated that differences in hydraulic parameters and topography on hydrostratigraphic unit surfaces have significant influence on plume evolution and progressive breakthrough distribution in zones in A1, including: (a) earlier breakthrough in the lower zones; (b) extended breakthrough in Unit 2; and (c) limited and delayed breakthrough in Unit 3 with almost no breakthrough in the upper zones in A1.

4. Two tracers were used for the TTLT that were believed to be conservative tracers: (a) bromide, an electrically conductive inorganic salt; and (b) uranine, an organic fluorescent dye. These two tracers were injected into a 4-m-thick interval in well B3 spanning the contact between two hydrostratigraphic units having differences in porosity and permeability (Unit 2 with relatively greater porosity and permeability, and Unit 3 with relatively lower porosity and permeability). Bromide concentration and injection volume were designed to start with and evolve into combined concentration and dimension characteristics that would be detectable and resolvable by radar tomography through rising, peak, and declining conductivity (bromide concentrations) at A1.

5. Chemical results on conductivity at about 50 locations were available on sample runs approximately every four hours during the TTLT to provide near-realtime feedback on breakthrough behavior. Follow-up QA/QC evaluation indicates that field measurements of conductivity and uranine were accurate and repeatable.

6. Although the main breakthrough with conductivity at A1 occurred several days later than predicted with pre-test modeling, other plume evolution features occurred including: (a) initial breakthrough in the lower zones of A1; (b) primary and extended breakthrough in Unit 2; (c) limited

and later breakthrough in Unit 3; and (d) virtually no breakthrough at the top zones in A1. Differences in detail, including an early injection peak at A1 and all B wells and a second main breakthrough peak, should provide valuable information about heterogeneity in the investigated volume.

7. Level runs across the plume path prior to and during plume passage exhibit clear differences associated with the absence or presence of a conductivity anomaly.

8. The behavior of the second tracer, uranine (organic fluorescent dye), was not conservative and differed considerably from that of bromide or its proxy, conductivity. In particular, relative to conductivity, uranine exhibited: (a) significantly less relative concentration at breakthrough in A1; (b) significantly delayed breakthrough at A1; and (c) somewhat different breakthrough pattern at A1.

9. Follow-up investigation suggests that the cause(s) for the non-conservative uranine behavior may be biological and/or microbiological activity associated with cottonwood roots in the aquifer.

10. Operational problems (long and short power outages) interrupted pumping and data collection with some head-change and flow measurement and recording systems. Prototype fiber-optic transducers permitted data collection from 14 zones in A1 and B wells through small-diameter access tubes, but software and hardware stability problems resulted in additional data gaps and a significant number of unreliable channels.

11. A follow-up field test was conducted in June, 2002 to recreate the start and various pumping and recovery conditions of the TTLT in order to capture head-change information at numerous zones with more-stable fiber-optic transducers. Review of data indicates that high-quality head-change data were collected from 22 of 33 zones monitored in A1 and B wells with the newer version of fiber-optic transducers used for the Restart Test in 2002.

INTRODUCTION

It is widely acknowledged that a major limiting factor in accurately and cost-effectively characterizing, monitoring, modeling, or remediating contaminated or sensitive environmental sites is the difficulty in knowing the heterogeneous distribution of parameters (especially permeability) and features (especially high- and low-permeability zones or lenses) that control the locations and rates of movement of water and contaminants in the subsurface (e.g., Anderson, 1997; Dane and Molz, 1991; Sudicky and Huyakorn, 1991; Gelhar, 1997; EPA, 1999). Also, it is recognized that non-invasive or minimally-invasive geophysical methods provide the most promising opportunity for cost-effectively supplementing the limited information that can be gained at wells (e.g., Rubin et al., 1992; McKenna and Poeter, 1995; Hyndman and Gorelick, 1996; Neuman, 1997; EPA, 1999). Indeed, two of EPA's highest research priorities for groundwater-contaminated sites (e.g., Tables ES-1 and 2-5 in EPA, 1999) are: (a) developing subsurface methods (including non-invasive methods) to characterize the inherent complexity of the subsurface and to detect and quantify the presence and movement of contaminants in the subsurface; and (b) improving fate and transport modeling to reduce uncertainty in site-specific risk assessment and cleanup decisions. Time-lapse imaging of subsurface planes or volumes of interest with geophysical methods is a new class of non- or minimally-invasive methods for detection and quantification of fluid and contaminant movement, and for determination of the distribution of parameters and features controlling subsurface water and contaminant movement.

The basic concept of time-lapse imaging is that variations in the presence of water and/or contaminants (i.e., depending on degree of water saturation and on the contaminants and their physical properties) may be detectable and quantifiable by recognizing changes in tomographic images collected in the same location at different times (e.g., Day-Lewis et al., 2000). Examples of such possible locations with environmental concerns are: (a) horizontal planes in the unsaturated zone beneath a pit, tank, or landfill containing or leaking waste; (b) vertical plane(s) in a contaminated aquifer at or up-gradient of a compliance boundary or a drinking water supply well, or immediately up- and down-gradient of a treatment system; and (c) a volume being remediated by air-sparging or being influenced by infiltration. In addition to using time-lapse changes in images to detect and quantify the movement of water and/or contaminants, this same information can also be used to verify or improve models of the three-dimensional distribution of permeability in the shallow subsurface.

A combined tracer and time-lapse (radar imaging) field experiment was conducted at a research wellfield (Boise Hydrogeophysical Research Site, or BHRS) in 2001 to examine the capabilities of time-lapse imaging with cross-hole radar tomography to detect the movement and both temporally- and spatially-varying concentrations of an electrically conductive tracer (analogue for high conductivity or high TDS contaminant plume) in a shallow, unconfined, heterogeneous, fluvial aquifer (common type of aquifer system that is easily contaminated and difficult to remediate). This tracer/time-lapse test (TTLT) builds on current efforts by research teams at Boise State University to develop methods for using geophysical techniques in conjunction with hydrologic and geologic techniques to determine the distribution of permeability in shallow, heterogeneous, fluvial aquifers

(Barrash and Knoll, 1998; Barrash et al., 1999; Clement et al., 1999). This report presents design, operation, and preliminary results from the 2.5-week TTLT conducted in August 2001, with follow-up laboratory and field measurements.

TRACER/TIME-LAPSE IMAGING TEST GOALS

Goals of the tracer/time-lapse imaging test were to:

1. Conduct time-lapse radar tomography during a controlled tracer test to demonstrate the ability of this method to detect the presence of, and also temporal and spatial variations in, a tracer plume through cross-sectional and longitudinal planes of imaging;

2. Quantify attenuation magnitudes and differences in terms of concentration magnitudes and differences at a central location along the path of the plume where a well that is in line with two of the time-lapse radar imaging planes will be instrumented for multilevel sampling for tracer concentration;

3. Assess issues of resolution and uncertainty associated with the time needed for collecting the tomographic data compared with the flow rate of plume passage through the imaging plane;

4. Identify operational and equipment features that can be modified to improve efficiency of field data collection and subsequent image generation and interpretation; and

5. Provide a data set for hydrologic modeling to estimate the 3D distribution of permeability from head, injection/pumping, tracer, and time-lapse geophysical data.

HYDROGEOLOGIC SETTING

The TTLT and follow-up field tests were conducted at the BHRS. The BHRS is located on a gravel bar adjacent to the Boise River ~15 km from downtown Boise, Idaho (Figure 1). The wellfield consists of 13 wells in the central area (~20 m diameter) and five boundary wells about 10-35 m from the central area (Figure 1). The general design of the 13 central area wells is two concentric rings of six wells each around a central well. All wells were cored and drilled in the same manner without the use of mineral solids for drilling mud to minimize disturbance to the surrounding formation (Morin et al., 1988; Barrash and Knoll, 1998). All wells were constructed with 4-in ID PVC, including slotted casing throughout the saturated interval (Figure 2). This design and the method of well construction support a wide variety of single-well, cross-hole, and multiple-well hydrologic and geophysical tests for thorough three-dimensional characterization of the central area (Barrash and Knoll, 1998; Barrash et al., 1999; Clement et al., 1999). Well locations at the BHRS are given in Table 1.

The shallow aquifer at the BHRS consists of late Quaternary, coarse (dominantly cobble-and-sand), fluvial deposits similar to nearby exposures in road cuts (Figure 3) and quarries. Saturated thickness

of this aquifer ranges between ~16-18 m depending on seasonal variation in river stage and local depth to a tight red clay that underlies the site (Figure 2).

Hydrostratigraphic understanding of the subsurface at the BHRS is important for design and interpretation of tracer/time-lapse tomography experiments. Hydrostratigraphic understanding of the coarse fluvial deposits at the BHRS is based on: porosity profiles derived from neutron logs (Barrash and Clemo, 2000; 2002); radar and seismic tomography (Liberty et al., 1999; 2000; Peterson et al., 1999; Clement and Knoll, 2000); characteristics of core samples Reboulet and Barrash, 1999; 2000); GPR reflection profiles (Peretti et al., 1999; 2000); and preliminary permeability profiles (Purvance and Barrash, 2000; Barrash and Johnson, unpubl. data). Five hydrostratigraphic units in the coarse fluvial deposits (Figure 4) overlie a very thin (<1-m thick) portion of a basalt flow and a tight red clay (>3-m thick). These five units are, from older to younger: Unit 1, the lower low-porosity cobble-dominated unit; Unit 2, the lower variable-porosity cobble-dominated unit; Unit 3, the upper low-porosity cobble-dominated unit; Unit 4, the upper variable-porosity cobble-dominated unit; and Unit 5, an uppermost channel sand that thickens toward the Boise River and pinches out near the center of the wellfield (Barrash and Clemo, 2000; Reboulet and Barrash, 2000). The four cobble-dominated units pinch and swell in thickness, and have internal variations in porosity and permeability that may be related to relative proportions of sand to cobbles and/or to variations in sorting and packing.

Historical water level measurements at the site and measurements prior to the TTLT indicate a gradient with an azimuth approximately co-linear with the alignment of B3 and B6 (Figures 1 and 5). The Boise River forms a boundary on the western side of the site. The TTLT occurred during the time of year when flow rate and stage in the Boise River near the BHRS are relatively steady due to relatively steady outflows from the Lucky Peak Reservoir and diversions into the New York Canal for irrigation down valley. Such was the case during the time of the TTLT.

In addition to the stage of the Boise River, influences on water levels at the BHRS include daily cycles associated with evapotranspiration and having amplitudes ranging from ~.009 m to .027 m. Boundary conditions on the east side of the site are indeterminate beyond projection of the steady-state gradient to a lateral boundary to maintain that gradient. Recharge was negligible prior to and during the TTLT.

TRACER/TIME-LAPSE IMAGING TEST DESIGN

General descriptions are given below for a combined hydrologic and geophysical field experiment to test the capability of time-lapse radar imaging to detect temporal and spatial concentration changes at specified imaging planes and to learn from experience how to improve or optimize operational parameters for time-lapse imaging.

The TTLT was designed to be conducted between two wells (up-gradient injection well B3, and down-gradient withdrawal well B6) that are 6.9 m apart and are approximately in line with the natural gradient during summer months at the BHRS (Figures 5-6). A third well (A1) is located

between wells B3 and B6 along the line of the natural gradient; during the TTLT A1 was equipped to collect water samples from 20 zones isolated by packers and accessed by ports and dedicated tubing.

A central design concept was for injection and withdrawal wells to be equipped with log-through packers and ports that allow radar instruments to be lowered and raised through the well for the collection of tomographic data on an approximately axial plane through the plume as it developed and moved down-gradient (Figure 6). Similarly, nearby wells (B1, B2, B4, and B5) that are marginal to the plume path would be equipped with log-through packers and ports to allow head measurements, collection of water samples to detect if plume spreading has occurred to those locations, and to allow radar instruments to be lowered and raised through the wells for the collection of tomographic data on cross-flow planes through the plume (e.g., B4-B2 and B4-B1 as in Figure 6) as the plume moved down-gradient.

Well A1 (densely instrumented for water chemistry sampling) is in the middle of the tomographic panels that were collected between wells B4-B1 (cross-flow panel) and wells B3-B6 (longitudinal panel), and will provide the independent quantitative calibration information needed to check variations in time-lapse images against measured changes in tracer concentrations at different levels of the plume and at different times during plume passage through well A1.

Non-toxic, conservative tracers (bromide and uranine or Na-fluoroscein) were injected into two hydrostratigraphic units (Unit 2 and Unit 3) in the middle 4 m of the aquifer at well B3 (Figures 4 and 6). Unit 2 is generally more porous and permeable, and more variable in porosity and permeability than Unit 3 (Barrash and Clemo, 2000; 2002). This injection interval was chosen because the contrast in permeability was expected to cause the plume to move at different rates in the two units and thereby develop a changing geometry that should be a good target for examining imaging capabilities. Also, by limiting the tracer injection to a 4-m-thick interval in these two units, resources could be concentrated for measurement and analysis, including focusing the tomographic imaging data collection and high-resolution chemical sampling for calibration of radar image changes on a 4 m-thick portion of the system rather than the full 18-m thickness of the system.

TRACER SELECTION

Two conservative tracers (bromide and uranine) were selected for simultaneous use in the TTLT. Conservative tracers were selected to simplify test analysis because the focus of the experiment was on the ability to detect changes in tracer concentration with geophysical methods and to determine the distribution of hydraulic parameters — not on examining chemical interaction of tracers with substrate or biological components of the environment. The use of two conservative tracers with different chemistry provides a test of the assumption of conservative behavior and could provide insight into unexpected aquifer conditions if the behavior differed between the two tracers.

Bromide was selected because it is electrically conductive and would thereby influence the radar signal and support testing of the capabilities of time-lapse radar imaging. Also bromide is non-toxic,

highly soluble, inexpensive, has low background concentration at the BHRS, and is easy to detect in the field at low concentrations as conductivity. One concern with the use of bromide is the potential for density effects on the flow field with initial concentrations near 10,000 ppm. If such effects occur, they complicate the analysis but do not negate the value of the tracer in other respects.

Uranine was selected as the second tracer because it is a conservative organic dye under stable chemical and photochemical conditions (e.g., Davis et al., 1985; Kass, 1998). For example, uranine and several other organic and inorganic tracers exhibited conservative behavior in a recent tracer test in a similar type of aquifer (shallow, coarse fluvial aquifer adjacent to a river) in Germany (Bosel et al., 2000). Being an organic dye, uranine is different in chemical behavior from the inorganic anion bromide. Uranine also is non-toxic, inexpensive, highly soluble and easy to detect in the field at low concentrations with a fluorometer.

PRE-TEST FLOW AND TRANSPORT MODELING

Pre-test flow and transport modeling was conducted to estimate breakthrough time and plume shape considering the effect of different aquifer and test parameters. Transient three-dimensional (3D) modeling was conducted using the finite-element code: FEMWATER. Design parameters used in the TTLT based on this modeling (described below) were: injection rate of 30 gpm for 35 min through the 4-m injection interval in B3 to achieve an average plume diameter of ~2 m in Unit 2 at ~75-100% relative source concentration; and pumping rate of 5 gpm from the same 4-m elevation interval in B6 to help guide the plume along the desired pathline at a rate conducive to both collection of radar tomography data in daily cycles and completing breakthrough at well A1 in 2.5 weeks, while limiting the forced-gradient effect on plume movement in the region between wells B3 and A1.

The modeling focused primarily on the central region of the BHRS (Figure 1) where information is available from wells on subsurface variations in hydrostratigraphic unit contacts and on hydraulic parameters (Figure 4). Positions of unit contacts for the model were generated by kriging. Hydraulic parameters varied by unit but were held constant within units (Table 2). Similar hydraulic conductivity values were assigned to Units 1 and 3 (relatively lower porosity and permeability) and Units 2 and 4 (relatively higher porosity and permeability) based on their similarity in porosity (Barrash and Clemo, 2000; 2002) and preliminary permeability measurements (Barrash and Johnson, unpubl. data). Units 2 and 4 were given hydraulic conductivities four times greater than Units 1 and 3. Hydraulic conductivity for the channel sand was highest of all, but present only in the western half of the model and generally was above the region of the aquifer involved in plume transport. A 2:1 horizontal to vertical anisotropy was assumed for all units. Constant longitudinal and transverse dispersivities were assigned to all units (Table 2); it is believed that these values are low but, when used in combination with the relatively higher numerical dispersion associated with use of the FEMWATER code, apparently reasonable results were obtained.

Constant head boundaries were assigned around the BHRS in keeping with the natural gradient and the position of the Boise River. A no-flow boundary was set at the base of the coarse fluvial

sediments (known from coring and drilling) where these coarse sediments overlie a thin (<1-m thick) basalt flow edge and a tight red clay. This lower surface is approximately horizontal under most of the site but is deeper, perhaps cut out by a paleo-river channel, on the west (river) side of the site.

Operational test conditions that were variables in pre-test modeling included: injection rate and time at B3, and pumping rate at B6. Injection and pumping were allowed only from the target 4-m injection interval spanning the contact between Units 2 and 3, but the wells were given finite dimensions equal to their geometry to account for hydraulic influence of open wells above and below the packers. In particular, equalization of hydraulic head and tracer concentration occurring at injection well B3 could have significant flow and transport effects locally.

Model results are shown at four model times for the tracer/time-lapse test for a horizontal plane ~0.5 m above the mid-elevation of the injection interval (~839.65 m elevation) and for a cross-section through the center of the plume. These times are: (a) immediately after injection (i.e., 35 min after start of injection) (Figures 7-8); (b) near peak breakthrough at well A1 (~3.7 days) (Figures 9-10); (c) significant portion of plume dominated by pumping at B6 (~9.8 days) (Figures 11-12); and (d) substantial passage of the tracer plume through well A1 (~16.6 days) (Figures 13-14). Figure 15 shows model breakthrough curves at A1 for relative concentration at the elevation of the plan view figures (upper portion of Unit 2) and at a horizontal plane 1.6 m below where the peak breakthrough concentration occurs in the model.

A number of points are illustrated in these figures. With injection, the plume is nearly radially symmetrical (Figure 7) but it is wider in Unit 2 than Unit 3 (Figure 8) because of higher permeability in Unit 2. The plume extends above and below the injection interval in the formation because vertical gradients are generated adjacent to the packers. Diameter of 70% relative concentration contour is ~2.9 m in Unit 2, and ~1.9 m in Unit 3. Also, vertical flow components arise from topography on the unit contacts between wells (especially the rise of contacts between Units 2 and 3 and between Units 3 and 4 from injection well B3 to well A1).

After ~3.7 days of pumping from B6 at 5 gpm, the up-gradient portion of the plume is largely past B3 (Figure 9) and the down-gradient portion of the plume is being drawn out of well B6, but only from Unit 2 (Figure 10). The shape of the plume and orientations of velocity arrows illustrate that a flow field with parallel flow in the horizontal dominates between wells B3 and A1, and a flow field with convergent flow (i.e., influenced by forced gradient due to pumping at B6) dominates between wells A1 and B6 (Figure 9). Tracer discharge at B6 and breakthrough at A1 are almost entirely in the lower half of the 4-m (injection) interval at A1 (Figure 10). A significant fraction of the plume is traveling below the injection interval between wells B3 and A1. The slow-moving core of the plume in Unit 3 is partially being drawn into Unit 2.

After ~9.8 days of pumping from B6 at 5 gpm, the plume is almost fully past B3 (Figure 11) and is being removed from B6 in both Units 2 and 3 (Figure 12). The core of the plume is approaching A1 in the plane of view; breakthrough in the lower portion of the injection interval in A1 is extended

in time due to the downward component of flow bringing additional tracer mass from Unit 3. Plume shape in the horizontal plane is not symmetrical due to topography on the contact between Units 2 and 3. The plume is being drawn out of Unit 3 at both well B6 and Unit 2 (Figure 12).

After ~16.6 days of pumping from B6 at 5 gpm, the plume shape in the horizontal plane is elongated and converging because it is largely influenced by the forced-gradient due to pumping at B6 (Figure 13). The plume is largely past A1 (Figure 14).

INJECTION, MEASUREMENT, AND PUMPING SYSTEMS AND METHODS

Detailed design for tracer delivery and recovery, and for chemical, hydrologic, and geophysical measurements during the TTLT are described below. The overall arrangement of infrastructure for conducting the TTLT at the BHRS are shown in Figures 16 and 17. Here we note that the BHRS is a natural area without line power service, so generators were used to power most instruments used during the TTLT.

INJECTION

The injection system includes the above-ground components for storage, mixing, sampling, recording, and pumping, and the in-well system for isolating the 4-m injection zone and for measuring head change below, within, and above the injection zone (Figures 18-19). A 1000+ gallon plastic water tank was the reservoir for mixing the two tracers prior to injection; a double layer of tarp was used to cover the tank to limit light exposure (Figure 20).

TECHNOLOGY FOR COINCIDENT SAMPLING AND MEASUREMENT

Only wells already present at the BHRS (Figure 1) were available for use during the TTLT and wells at the TTLT had to be left without instrumentation after the test — so all installations in wells for the TTLT had to be removable. With this requirement, two types of modular in-well technology were designed and constructed for the TTLT: (a) log-through packer-and-port systems; and (b) a many-zone high-resolution packer-and-port system. These two types of custom-designed in-well technology are described briefly below.

Log-Through Packer-and-Port Systems

In-well technology was needed to allow collection of water samples and information on head changes from discrete zones at the same time that: (a) cross-hole radar data were being collected; or (b) pumping was occurring from the same well. Log-through packer-and-port systems were custom designed in collaboration with Michigan State University, and were manufactured at Michigan State University. These systems had the following design characteristics: operate in 4-in ID PVC-screened wells; have 2-in ID riser; use minimal metal to avoid interference with geophysical equipment; isolate 1-m zones; have sampling access to zones for collection of water samples and/or measurement of head through small-diameter access tubes; inflate short-length packers for zone-

isolation with a single pressurized-gas inflation line; and have systems consist of 2-m sections that can be transported, assembled, and disassembled easily (Figure 21).

Five such systems with six 1-m zones per well were used for the TTLT. Four of these systems were installed in B wells (B1, B2, B4, and B5) for sampling while collecting cross-hole radar data (Figure 22); and one system was constructed in a similar manner but holes were drilled in four of the six 1-m intervals to: (a) permit pumping at well B6 from four 1-m zones set at the same elevations as the 4-m injection zone in B3; and (b) also allow discrete-zone sampling from these four zones and two additional 1-m zones above and below these four zones. Table 3 identifies the specific locations of packed-off zones in wells for the TTLT. This configuration of packers and ports in B wells was designed to allow determination of head change and tracer concentrations by zone for tracer transport modeling, and allow radar tomography through the tracer plume, including tomography between wells B3 and B6 by periodically pulling the pumping hose from well B6 and logging as in the other four B wells, while continuing to collect periodic water samples and head-change data.

High-Resolution Packer-and-Port System

A packer-and-port system for high-resolution information was needed in calibration-well A1 to collect tracer breakthrough and head-change information in the planes of cross-hole radar data collection between wells B4 and B1, and B3 and B6 (e.g., Figures 6 and 23). Data collected through this system permits quantitative calibration of radar attenuation differencing with water conductivity magnitudes and changes; this capability is critical to modeling time-lapse radar imaging and groundwater flow and tracer transport. Such a system was custom designed as a collaborative effort by Boise State University and Michigan State University, and was manufactured at Michigan State University with the following design characteristics: operate in 4-in ID PVC-screened wells; use minimal metal to avoid interference with geophysical measurements; isolate twenty .25-m zones; have sampling access through small-diameter access tubes to all 20 zones for collection of water samples and to four of these zones also for measurement of head change; inflate short-length packers for zone-isolation with a single pressurized-gas inflation line; and have systems consist of 2-m sections that can be transported, assembled, and disassembled easily (Figure 24). Table 3 and Figure 25 identify the locations of zones isolated in A1 for the TTLT.

TRACER SAMPLING AND ANALYSIS

Tracer sampling was needed at sufficient frequency to capture concentration changes and thereby to define breakthrough curves and calibrate radar attenuation tomography. In-field analysis of water samples was needed to provide near-realtime feedback on the progress of the test in case changes in operational parameters (e.g., pumping rates, frequency or intervals of radar tomography) were needed, and to know when to end the test. Sampling and sample management procedures were needed to assure orderly data collection and analysis in the field, and for storage and subsequent analyses as needed for QA/QC and/or delayed or repeated analyses (Barrash and Knoll, 2001).

Sample Collection Method, Frequency, and Handling

Five peristaltic pumps with ten sampling lines each were used to collect samples from six zones in each of wells B1, B2, B4, B5, and B6, and from 20 zones in A1 (Figure 26). These pumps were run continuously throughout the test to ensure samples did not include stagnant water. Pumping rates with the sample pumps were adjusted from 5 ml/min (between sampling events) to 30 ml/min (during sampling events), although some variation from this regimen occurred. Calculation of transit times from individual zones based on pumping rate, tubing diameter, zone depth, and length of surface tubing allow adjustment of sampling time from that marked on the sample vial as needed. In general, sample transit times range from ~2 to ~27 min (Figure 27; Hausrath et al., 2002).

Water samples were collected in 30 ml amber plastic vials. Amber color was used to help limit exposure of samples to light because uranine decomposes with exposure to light (e.g., Kass, 1998). Prior to the test, sample vials were pre-labeled with sample location (well and zone), or with identification as a QC sample from an as-yet-undetermined location, and all vials were grouped into boxes for each sampling event. During a sampling event, sampling tubes were rinsed with distilled water prior to insertion in the sample vials (Figure 28A) to prevent cross-contamination. Vials were loaded into labeled trays and set in collection troughs where labeled, dedicated sampling tubes from isolated zones in wells were fixed at the discharge side of peristaltic pumps (Figure 28B).

A complete sampling event during the test included collection of samples from the 50 zones in wells, 5 or 6 duplicate (QC) samples from zones selected at the discretion of the sampling person(s), and a sample from the discharge line (Figures 26 and 29). Also, samples were collected prior to injection to get background measurements. Samples were collected from the mixing tank prior to injection, and from the injection line at 4 minute intervals during injection. Samples were collected from well B3 after the straddle packer was removed; the line from B3 was substituted for the line from B4-6 (i.e., zone 6 in well B4) starting with sampling event 32 (e.g., Appendix 1) because the B4-6 line was not maintaining production.

Sampling frequency after injection was every four hours through August 17 (test day 16), with some variation from this during the early stages of the test (e.g., Appendix 1). After test day 16, pumping ceased from well B6 and was moved to A1 (to remove residual tracer from the central portion of the wellfield) with samples collected from six zones in well A1 for one more day. Appendices 1-3 list sampling event times and numbers and types of samples collected during the TTLT.

Following collection and/or analysis in the field, vials from a given sampling event were returned to the event box which was labeled and stored in a black plastic bag and a cardboard box. Event boxes were transported to temperature-controlled storage at Boise State University and kept there in black plastic bags.

Field Laboratory and Near-Realtime Analyses

A field laboratory (Figures 26 and 30) was set up to run analyses for fluorescence (as an analogue for uranine concentration) with a Turner Designs 10AU fluorometer, and for conductivity (as an analogue for bromide concentration) with probes. Also, measurements for pH were taken periodically from a subset of samples, and temperature measurements were taken on all samples. Calibration checks were run before analyses for each sampling event. Additional detail is provided in the report on chemical analyses during and after the TTLT (Hausrath et al., 2002).

Samples from well A1 were the top priority for analysis, and analyses on samples from A1 were completed within four hours of collection for all sample events during the test. Data were entered into a spreadsheet at the field laboratory to provide near-realtime feedback on breakthrough behavior.

HYDRAULIC HEADS AND FLOWS

Hydraulic head measurements in open wells, in zones isolated in wells with packers, and in the Boise River were taken prior to and during the TTLT, primarily with transducers and recorded on data loggers (Figures 31-32). Periodic checks also were made with electric tape measurements in accessible open wells (C and X wells). Also, atmospheric pressure measurements were collected during the test.

Flow rate measurements were taken with a digital flowmeter and recorded on a data logger for both injection from B3 and subsequent pumping from B6. Pumping rates from peristaltic pumps were checked periodically on a line-by-line basis with the nominal flow rate displayed on the readout of the pump. It was not uncommon to have variation of up to 50% among the lines of a given peristaltic pump at low nominal flow rates.

Discharge from dedicated lines run through the peristaltic pumps was collected at each pump station and routed to a collection barrel for waste water at the field laboratory (Figures 26 and 29). Water from this barrel was injected into the discharge line from B6 that was routed to the slough area under the SH21 bridge about 140 m from the central wellfield (Figure 1).

Measurements of head-change at zones isolated with packers in well A1 and in B-ring wells were taken with small-diameter (2 mm) fiber-optic transducers with a measurement range of 0-5 psi. These are total pressure transducers requiring data adjustment for atmospheric pressure. This is a new technology which allows ease of access to isolated zones in wells by threading the thin cable down small-diameter access tubes as were used for water chemistry sampling. Other attributes include high sensitivity of measurement (<.01 psi), fast sampling rate (100 Hz), and synchronized sampling from up to 64 channels. However, the hardware and software for this technology are prototype rather than stock production and, despite successful use in short-test applications, several failures occurred during the longer-running TTLT necessitating a rerun of the start of the test with revised transducers in 2002 (see below).

C-ring and X-ring wells were measured as open wells (i.e., without separation into zones) using conventional strain-gauge transducers linked to data loggers (Figure 31). Also, these wells were measured periodically by hand with electric tapes. Stage changes in the Boise River were measured with a strain-gauge transducer linked to the data logger used for the C wells (Figure 31).

RADAR SYSTEMS

Information on the types of radar systems and antenna frequencies used, the length of measurement runs and intervals between measurements in wells, and other operational data are presented in Knoll (in prep.). Figure 33 shows near-realtime review of radar data during the TTLT.

TRACER/TIME-LAPSE IMAGING TEST 2001

In this section, first the events or chronology of the TTLT are described and then preliminary hydrologic, water chemistry, and radar results are given.

CHRONOLOGY

Chronology of the TTLT in 2001 (Appendix 4) is described below by major stages and noteworthy events.

Preparation and Background: July 29 to August 1, 2001

Instrumentation to support the TTLT was set up at the BHRS during the week prior to the start of the test. Background measurements were initiated on July 29, 2001. A practice injection test was run on July 31 to test plumbing and measurement systems, and to adjust valving to achieve the desired injection rate as quickly as possible during the real test. Similarly, data for background radar tomograms were collected and other experiments were conducted for calibration and data optimization purposes.

The two tracers used in the TTLT were mixed together in the 1000+ gallon tank that was full of water pumped from well X2 at the BHRS between 0930 hr and 1030 hr on August 1, 2001; 31.5 kg of potassium bromide and 378.5 mg of uranine were mixed to achieve ~8300 ppm bromide and ~100 ppb uranine, assuming 1000 gallons at the source. Actual concentrations in the injection tank were ~7600 ppm bromide (8410 uS/cm conductivity) and 88 ppb uranine; these values were less than the design because the water tank held approximately 1100 gallons. The tank was covered with a double layer of blue plastic tarp to reduce exposure of uranine to light (Figure 20). Water in the tank was circulated vigorously at ~50 gpm to assist mixture of bromide and minimize the possibility of density stratification in the source tank. Temperature of the water was monitored periodically because air temperature was rising rapidly. Water temperature at the time of injection was 19.8 ^{o}C.

Test Period: August 1-18, 2001

Injection into well B3 at ~29.5 gpm began at 1140 hr on August 1, 2001 and continued for 33 min and 20 sec (Figure 34A). Approximately 35 minutes after injection was completed, pumping was started from well B6 at ~5 gpm from the same 4-m elevation interval that was used for injection. It was intended for pumping to continue at this rate for the duration of the test except for periods needed for collection of tomographic data between wells B3 and B6; Figure 34B shows the pumping history for the whole TTLT. Injection-line bromide "concentration" as conductivity averaged 8375 uS/cm; injection-line concentration of uranine averaged 88.5 ppb (Hausrath et al., 2002).

A power failure at ~0700 hr on August 7 caused a cessation of pumping that lasted longer than the buffer capacity of the two uninterruptable power supply (UPS) units that were in line to all instruments and equipment except the pump at B6 and the data loggers in the X wells. As a result, recording stopped at data loggers for the fiber-optic transducers and the strain-gauge transducers in the C wells, Boise River, and upper zone of B3. Power was restored by ~1030 hr. Although data collection continued at the data logger directly connected to the flow meter, atmospheric pressure transducer, and transducers in the lower two zones of B3, the power failure caused a non-linear loss of time standard at this logger, so its records after the power failure might only be placed approximately in time by projection after matching identifiable events on other loggers.

An unscheduled stoppage of pumping at B6 occurred again at ~1343 hr on August 7. A back-up pump was installed and pumping was re-established at ~1400 hr on August 7. A second power failure occurred at ~2010 hr on August 7 which caused a pumping stoppage, but the duration of power loss was short and power was restored at ~2017 hr before the buffer capacity at the UPS units was exhausted.

The straddle packer system was deflated and pulled from well B3 prior to 1000 hr on August 10 after it was determined that the up-gradient portion of the initial injected plume had almost completely passed through well B3. Pumping was stopped from B6 at ~1000 hr for collection of radar tomography data between wells B3 and B6. Radar tomography was completed and pumping re-established at B6 at ~1930 hr (Appendices 4-5).

Cessation of pumping at B6 and radar tomography between B3 and B6 occurred again between ~0710 hr and ~1345 hr on August 13, and between ~0710 hr and ~1400 hr on August15 (Appendices 4-5). During the time that tomographic data were collected on August 15, the discharge point for pumpage from the wellfield was moved from the location at the slough just north of the SH21 bridge, to a location at the slough northeast of well X1 (see Figure 1) which allowed significant shortening of the discharge line, but which brought the discharge point closer to wells. When pumping resumed on August 15, the pumping rate was increased to 26 gpm to expedite removal of residual tracer from the wellfield.

Pumping was stopped at B6 at ~1400 hr on August 17. Packer-and-port strings were removed from all wells, and the string that had been in B6 was placed in A1. Pumping then was started at ~26 gpm

from well A1 to help remove residual tracer from the wellfield. Abbreviated sampling was conducted only from the six 1-m zones in A1 and from the discharge line for sample event numbers 98 to 102 between 1900 hr on August 17 and 1100 hr on August 18 (Appendices 1-3).

PRELIMINARY RESULTS

Descriptions of measurements associated with the TTLT are given below. These results are preliminary in that thorough review has not been completed on some data sets.

Hydrologic Responses During the TTLT

Injection for the TTLT began at 1140 hr on August 1, 2001. Initial injection rates rose above 30 gpm but rapidly declined and the stable injection rate of 29.5 $\pm$ .5 gpm was established by ~.33 min elapsed time and was maintained until injection stopped 33 min 20 sec later (Figures 34-35). All wells and monitored zones in wells registered responses to injection. Head build-up in the injection zone in B3 (~1.2 m) and in the open well above and below the packers around the injection zone in B3 (~.28 m and ~.16 m, respectively) are shown in Figure 35. Sporadic early-time head changes in opposition to pumping rates likely are due to trapped air in the injection line. Head build-up during injection at packed-off zones in A1 and B wells largely follow expected patterns of: (a) greater head build-up in well A1 in zones at elevations within the injection zone than above or below the injection zones (Figure 36A); (b) greater head build-up in wells B1, B2, B4, and B5 in zones 2 (i.e., in Unit 2 with higher porosity and permeability) than in zones 5 (i.e., in Unit 3 with lower porosity and permeability) (Figure 37A); and (c) greater head build-up for any given packed-off zone in wells B2 and B4 which are closer to injection well B3 than wells B1 and B5 (Table 1, Figures 1 and 37A).

Head changes in C wells during injection (unadjusted for evapotranspiration trend) ranged from ~.027 m in C5 (Figure 38) to ~.075 m in C2. Head changes in X wells during injection (unadjusted for evapotranspiration trend) ranged from ~.001 m in X5 to ~.019 m in X2 (Figure 39).

Here it is important to note that head-change measurements with fiber-optic transducers in zones of A1 and B wells have some uncertainty due to apparently random occurrences of drift and/or shifts (Figures 36B and 37B) after removal of atmospheric pressure changes (Figure 40). Drift was more pronounced for some transducers (e.g., transducers in zones A1-2, A1-6, B1-6, B2-2, B2-5, B4-5, B6-2, B6-5). Data from A1 and the B wells are considered semiquantitative; because of this, a rerun of the start of the TTLT and several pumping configurations similar to the TTLT was performed in June 2002 with more stable fiber-optic transducers (see Test Restart 2002 section below).

Also, gaps in coverage are evident for A1 and B wells from 0004 hr August 2 to 1445 hr August 3, and 1358 hr August 6 to 1036 hr August 7 (Figures 36B and 37B). The first gap was due to a software problem; the second gap was due to equipment and software changes and the long power outage. A gap in C well coverage is due to the long power outage on August 7. Data from the digital in-line flow meter, the atmospheric pressure transducer, and transducers in well B3 (above, within,

and below the injection zone) were recorded initially on a separate data logger; duplicate measurements were collected on the logging system for the fiber-optic transducers starting at 0725 hr August 1 for the flowmeter and at 1036 hr August 7 for the atmospheric pressure transducer and transducers in the injection zone and the zone below injection in B3 (Appendix 4). Unfortunately the loss of power to the separate data logger during the long power outage on August 7 caused a time-transgressive scaling problem for time recording, and recreation of data for the gaps in the fiber-optic logging system from the post-loss continuous, but time-uncertain, record on the separate logger can only be approximate.

Head changes during changes in pumping regimes are recognizable in A1, B wells, and C wells (Figures 36-38). All X wells responded during injection and pumping at 26 gpm; only X4 and X5 responded to periods of cessation of pumping at B6 for radar tomography or resumption of pumping at 5 gpm at B6 (Figure 39). Head change associated with pumping (or cessation of pumping) at 5 gpm ranged from ~.006 to .026 m in zones in A1 and B wells; from ~.007 m in C4 to ~014 in C6 in C wells; and from ~.002 m in X5 to ~.006 m in X4 in X wells. Head change associated with pumping at 26 gpm ranged from ~.03 m in C3 and C4 to ~.053 m in C6 in C wells; and from ~.012 m in X1 to ~.12 m in X4 in X wells. Data logging was suspended for A1 and B wells prior to starting of pumping at 26 gpm from well B6 on August 15.

Daily head fluctuation cycles due to evapotranspiration are evident during the test in all wells and monitored zones. Although head changes associated with injection, pumping, and recovery from injection and pumping are recognizable at most wells, accurate determination of long-term head changes will require removal of the local trend associated with these cycles at a given well or zone. Also, a minor decreasing trend in river stage is recognizable after day six; this trend corresponds with minor increasing diversion rates to the New York Canal (Figure 41).

Water pumped during the first 14 days of the TTLT was discharged to a point just north of the SH21 bridge (Figure 1) ~140 m down-gradient of the TTLT area; water pumped thereafter (after the discharge rate was increased to 26 gpm) was discharged to the slough northeast of well X1. It is unlikely that the head field around the test was influenced by 5 gpm discharge north of the SH21 bridge; however heads at X1 were influenced by the 26 gpm discharge northeast of X1 at the end of the TTLT (see relative head increase after ~14.5 days in Figure 39).

Water Chemistry: Field and Laboratory Measurements, and QA/QC

A total of 5521 samples were collected for the TTLT between July 29 and August 18, 2001 including background, pre-injection mixing-tank samples, and duplicate QA/QC samples (Appendices 1-3). Of these, 4735 samples were collected from isolated zones during the main portion of the test and an additional 495 samples, or 10.5%, were collected as QC duplicates. Also, 153 samples were collected from B3, and from the discharge line downflow from B6. Samples were analyzed in the field for uranine, pH, conductivity, and temperature (Figures 26 and 30).

From the field results it became clear that conductivity (Figures 42-48) and uranine (Figures 49-55) exhibited significantly different transport and breakthrough behavior. In particular, uranine: (a) was reduced in relative concentration compared with conductivity; (b) was delayed in breakthrough occurrence compared with conductivity; and (c) had different vertical distribution of breakthrough timing and relative concentrations than conductivity. Because the focus of the TTLT was on time-lapse imaging of a conductive plume, time available for field and laboratory analyses was apportioned preferentially for conductivity once the anomalous behavior of uranine was recognized. Still, uranine was analyzed for all zones in A1 throughout the TTLT and for other zones in B wells as possible. And, reconnaissance investigation into the cause for the unexpected uranine behavior was pursued after conductivity analyses were finished (see below, and Hausrath et al., 2002).

More complete examination of field data, outliers, laboratory analyses on samples not analyzed in the field, and QA/QC are given in Hausrath et al. (2002). Here we note that, even without removal of outliers, field samples and QC duplicates of field samples correlate at $R^2 = .99$ for conductivity (Figure 56) and uranine (Figure 57). As an additional QC check, a selection of conductivity samples spanning the range of values measured during the TTLT was sent to a commercial laboratory for analysis; excellent agreement was found between the external laboratory results and the field results (Hausrath et al., 2002). For pH, the repeatability of samples and QC duplicates was $R^2 = .99$ (Figure 58). Greater local scatter in pH data is likely due to problems in achieving full calibration with the probes we used in the field; apparently poorer correlation for pH ($R^2 = .83$) results if the data are not forced through zero for the correlation analysis. Considering the degree of correlation between samples and QC duplicates, it is reasonable to present preliminary interpretation of tracer breakthrough behavior in following sections.

Conductivity Breakthrough

Conductivity increased from background with an early minor peak ("injection peak") at all zones of all monitored wells (except zones 1-5 in well A1) between events 6 or 7 and events 13 or 14. Except for significantly higher peak conductivity of ~800 uS/cm in well B4, values of peak conductivity were largely similar for zones registering the injection peak: peak conductivity of ~330-350 uS/cm in wells B1, B2, B5, and B6; and peak conductivity of ~250-400 uS/cm with upward-increasing trend in well A1. The shape of the injection peak varied progressively from steep front and extended tail in the upper portions of A1 to a symmetrical peak at the bottom of the breakthrough region in A1 (i.e., zone A1-6). The injection peak in the B wells occurred earlier (about events 3-4 in wells B1, B2, B5, and B6; about events 2-9 in B4) and was much shorter in duration than in A1.

After the injection peak, conductivity returned to background levels for the remainder of the test for wells B2, B4, and B5 (Figures 44-46), but exhibited a second breakthrough peak in well B1 between about event 47 and event 59 (Figure 43), and exhibited a range of second (main) breakthrough behaviors in well A1. The main breakthrough behaviors in well A1 generally have complicated and extended shapes, including a distinctive second peak for a significant portion of the investigated vertical interval in well A1. The highest conductivity for any zone during the main breakthrough

was ~2600 uS/cm in zone A1-5 (Figure 42B), which is ~0.31 C_o compared to the injection-line concentration, in terms of conductivity, of 8375 uS/cm (Hausrath et al., 2002).

Main breakthrough behavior for conductivity in well A1 can be subdivided into five vertically contiguous types based on the presence or absence of the main breakthrough and on similarities in the time of onset, the overall magnitude, and the details of concentration changes during the main breakthrough period. In order from lower to upper, these five subdivisions in well A1 are: (1) zones 1-4; (2) zones 5-7; (3) zones 8-12; (4) zones 13-14; and (5) zones 15-20.

In particular, main breakthrough behavior in zones 1-4 of well A1 (Figure 42A) follows a sequence of: (a) slow increase from background from about event 20; (b) steep rise from event 37 to a first peak of ~2000 uS/cm at about events 52-59; (c) less-steep decline (compare with pre-test model breakthrough curve shape — Figure 15) until event 73 when (d) an abrupt rise occurs to a second peak within the main breakthrough period; and then (e) at event 86 an abrupt decline occurs to resume the tail of the main breakthrough period.

For zones 5-7 in well A1 (Figure 42B), the main breakthrough period is somewhat similar to behavior described above for zones 1-4 with respect to stages that occur and magnitude of peaks, but there are significant differences in timing. In particular: (a) the increase from background begins about event 22; (b) has a relatively smooth increase to first peak maximum (events 60-71) – rather than a two-stage increase as in zones 1-4; (c) has an abrupt rise to the second peak at event 73 immediately after the first peak; and then (d) there is an abrupt decline starting at about event 86.

Zone A1-8 exhibits some similar behavior to zones 5-7 (early rise to main breakthrough period, magnitude of first peak in this period, end of first peak), but also differs significantly in that there is a decline after the first peak until about event 84 when the second peak of this period begins, and the second peak begins its steep decline at about event 91 (Figure 42C). Overall, zones 8-14 in well A1 are transitional between the significant main breakthrough peaks of zones 1-7 below and the general lack of main breakthrough in zones 15-20 above. Within zones 8-14 there is an upward dampening of magnitude, and the onset of increase from background is significantly delayed for zones 13-14. Also of note is the shape of the main breakthrough curves for zones 9-12: after the initial gradual rise from background starting about event 23 (as in zones below), conductivity appears to synchronously increase to three plateau levels (with synchronous fluctuations at the start or end of these plateau periods), then decrease to fourth, and perhaps fifth, plateau levels by the end of the test (Figure 42C). For zones 13-14, conductivity rise from background occurs at about event 64 and continues very gradually until the end of the test (Figure 42C).

Conductivity values after the injection peak in zones 15-20 in well A1 (Figure 42D) stay at background values with the exception of increases in zones 15 and 16 starting at late time (events 89 and 91, respectively).

Conductivity-Bromide Relationship

Conductivity may be converted to bromide concentration with the following relationship (Figure 59) based on post-test laboratory measurements:

$$\text{Bromide} = (C_{25} - C_{background}) * 0.9255 + 0$$

where bromide units are ppm, conductivity units are uS/cm, and background conductivity was ~206 uS/cm based on 94 samples collected before tracer injection (Hausrath et al., 2002).

Uranine Breakthrough

Uranine concentration (determined from fluorescence) increased from background with a minor injection peak at wells B1, B2, and B4 between about event 2 and event 10 after injection, and then returned to background levels for nearly the remainder of the test (Figures 50-52). No later main peak was observed in B wells, except perhaps a low-amplitude pulse passing through zones 2-5 of B1 starting before event 50 and ending by about event 90 (Figure 50). The injection peak passed through A1 later than in the B wells, starting about event 13 or 14 in most zones in A1 (Figures 49A-D). All wells and zones show approximately synchronous, very low-amplitude (.01-.02 ppb), daily cycles (Hausrath et al., 2002).

Main breakthrough for uranine was observed in the lower 3 m of zones in well A1 starting about 10.3 days into the test (Figures 49A-D) and moving progressively upward — as with main conductivity breakthrough behavior in A1. The highest concentration of uranine for the main breakthrough (Figure 49B) was at a greatly reduced concentration of ~12 ppb (~.13 C_o) in zone A1-9 compared to the injection-line concentration of 88.5 ppb, and compared to the relative maximum breakthrough magnitude of conductivity (~.31 C_o or about 2.5 times greater than for uranine). The shape of the main breakthrough curves in A1 generally have a relatively low build-up slope and then a steeper rise to a narrow peak starting about 14 days into the test (Figures 49A-C).

Main breakthrough behavior for uranine in well A1 can be subdivided into several vertically contiguous groups based on the presence or absence of the main breakthrough peak and on the steepness of the rise to this peak. In order from lower to upper subdivisions: (1) zones 1-7 have "moderate" relative breakthrough rate increases at about event 63 and again at about event 86, and reach maximum concentrations of ~2 to 3.5 ppb (Figure 49A); (2) zones 8-11 have steepest relative breakthrough rate increases at about events 63 and 86, and reach maximum concentrations of >3 to12 ppb (Figure 49B); (3) zone 12 is transitional from zones 1-11 (which have similar breakthrough behavior after event 86 [Figure 49C]) and zones 13-14 which have little change from background until about event 91 when both have minor but recognizable concentration increases to ~1 ppb (Figure 49C); and (4) zones 15-20 show no, or very minor, concentration increases toward a second peak above background (Figure 49D). These vertical subdivisions in uranine main breakthrough behavior at A1 differ in timing and magnitude of breakthrough from those for conductivity (Figure 42).

pH

Uranine fluorescence is highly pH dependent with fluorescence decreasing rapidly as pH decreases below ~7.5 (e.g., Kass, 1998). A general trend of increasing pH with depth during the TTLT may be recognized from pH ~6.6-6.7 at upper zones to pH ~7.5 at zone 1 (Figure 60). Previous reconnaissance pH profiles in wells at the BHRS (Johnson and Barrash, unpubl. data) similarly indicated a downward increasing trend in pH in wells at the BHRS.

Here we note that although the pH meter used during the TTLT did not register full calibration for a significant number of measurement cycles, the results show systematic trends within and between wells rather than random behavior (Figure 60). Also, results are generally consistent with previous measurements taken with a different instrument (Johnson and Barrash, unpubl. data).

Uranine and Aquifer Ecology

The unexpected reduction in uranine concentration and retardation in uranine transport rate likely are not due to inorganic causes such as pH reduction, exposure to aggressive oxidizing agents, or light exposure (Hausrath et al., 2002). Uranine removal from groundwater can occur due to microbiological degradation (e.g., Kass, 1998), and perhaps due to sorption at plant roots or root hairs (e.g., Vakhmistrov and Zlotnikova, 1990). To test for the possibility of such biological and/or microbiological interaction with uranine, site water was collected in 2002 from the injection zone in well X3 which is up-gradient from the region exposed to uranine during the TTLT (Figures 1 and 6). Site water, autoclaved site water, and autoclaved Boise tap water were treated to achieve initial uranine concentrations of 100 ppb, 50 ppb, 10 ppb, and 1 ppb. Also, roots from well X2 (also up-gradient from the region of the TTLT [Figure 1]), were treated with uranine at a concentration of 100 ppb. Concentration (i.e., fluorescence) showed an exponential decay in the flask with roots, but no reduction occurred in flasks with water alone, autoclaved or not (Figure 61, and Hausrath et al., 2002). It appears likely that biological and/or microbiological activity associated with cottonwood roots in the aquifer has played a major role in reducing uranine concentration, delaying uranine transport during the TTLT, and causing a different distribution pattern for breakthrough at A1 relative to conductivity (e.g., compare Figures 42A-D and 49A-D).

Cross-Hole Radar

The schedule of cross-hole radar measurements prior to, during, and after the TTLT is given in Appendix 5. Results from cross-hole radar measurements during the TTLT will be given in Knoll (in prep.). Figures 62-63 show level run results which demonstrate the ability of radar methods to detect changes from background with time-lapse measurements across two planes (B4-B2 plane and B4-B1 with A1 in the middle) during the TTLT at the BHRS in 2001.

TEST RESTART 2002

Follow-up testing was conducted because of the failure of eight of 14 of the prototype fiber-optic transducers to accurately measure head changes during the TTLT in 2001 in isolated zones in well

A1 and the B wells (Figures 36-37). Such data are important for hydrologic model calibration and provide direct information on aquifer heterogeneity. New fiber-optic transducers with a modified design were placed in 33 isolated zones (Figure 25) for a Test Restart (i.e., re-enactment of significant events and pumping configurations of the TTLT) that was run in June, 2002.

The following TTLT events and configurations were re-enacted in 2002: (a) the initial injection into B3 and change to pumping from B6; (b) periods without pumping to match power-outages and radar tomography between wells B3 and B6; (c) pumping at both 5 gpm and 26 gpm from B6; and (d) running a peristaltic pump at rates of 5 ml/min and 30 ml/min from 10 zones in A1. Also, the Test Restart provided the opportunity to collect water samples from 10 zones to see if residual concentrations of tracers (bromide and uranine) remained in the aquifer 10 months after the TTLT ended.

The sequence of activities for the Test Restart is given in Appendix 6. Injection and pumping rates, and head changes in A1 and B wells are shown in Figures 64-70. Supporting data for absolute-pressure fiber-optic transducers (i.e., atmospheric pressure) are given in Figure 71. Head changes in C wells and the Boise River are given in Figure 72; discharge rates from Lucky Peak Dam to the Boise River and from the Boise River to the New York Canal nearby upstream from the BHRS are given in Figure 73. Head changes in three X wells are given in Figure 74. Natural hydraulic gradients at the BHRS (e.g., Figure 5) were similar for both the TTLT in 2001 and the Test Restart in 2002, although the ambient depth to water was approximately 0.3 m shallower across the BHRS during the TTLT in 2001 than during the Test Restart in 2002.

PRELIMINARY RESULTS

Data from 22 of the 33 new fiber-optic transducers (Table 4) provide high-quality data at isolated zones for model calibration (compared with six of the original 14 during the TTLT). The 22 operating locations include: six in A1, two in B1, four in B2, three in B4, four in B5, and three in B6 (Figure 25). Care was taken to collect data at high frequency sampling rates at each change in pumping rate including changes from pumping to non-pumping, initiation of pumping after non-pumping, and change in pumping rate. Resulting head-change sequences are highly resolved (Figures 65-70). As with head change measurements during the TTLT in 2001, pronounced diurnal secular head changes overprint much of the test in 2002 (Figures 65-70, 72 and 74); these changes are due principally to evapotranspiration at the BHRS (Johnson and Barrash, unpubl. data). Flow and head data from different segments of the Test Restart will be used for numerical flow model calibration and verification.

Water samples were collected from 10 zones with tubing to the peristaltic pump (Figure 25) to measure residual presence of tracers. Conductivity values were at or lower than background values prior to the TTLT in 2001 (compare Table 5 and Figures 42-44), and uranine values were comparable to the lowest measured values during the TTLT (compare Table 5 and Figures 49-51).

SUMMARY

1. A tracer/time-lapse radar imaging test (TTLT) was conducted in a heterogeneous fluvial aquifer at the Boise Hydrogeophysical Research Site (BHRS) between August 1-18, 2001 to demonstrate, evaluate, and improve the capability to image temporal and spatial changes in an electrically conductive plume during a tracer test, and to provide quantitative results for geophysical, hydrologic, and combined hydrologic and geophysical modeling of plume detection, plume evolution, and permeability heterogeneity.

2. Custom in-well equipment was designed with and manufactured by collaborators at Michigan State University to allow: (a) simultaneous logging with radar instruments for cross-hole imaging and collection of water samples and head-change measurements from isolated zones in the same wells; and (b) collection of high-resolution water chemistry samples and head-change data in the middle region of two tomographic planes for quantitative calibration of attenuation differences detected by radar tomography.

3. Pre-test flow and transport modeling with generalized aquifer parameter estimates, and better-known topography on hydrostratigraphic contacts, was run to help select a pumping rate at withdrawal well B6 that would assure passage of the tracer plume through A1 with limited distortion of the plume up-gradient of well A1, and with complete breakthrough at A1 within two weeks. The modeling indicated that differences in hydraulic parameters and topography on hydrostratigraphic unit surfaces have significant influence on plume evolution and progressive breakthrough distribution in zones in A1, including: (a) earlier breakthrough in the lower zones; (b) extended breakthrough in Unit 2; and (c) limited and delayed breakthrough in Unit 3 with almost no breakthrough in the upper zones in A1.

4. Two tracers were used for the TTLT that were believed to be conservative tracers: (a) bromide, an electrically conductive inorganic salt; and (b) uranine, an organic fluorescent dye. These two tracers were injected into a 4-m thick interval in well B3 spanning the contact between two hydrostratigraphic units having differences in porosity and permeability. Bromide concentration and injection volume were designed to start with and evolve into combined concentration and dimension characteristics that would be detectable and resolvable by radar tomography through rising, peak, and declining conductivity (bromide concentrations) at A1.

5. Chemical results on conductivity at about 50 locations were available on sample runs approximately every four hours during the TTLT to provide near-realtime feedback on breakthrough behavior. Follow-up QA/QC evaluation indicates that field measurements of conductivity and uranine were accurate and repeatable.

6. Although the main breakthrough with conductivity at A1 occurred several days later than predicted with pre-test modeling, other plume evolution features occurred including: (a) initial breakthrough in the lower zones of A1; (b) primary and extended breakthrough in Unit 2; (c) limited and later breakthrough in Unit 3; and (d) virtually no breakthrough at the top zones in A1. Differences in detail, including an early injection peak at A1 and all B wells and a second main

breakthrough peak, should provide valuable information about heterogeneity in the investigated volume.

7. Level runs across the plume path prior to and during plume passage exhibit clear differences associated with the absence or presence of a conductivity anomaly.

8. The behavior of the second tracer, uranine (organic fluorescent dye), was not conservative and differed considerably from that of bromide or its proxy, conductivity. In particular, relative to conductivity, uranine exhibited: (a) significantly less relative concentration at breakthrough in A1; (b) significantly delayed breakthrough at A1; and (c) somewhat different breakthrough pattern at A1.

9. Follow-up investigation suggests that the cause(s) for the non-conservative uranine behavior may be biological and/or microbiological activity associated with cottonwood roots in the aquifer.

10. Operational problems (long and short power outages) interrupted pumping and data collection with some head-change and flow measurement and recording systems. Prototype fiber-optic transducers permitted data collection from 14 zones in A1 and B wells through small-diameter access tubes, but software and hardware stability problems resulted in additional data gaps and a significant number of unreliable channels.

11. A follow-up field test was conducted in June, 2002 to recreate the start and various pumping and recovery conditions of the TTLT in order to capture head-change information at numerous zones with more-stable fiber-optic transducers. Review of data indicates that high-quality head-change data were collected from 22 of 33 zones monitored in A1 and B wells with the newer version of fiber-optic transducers used for the Restart Test in 2002.

ACKNOWLEDGMENTS

This project is supported by EPA grant X-970085-01-0 and U.S. Army Research Office grant DAAH04-96-1-0318. Instruments and equipment acquired under grants from the U.S. Army Research Office (DAAD19-00-1-0105) and the Murdock Charitable Trust were used in support of this research. Identification of brand names for instruments is for identification purposes only and is not an endorsement for any brand by Boise State University or any of the project sponsors. Cooperative arrangements with the Idaho Transportation Department, the U.S. Bureau of Reclamation, and Ada County allow development and use of the BHRS and are gratefully acknowledged. Significant assistance has been provided by Drs Michael Knoll, William Clement, and Gary Weissmann, and by the following students and research assistants: Jason Broome, Marc Buursink, Frances Clark, Jessica Fox, Alex Gret, Clint Hughes, Tim Johnson, Linda Kenoyer, Carsten Leven, Aaron Marshall, Jay McMindes, Geoff Moret, James Nelson, Greg Oldenborger, Mike Procsal, J.D. Spalding, and Whitney Trainor. Tom Palazzolo provided significant assistance on the design and with the production of custom packer and port systems including log-through systems. Contribution no. 02-02 of the Center for Geophysical Investigation of the Shallow Subsurface at Boise State University.

REFERENCES CITED

Anderson, M.P., 1997, Characterization of geological heterogeneity, in Dagan, G. and Neuman, S.P., eds., Subsurface flow and transport: A stochastic approach: International Hydrology Series, UNESCO, Cambridge University Press, p. 23-43.

Barrash, W. and Clemo, T., 2000, Hierarchical geostatistics of porosity derived from neutron logs at the Boise Hydrogeophysical Research Site, Boise, Idaho: Proceedings of TraM'2000, Liege, Belgium, May 23-26, 2000, IAHS Publ. no. 262, p. 333-338.

Barrash, W. and Clemo, T., 2002, Hierarchical geostatistics and multifacies systems: Boise Hydrogeophysical Research Site, Boise, Idaho: Water Resources Research, v. 38, no. 10, 1196, doi:10.1029/2002WR001436, 2002.

Barrash, W. and Knoll, M.D., 1998, Design of research wellfield for calibrating geophysical measurements against hydrologic parameters: 1998 Conf. on Haz. Waste Res., Snowbird, UT., Great Plains/Rocky Mountains Haz. Substance Res. Ctr., Kans. St. Univ., p. 296-318.

Barrash, W. and Knoll, M.D., 2001, Quality Assurance Project Plan for Tracer/Time-Lapse Imaging Test at the Boise Hydrogeophysical Research Site: CGISS, Boise State University.

Barrash, W., Clemo, T., and Knoll, M.D., 1999, Boise Hydrogeophysical Research Site (BHRS): Objectives, design, initial geostatistical results: Proceedings of SAGEEP99, The Symposium on the Application of Geophysics to Engineering and Environmental Problems, March 14-18, 1999, Oakland, CA, p. 389-398.

Bosel, D., Herfort, M., Ptak, T., and Teutsch, G., 2000, Design, performance, evaluation and modeling of a natural gradient multitracer transport experiment in a contaminated heterogeneous porous aquifer, in Dassargues, A., ed., Tracers and modelling in hydrogeology: Proceedings of TraM'2000 Conference, May 2000, Liege, Belgium, IAHS Publication no. 262, p. 45-51.

Clement, W.P. and Knoll, M.D., 2000, Tomographic inversion of crosshole radar data; confidence in results: Proceedings of SAGEEP2000, The Symposium on the Application of Geophysics to Engineering and Environmental Problems, February, 2000, Arlington, VA, p. 553-562.

Clement, W.P., Knoll, M.D., Liberty, L.M., Donaldson, P.R., Michaels, P., Barrash, W., and Pelton, J.R., 1999, Geophysical surveys across the Boise Hydrogeophysical Research Site to determine geophysical parameters of a shallow, alluvial aquifer: Proceedings of SAGEEP99, The Symposium on the Application of Geophysics to Engineering and Environmental Problems, March 14-18, 1999, Oakland, CA, p. 399-408.

Dane, J.H. and Molz, F.J., 1991, Physical measurements in subsurface hydrology: Reviews of Geophysics, Supplement to v. 29, Pt. 1, U.S. National Report 1987-1990, p. 270-279.

Davis, S.N., Campbell, D.J., Bentley, H.W., and Flynn, T.J., 1985, Ground-water tracers: National Water Well Association, 200 p.

Day-Lewis, F.D., Hsieh, P.A., and Gorelick, S.M., 2000, Identifying fracture-zone geometry using simulated annealing and hydraulic-connection data: Water Resources Research, v. 36, no. 7, p. 1707-1722.

EPA (Environmental Protection Agency), 1999, Office of Research and Development Waste Research Strategy: Washington, DC, EPA/600/R-98/154.

Gelhar, L.W., 1997, Perspectives on field-scale application of stochastic subsurface hydrology, in Dagan, G. and Neuman, S.P., eds., Subsurface flow and transport: A stochastic approach: International Hydrology Series, UNESCO, Cambridge University Press, p. 157-176.

Hausrath, E.M., Barrash, W., and Reboulet, E.C., 2002, Water sampling and analysis for the Tracer/Time-Lapse Radar Imaging Test at the Boise Hydrogeophysical Research Site: Report to EPA for Grant X-970085-01-0 and to the U.S. Army Research Office for Grant DAAH04-96-1-0318, Center for Geophysical Investigation of the Shallow Subsurface Technical Report BSU CGISS 02-03, Boise State University, Boise, ID, 86 p.

Hyndman, D.W. and Gorelick, S.M., 1996, Estimating lithologic and transport properties in three dimensions using seismic and tracer data, Kesterson aquifer: Water Resources Research, v. 32, no. 9, p. 2659-2670.

Kass, W., 1998, Tracing technique in geohydrology: Rotterdam, A.A. Balkema, 581 p.

Knoll, M.D., in prep., Design, Operation, and Preliminary Results from Radar Methods for the Tracer/Time-Lapse Radar Imaging Test, 2001: Boise State University, BSU CGISS Technical Report 02-04.

Liberty, L.M., Clement, W.P., and Knoll, M.D., 1999, Surface and borehole seismic characterization of the Boise Hydrogeophysical Research Site: Proceedings of SAGEEP99, The Symposium on the Application of Geophysics to Engineering and Environmental Problems, March 14-18, 1999, Oakland, CA, p. 723-732.

Liberty, L.M., Clement, W.P., and Knoll, M.D., 2000, Crosswell seismic reflection imaging of a shallow cobble-and-sand aquifer: An example from the Boise Hydrogeophysical Research Site: Proceedings of SAGEEP2000, The Symposium on the Application of Geophysics to Engineering and Environmental Problems, February, 2000, Arlington, VA, p. 545-552.

McKenna, S.A. and Poeter, E.P., 1995, Field example of data fusion in site characterization: Water Resources Research, v. 31, p. 3229-3240.

Morin, R.H., LeBlanc, D.R., and Teasdale, W.E., 1988, A statistical evaluation of formation disturbance produced by well-casing installation methods: Ground Water, v. 26, p. 207-217.

Neuman, S.P., 1997, Stochastic approach to subsurface flow and transport: A view to the future, in Dagan, G. and Neuman, S.P., eds., Subsurface flow and transport: A stochastic approach: International Hydrology Series, UNESCO, Cambridge University Press, p. 231-241.

Peretti, W.R., Knoll, M.D., Barrash, W., Clement, W.P., and Reboulet, E.C., 2000, Radar stratigraphy, lithostratigraphy, and hydrostratigraphy of coarse fluvial deposits at the Boise Hydrogeophysical Research Site (abs.): Geological Society of America Annual Meeting, November 13-16, 2000, Reno, NV, Abstracts with Programs, v. 32, no. 7, p. A410.

Peretti, W.R., Knoll, M.D., Clement, W.P., and Barrash, W., 1999, 3-D GPR imaging of complex fluvial stratigraphy at the Boise Hydrogeophysical Research Site: Proceedings of SAGEEP99, The Symposium on the Application of Geophysics to Engineering and Environmental Problems, March 14-18, 1999, Oakland, CA, p. 555-564.

Peterson, J.E., Majer, E.L., and Knoll, M.D., 1999, Hydrogeologic property estimation using tomographic data at the Boise Hydrogeophysical Research Site: Proceedings of SAGEEP99, The Symposium on the Application of Geophysics to Engineering and Environmental Problems, March 14-18, 1999, Oakland, CA, p. 629-638.

Purvance, D.T. and Barrash, W., 2000, The electrical-hydraulic conductivity correlation observed at the Boise Hydrogeophysical Research Site (abs.): Spring AGU Meeting, May 30-June 3, 2000, Washington, DC, EOS, v. 81, no. 19, May 9, 2000 Supplement, p. S212.

Reboulet, E.C. and Barrash, W., 1999, Identification of hydrostratigraphic facies in coarse, unconsolidated, braided-stream deposits at the Boise Hydrogeophysical Research Site (abs.): Geol. Soc. Am. Ann. Mtg, October 25-29, 1999, Denver, CO, Abs. with Progr., v. 31, no. 7, p. A350.

Reboulet, E.C. and Barrash, W., 2000, Statistical analysis of grain-size distribution and porosity data from coarse braided-stream deposits at the Boise Hydrogeophysical Research Site (abs.): Geological Society of America Annual Meeting, November 13-16, 2000, Reno, NV, Abstracts with Programs, v. 32, no. 7, p. A410.

Rubin, Y., Mavko, G., and Copty, N., 1992, Mapping permeability in heterogeneous aquifers using hydrologic and seismic data: Water Resources Research, v. 28, p. 1809-1816.

Sudicky, E.A. and Huyakorn, P.S., 1991, Contaminant migration in imperfectly known heterogeneous groundwater systems: Reviews of Geophysics, Supplement to v. 29, Pt. 1, U.S. National Report 1987-1990, p. 240-253.

Vakhmistrov, D.B. and Zlotnikova, I.F., 1990, Functional specificity of root hairs: Fiziologiya Rastenii (Transl., Plenum Publ. Corp.), v. 37, no. 5, p. 946-954.

Table 1. Well locations at the BHRS

well	x coord meters	y coord meters	distance (m) from B3	azimuth (radians from east=0 degr)	distance (m) from B	azimuth (radians from east=0 degr)
A1	0	0	4.18	5.749	2.93	1.602
B1	- 0.09	2.93	6.26	5.342	2.66	3.735
B2	3.03	1.76	3.93	4.858	5.34	3.202
B3	3.60	- 2.13	---	---	6.90	5.739
B4	0.07	- 2.64	3.57	0.143	4.72	5.239
B5	- 3.18	- 1.71	6.79	6.221	3.27	4.44
B6	- 2.30	1.44	6.90	5.739	---	---
C1	3.63	6.39	8.52	1.567	7.72	0.696
C2	8.17	0.05	5.06	0.445	10.56	6.151
C3	3.47	- 6.22	4.09	4.681	9.59	5.358
C4	- 4.84	- 8.46	10.55	3.785	10.22	4.461
C5	- 9.12	0.27	12.94	2.955	6.92	3.311
C6	- 4.14	7.26	12.17	2.26	6.10	1.877
X1	6.66	39.69	41.93	1.498	39.28	1.341
X2	29.88	- 3.02	26.29	6.249	32.49	6.145
X3	17.16	-36.23	36.70	5.091	42.4	5.189
X4	-14.11	-17.01	23.13	3.84	21.91	4.143
X5	-36.94	23.22	47.81	2.583	40.92	2.58

Table 2. Input parameter values for pre-test flow and transport modeling.

Unit	Kh cm/s	Kz cm/s	Porosity	Ss m^{-1}	Sy	Longitudinal Dispersivity m	Lateral Dispersivity m
5	2.	1.	.43	E-4	.385	.03	.015
4	.08	.04	.23	E-4	---	.03	.015
3	.02	.01	.17	E-4	---	.03	.015
2	.08	.04	.24	E-4	---	.03	.015
1	.02	.01	.18	E-4	---	.03	.015

Table 3. Locations of packers and packed-off intervals

Well(s)	Midpoint* of packer string	Packed-off intervals
A1	mid-packer of 11th packer from bottom (i.e., packer between zones 10 and 11)	.25 m between packer centers; 20 zones total
B1, B2, B4, B5, B6**	mid-packer of 4th packer from bottom (i.e., packer between zones 3 and 4) Note: *lowest zone is zone 0* for these wells)	1 m between packer centers; 7 zones total
B3	center of 4 m straddled zone (between packers) 1 zone total	4 m continuous zone; holes in pipe

* Packer locations midpoint elevation: ft AMSL = 2752.87, m AMSL = 839.075

** Note: Zones 2, 3, 4, 5 have holes for pumping

Table 4. Fiber-optic transducer locations and performance ratings for the TTLT Restart Test in 2002

Well and Zone	Performance Rating
A1-1	Bad
A1-2	Good
A1-4	Good
A1-6	Good
A1-8	Bad
A1-10	Good
A1-12	Bad
A1-15	Good until drift at late time
A1-17	Good until shift at late time
A1-19	Bad
B1-1	Good
B1-2	Good
B1-3	Bad
B1-5	Bad
B1-6	Bad
B2-1	Bad
B2-2	Good
B2-3	Good
B2-5	Good
B2-6	Good
B4-1	Bad
B4-2	Bad
B4-3	Bad
B4-5	Good
B4-6	Good
B5-1	Good
B5-2	Good
B5-3	Bad
B5-5	Good
B5-6	Good
B6-1	Good ????
B6-3	Good ????
B6-6	Good ????

Table 5. Water sample analyses for conductivity and uranine during the TTLT Restart Test in 2002

Sample Location	Conductivity uS/cm	Water Temp. °C	Corrected Conductivity uS/cm	Uranine ppb: low	Uranine ppb: high	Uranine ppb: ave
A1-2	200	22.5	210.5	0.024	0.027	0.0255
A1-6	200	22.6	210.1	0.049	0.051	0.05
A1-6 QC	199	22.6	209	0.052	0.054	0.053
A1-9	196	22.2	207.6	0.055	0.057	0.056
A1-13	191	22.7	200.2	0.076	0.078	0.077
A1-15	192	22.7	201.3	0.108	0.111	0.1095
A1-19	188	22.4	198.3	0.097	0.1	0.0985
B1-2	184	22.3	194.5	0.011	0.013	0.012
B1-5	166	22.6	174.4	0.01	0.011	0.0105
B2-2	155	22.7	162.5	0.006	0.007	0.0065
B2-5	161	22.5	169.5	0.017	0.019	0.018
Discharge	193	22.8	201.9	0.034	0.034	0.034
Disch QC	193	22.7	202.3	0.045	0.047	0.046

Samples collected ~0825 hr on June 19, 2002

Samples analyzed on June 19, 2002 between 1105 hr and 1149 hr for uranine and between 1309 hr and 1346 hr for conductivity

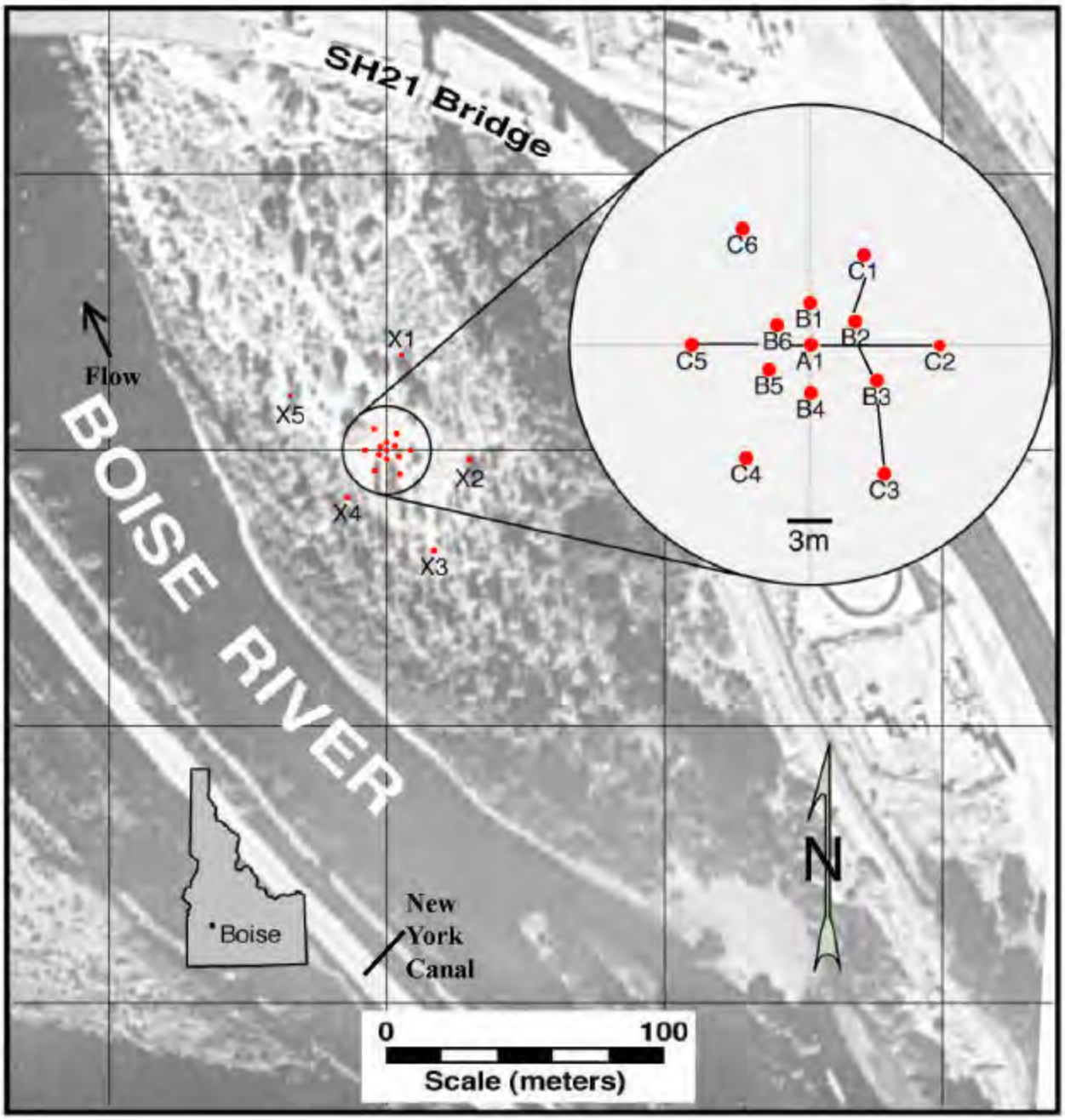

Figure 1. Air photo showing location of the Boise Hydrogeophysical Research Site and wells at the site; inset shows wells of central area and cross-sections used in Figure 4.

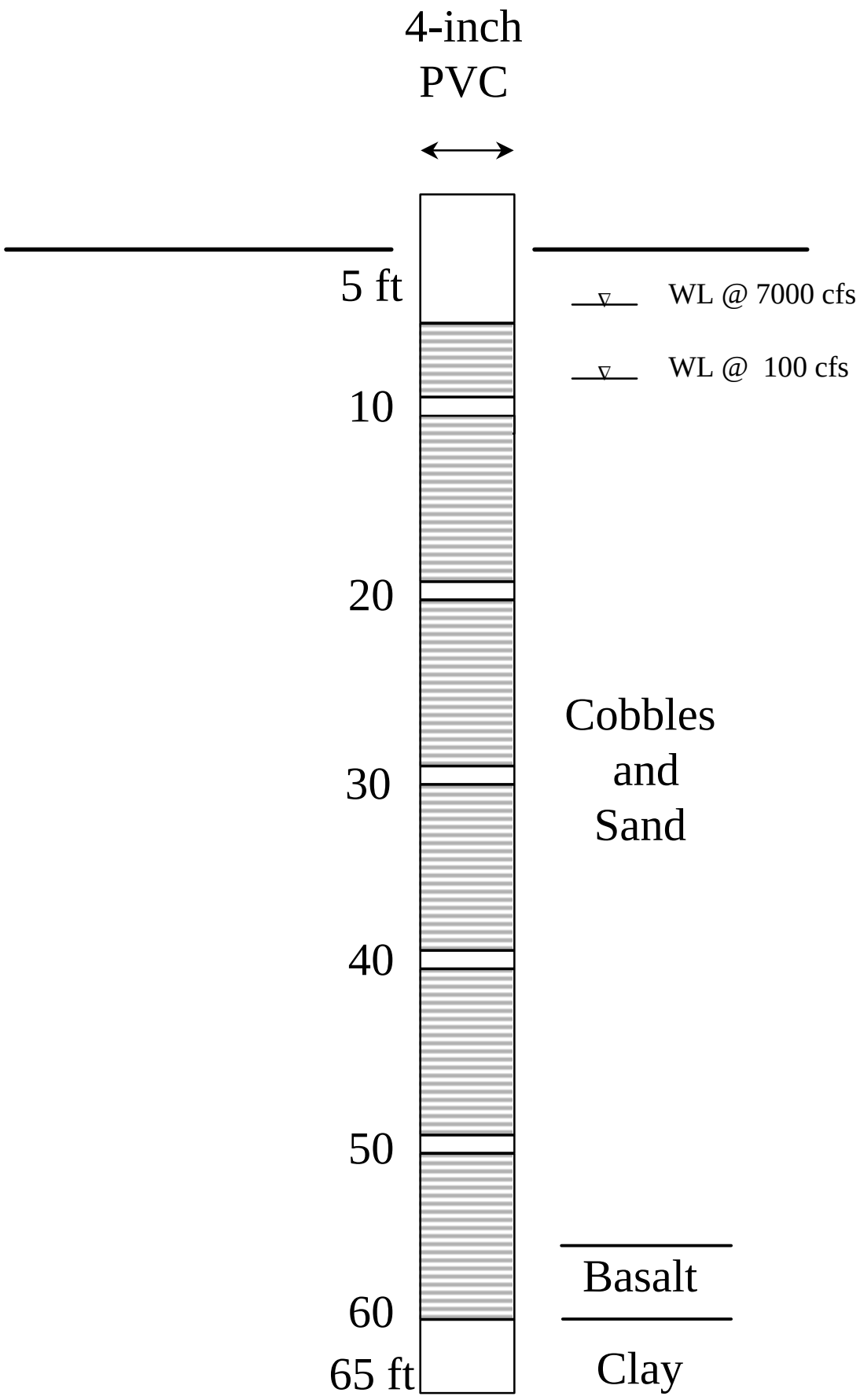

Figure 2. Schematic diagram of well construction, and generalized stratigraphy at the BHRS.

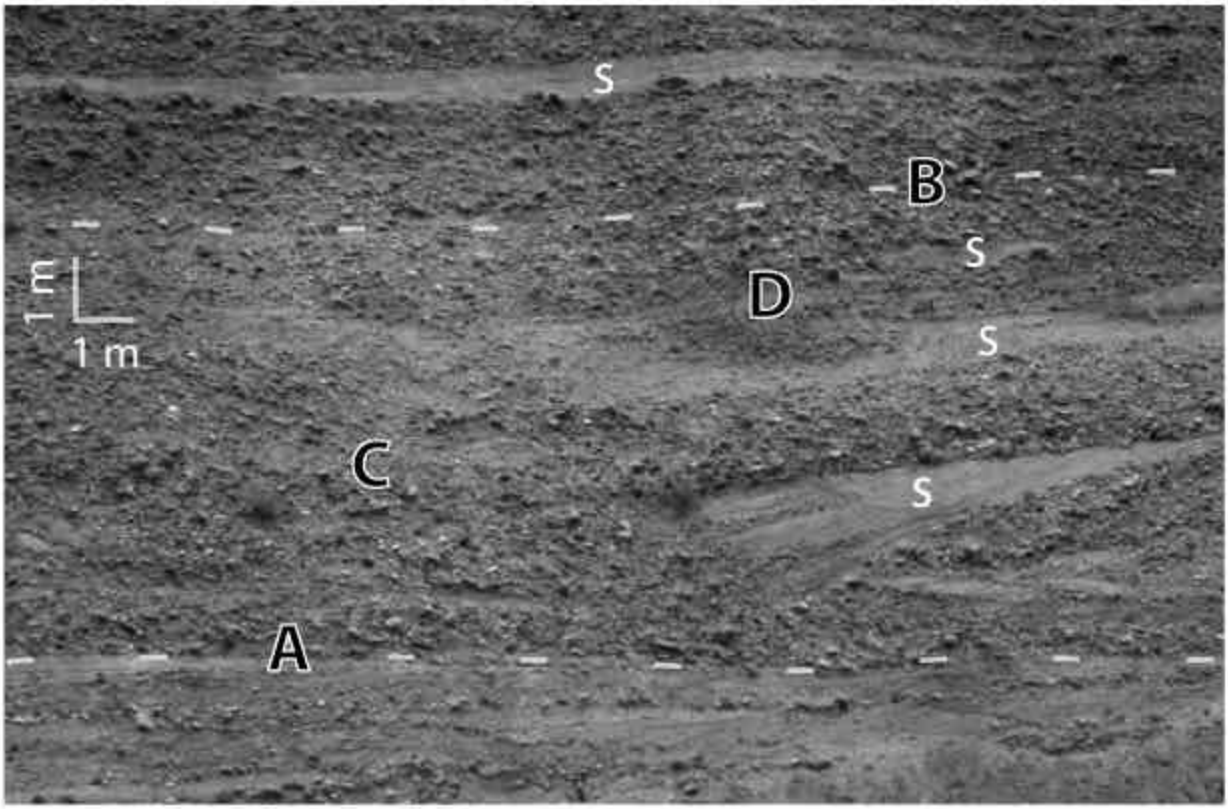

Figure 3. Photograph of coarse fluvial deposits in road cut 2.5 km upriver from the BHRS. Laterally persistent bounding surfaces (A and B) can be identified in addition to both gradual (e.g., C) and abrupt (e.g., D) changes of sedimentary structure and texture within the unit between bounding surfaces A and B. Note predominance of cobble-size framework clasts overall, but also the presence of distributed sand bodies (s), and sand-dominated unit below bounding surface A.

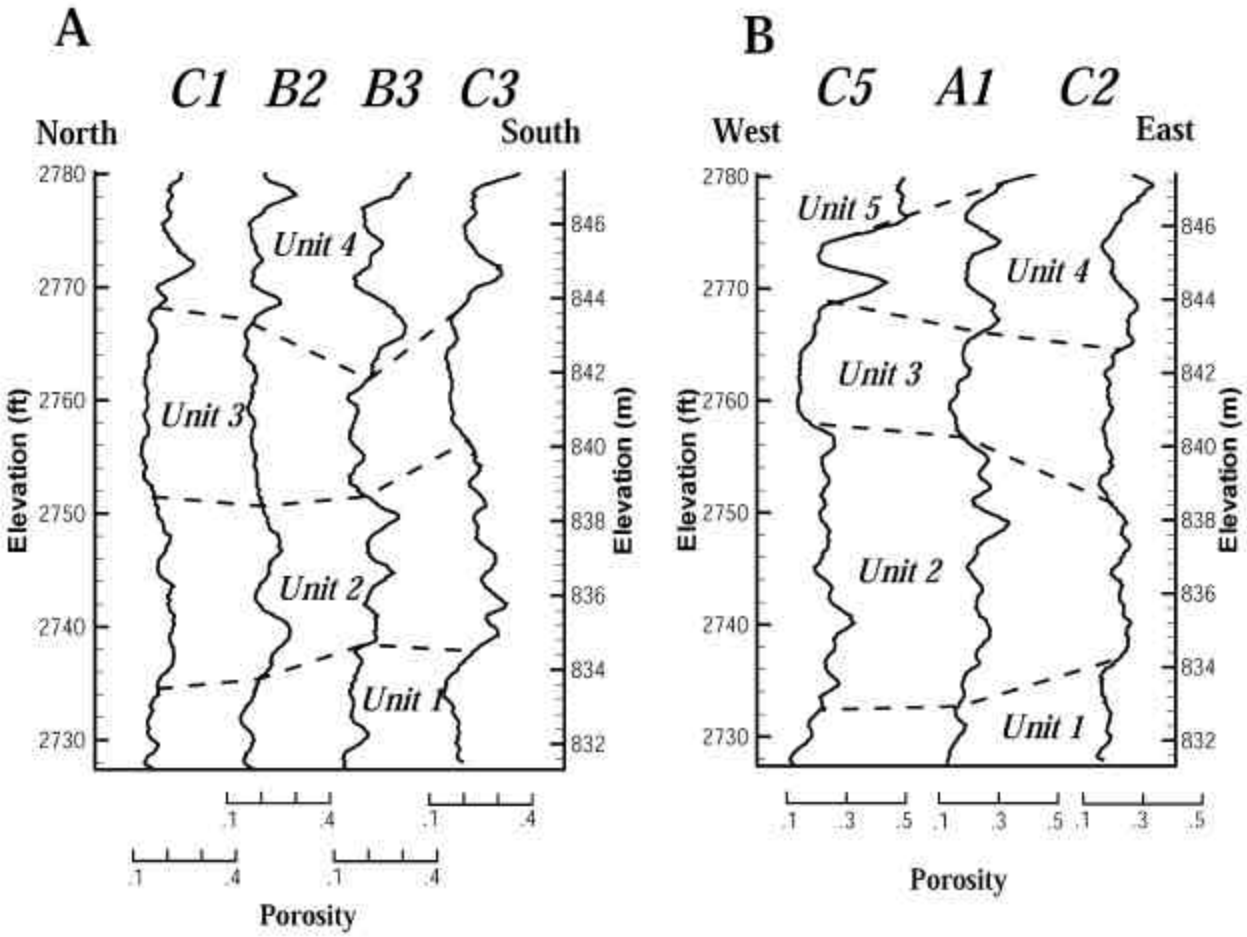

Figure 4. Stratigraphy at the BHRS interpreted from porosity logs. A. Porosity logs from water table to base of fluvial deposits. Orientation is in general direction of river flow. (See inset location map in Figure 1). Relative horizontal well positions not to scale. Units 1-4 are cobble-dominated units; Unit 5 is channel sand. B. Porosity logs from water table to base of fluvial deposits. Orientation is perpendicular to general direction of river flow (Figure 1). Channel sand thickens toward river and pinches out near center of wellfield.

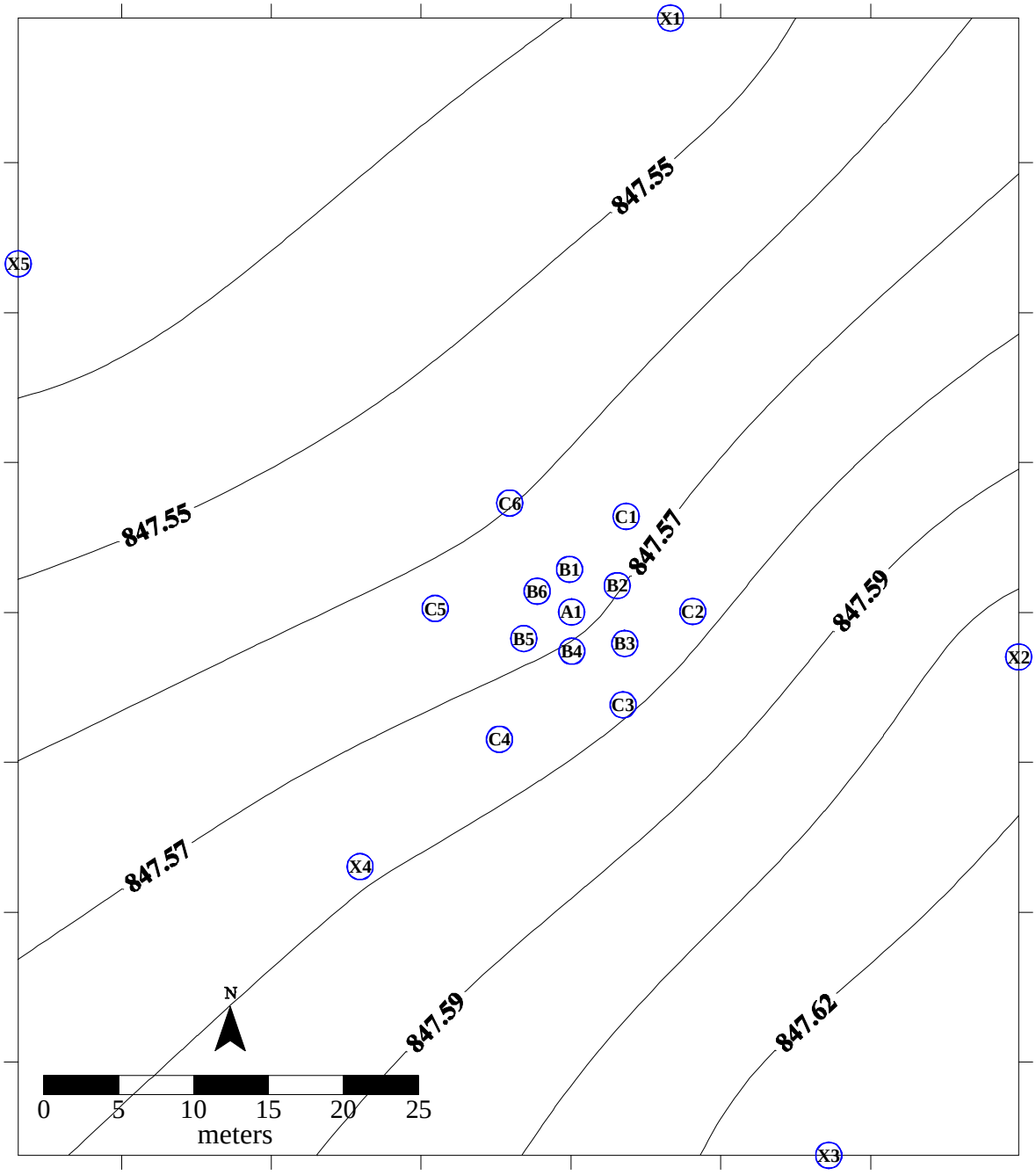

Figure 5. Water-level contours for the aquifer at the BHRS during summer season.

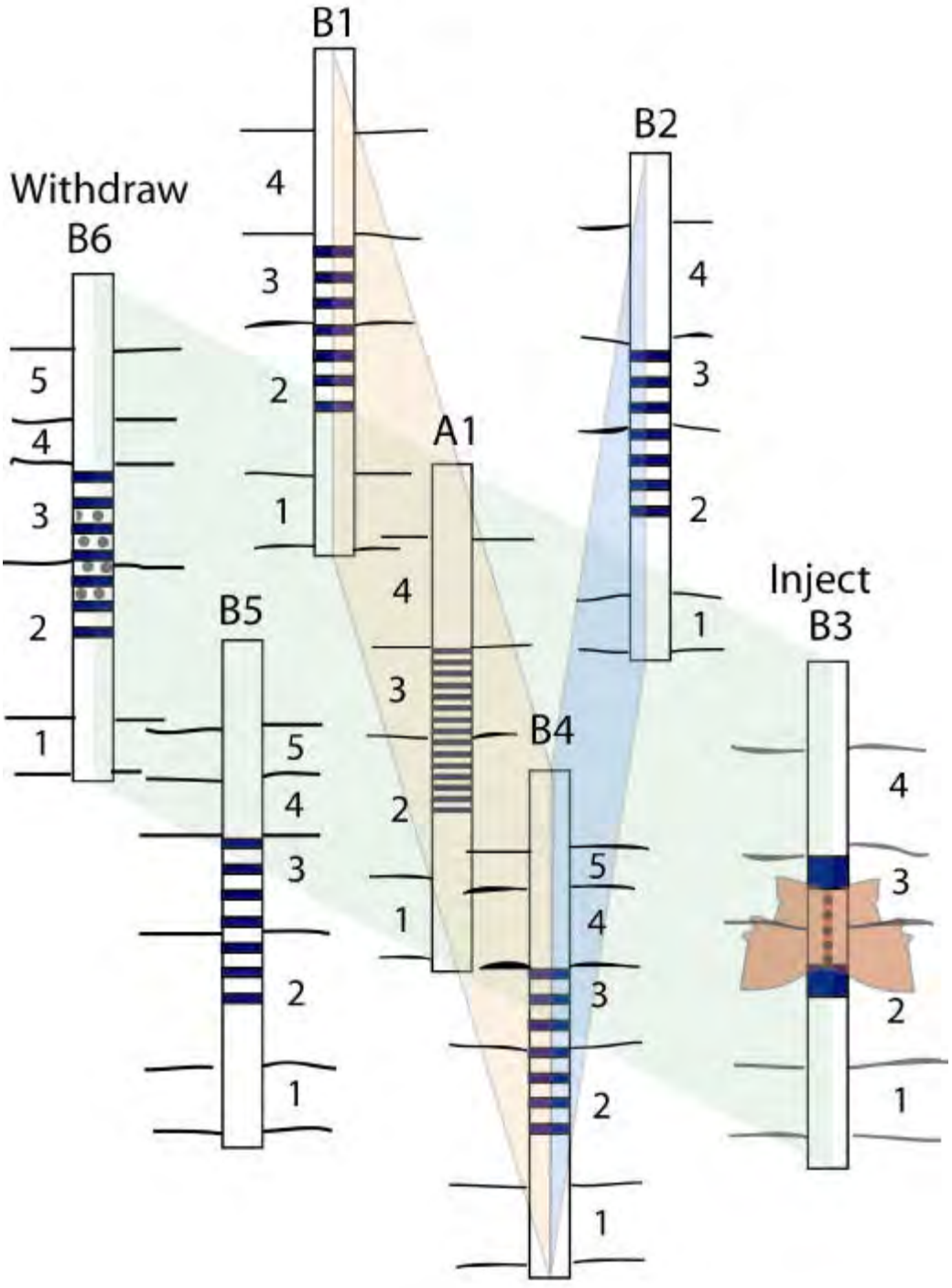

Figure 6. Schematic diagram of initial concept for tracer test with time-lapse radar tomographic imaging at the BHRS. Tracers injected into 4-m interval spanning contact between Units 2 and 3 at well B3. Natural gradient is along line between wells B3 and B6. Two cross-flow tomographic planes and a plane along the flow path for time-lapse monitoring of plume evolution. One cross-flow plane and the plane along the flow path pass through well A1 with 20 ports for water chemistry sampling to calibrate radar attenuation tomography and transport modeling. Not to scale.

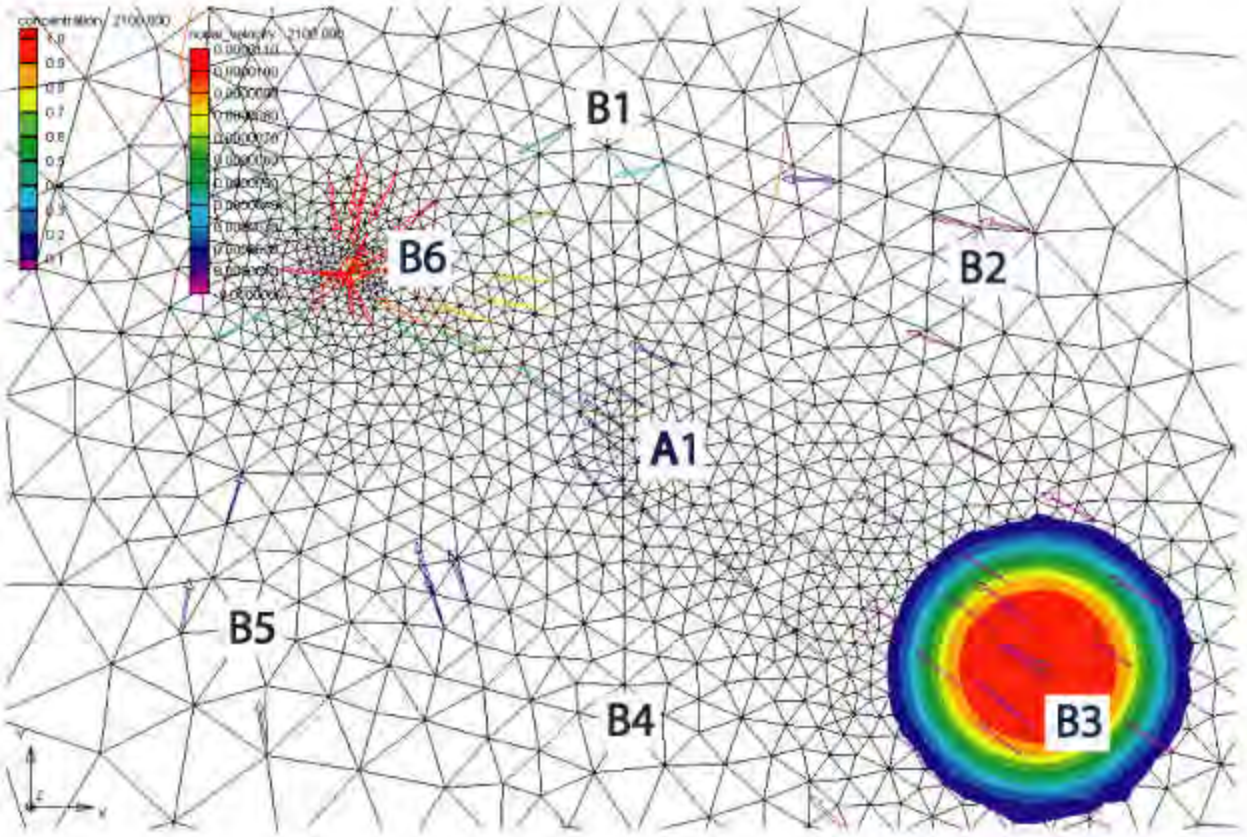

Figure 7. Plan view of pre-test 3D transport model with FEMWATER showing relative concentration distribution of bromide plume after injection for 35 minutes at 30 gpm (113.6 lpm) through 4-m vertical interval straddling the contact between Units 2 and 3 in well B3 (see Figure 8). Plane is at ~839.65 m elevation. Arrows indicate horizontal nodal velocities.

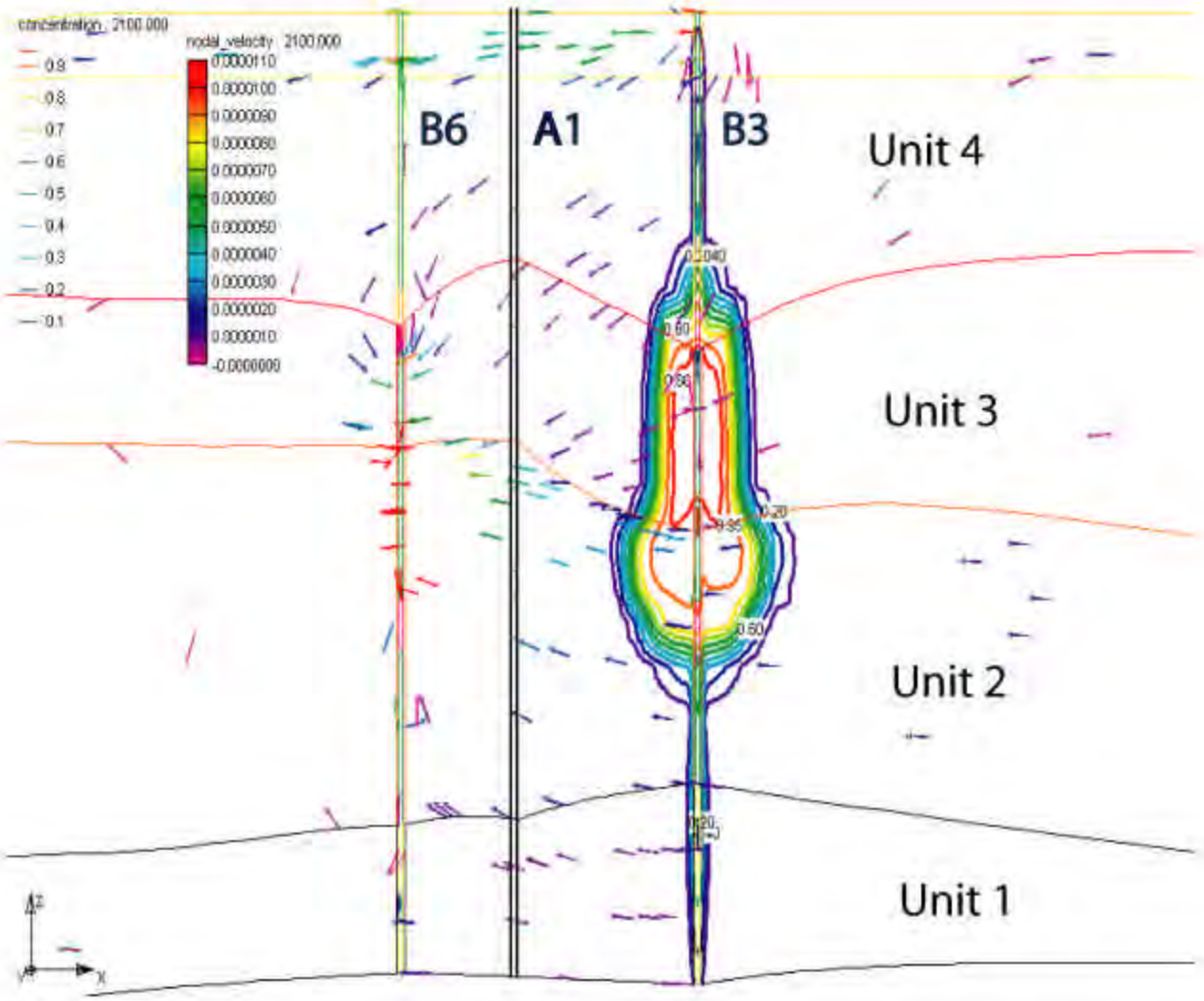

Figure 8. Cross-sectional view of pre-test 3D transport model with FEMWATER showing relative concentration distribution of bromide plume after injection for 35 minutes at 30 gpm (113.6 lpm) through 4-m vertical interval straddling the contact between Units 2 and 3 in well B3. Note smaller diameter in the upper portion of the plume in Unit 3 (lower permeability) than in the lower portion of the plume in Unit 2 (higher permeability). Also note topography on the unit contacts between wells (especially rise of contacts between Units 2 and 3 and between Units 3 and 4 from injection well B3 to well A1). Velocity arrows indicate nodal velocities; vertical components arise from partially penetrating pumping from well B6 (starting after injection stops) and from topography and permeability variation of units.

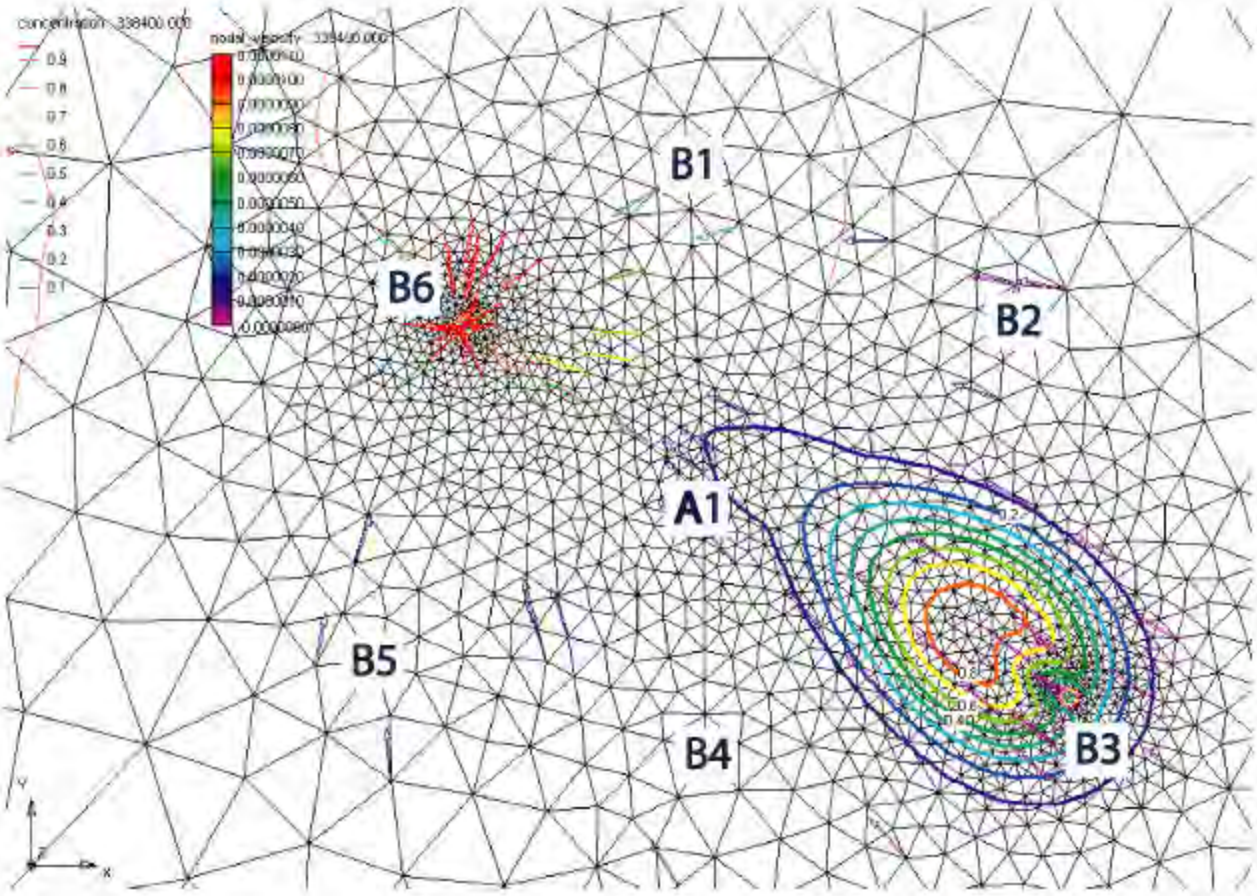

Figure 9. Plan view of pre-test 3D transport model with FEMWATER showing relative concentration distribution of bromide plume after ~3.7 days of pumping from B6 at 5 gpm (18.9 lpm). Note plane is at ~839.65 m elevation which is near the contact between Units 2 and 3, just above the lower, faster-moving portion of the plume (see Figure 10). Arrows indicate horizontal nodal velocities. Up-gradient portion of plume is largely past B3 and down-gradient portion of plume is beginning to be drawn out of well B6, but only from Unit 2. Shape of plume and orientations of velocity arrows illustrate horizontal component of flow is largely parallel between wells B3 and A1, but flow is more influenced by forced-gradient with convergent flow between wells A1 and B6.

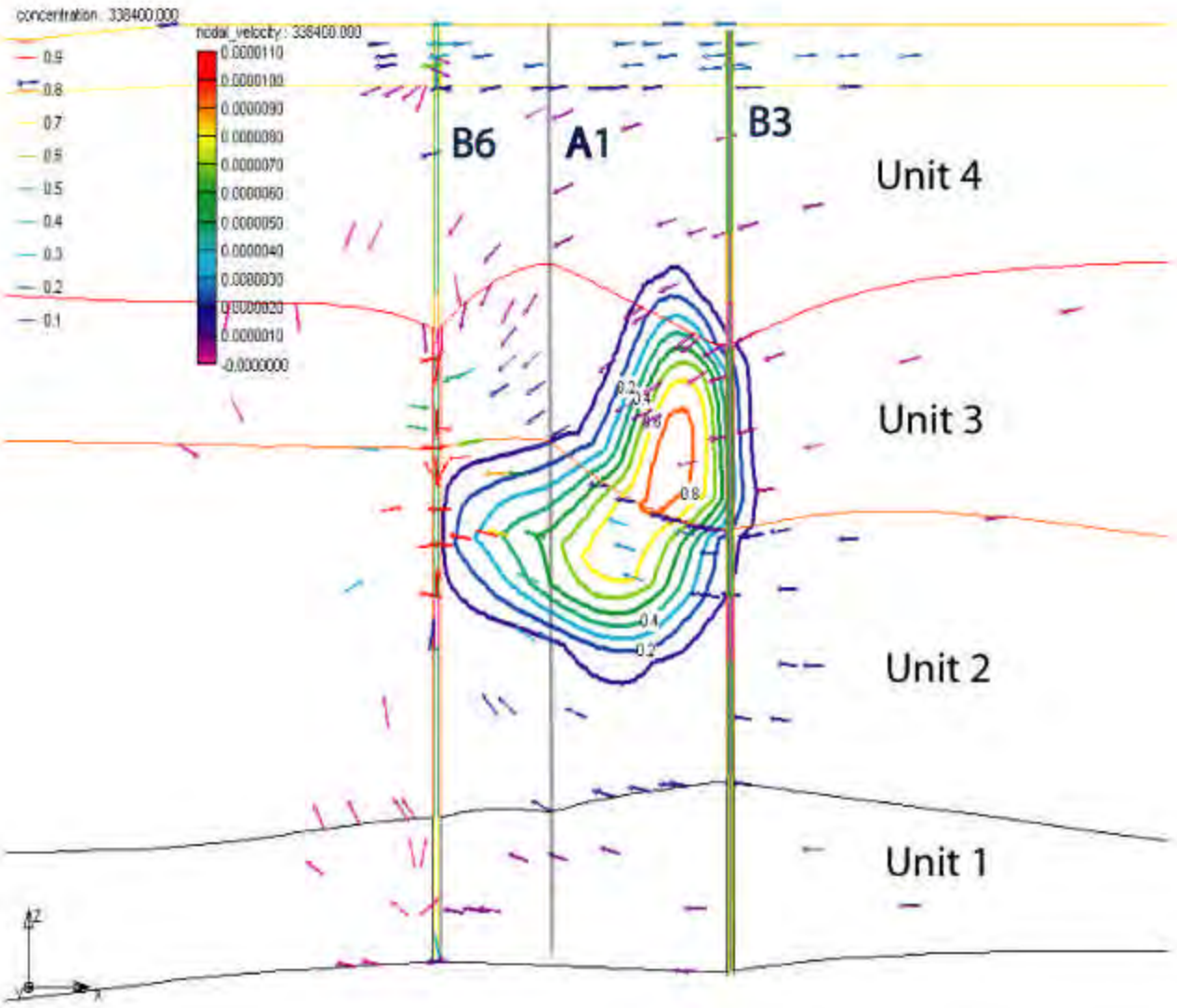

Figure 10. Cross-sectional view of pre-test 3D transport model with FEMWATER showing relative concentration distribution of bromide plume after ~3.7 days of pumping from B6 at 5 gpm (18.9 lpm). Plume is beginning to be drawn out of well B6 from Unit 2 only. Discharge at B6 and breakthrough at A1 are almost entirely in the lower half of 4-m (injection) interval at A1. Significant fraction of the plume traveling below the injection interval between wells B3 and A1. Slow-moving core of plume in Unit 3 is partially being drawn into Unit 2.

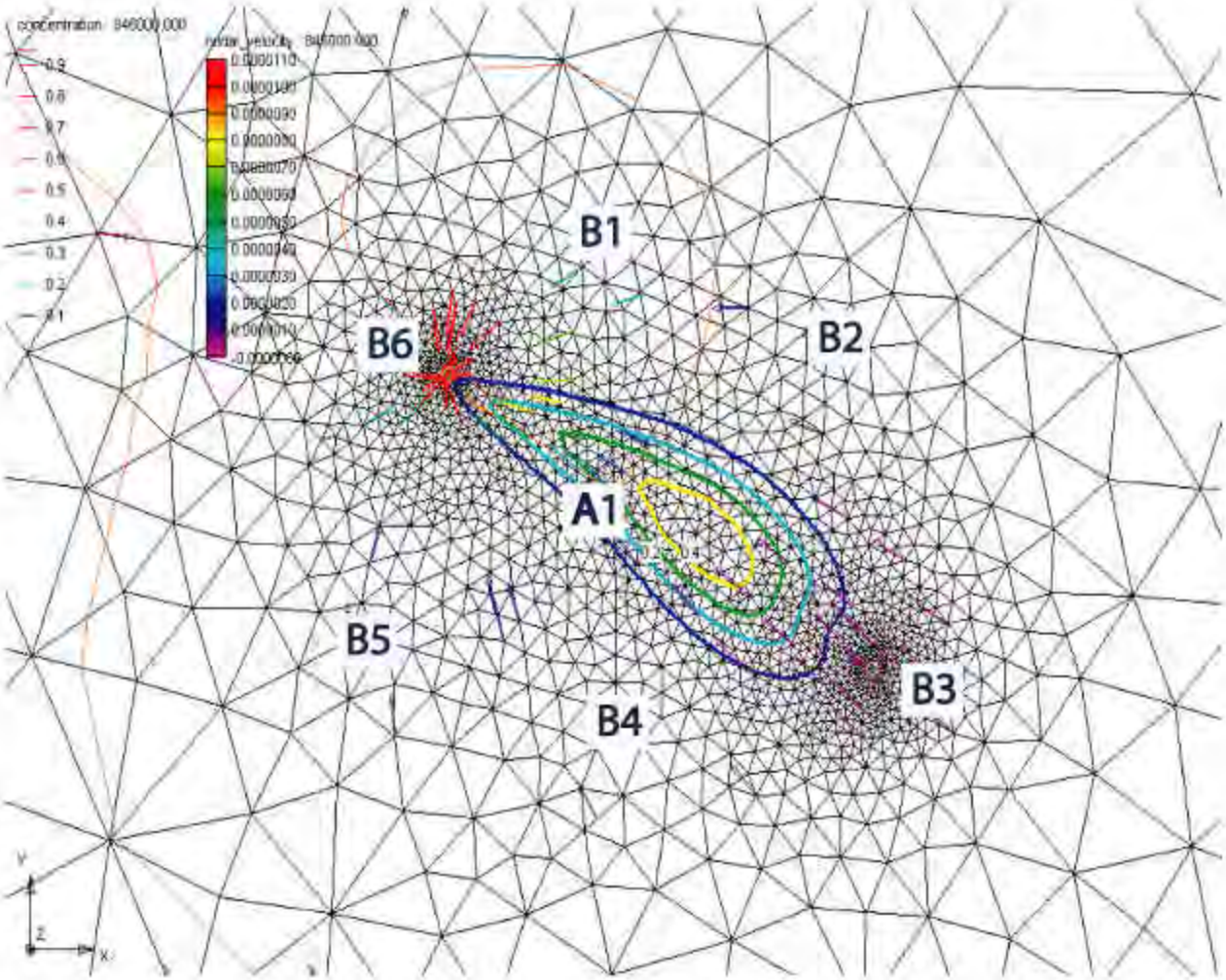

Figure 11. Plan view of pre-test 3D transport model with FEMWATER showing relative concentration distribution of bromide plume after ~9.8 days of pumping from B6 at 5 gpm (18.9 lpm). Note plane is at ~839.65 m elevation which is near the contact between Units 2 and 3, just above the lower, faster-moving portion of the plume (see Figure 12). Plume is fully past B3 and is being removed from B6 in both Units 2 and 3. Arrows indicate horizontal nodal velocities. Core of plume is approaching A1 in plane view; breakthrough in the lower portion of the injection interval in A1 is extended in time due to downward component of flow bringing additional tracer mass from Unit 3. Plume shape is not symmetrical due to topography on contact between Units 2 and 3.

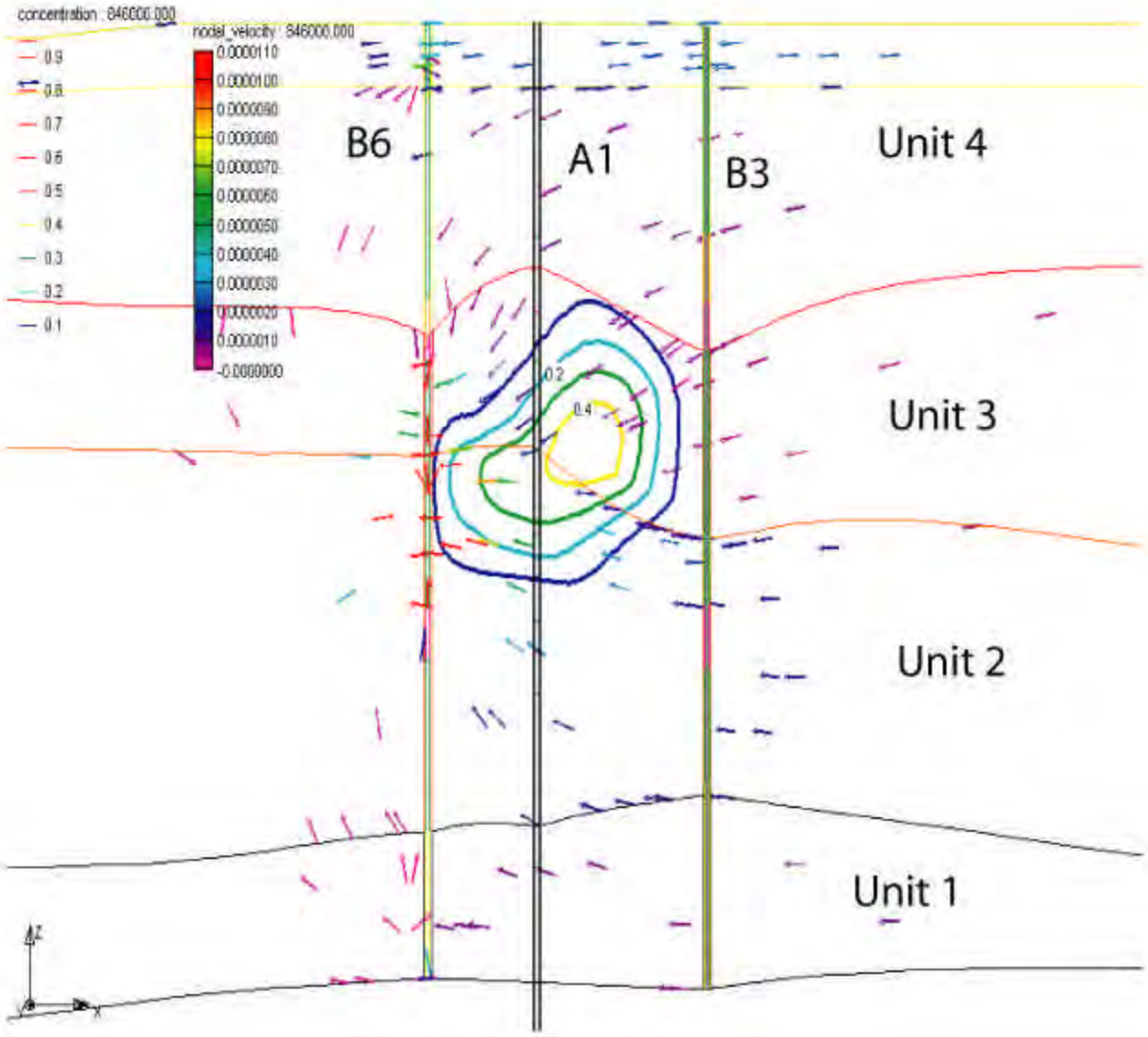

Figure 12. Cross-sectional view of pre-test 3D transport model with FEMWATER showing relative concentration distribution of bromide plume after ~9.8 days of pumping from B6 at 5 gpm (18.9 lpm). Plume is being drawn out of Unit 3 at well B6 in addition to Unit 2. Slow-moving core of plume in Unit 3 is largely being drawn into Unit 2. Core of plume passing through A1; breakthrough in the lower portion of the injection interval in A1 is extended in time due to the downward component of flow bringing additional tracer mass from Unit 3.

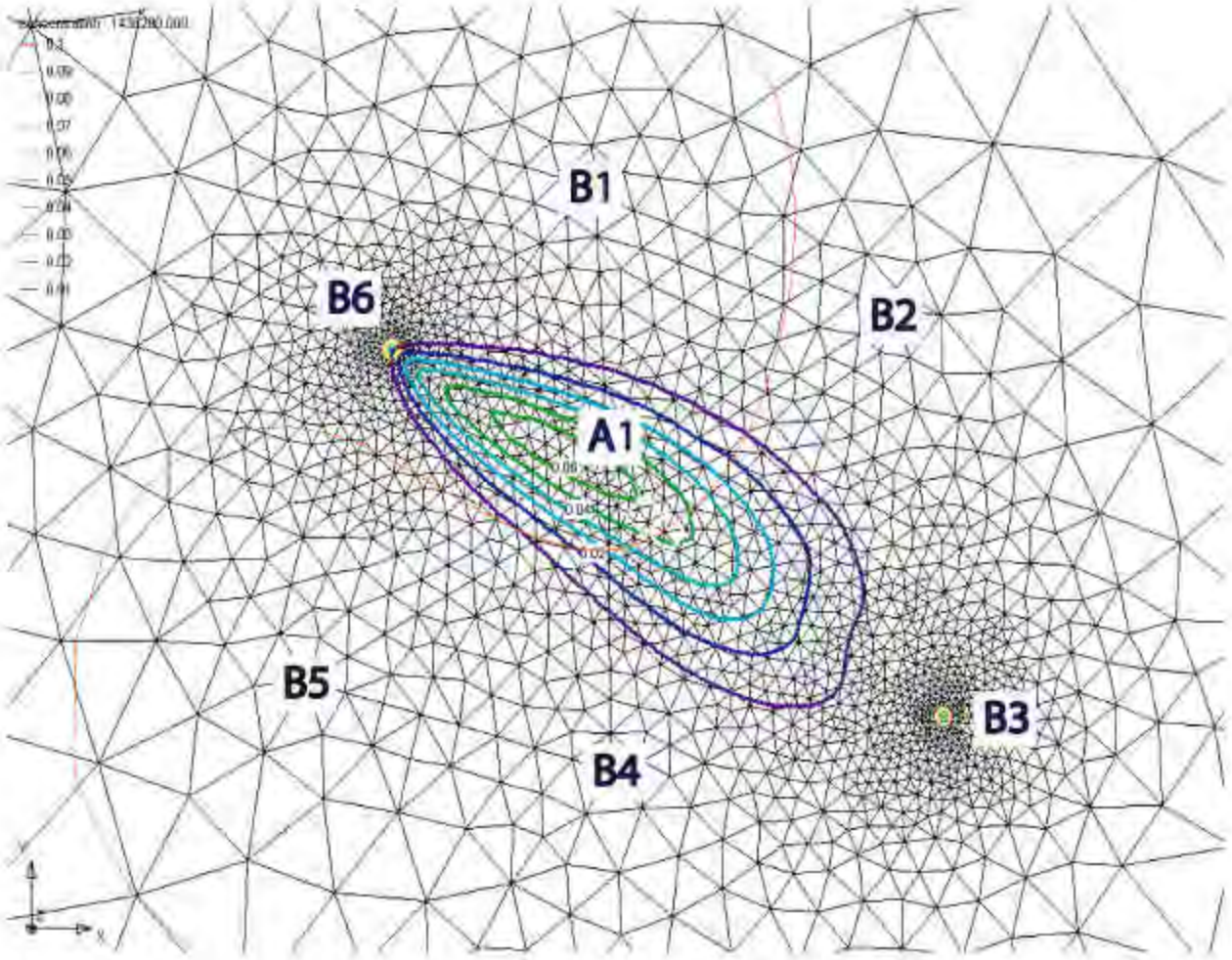

Figure 13. Plan view of pre-test 3D transport model with FEMWATER showing relative concentration distribution of bromide plume after ~16.6 days of pumping from B6 at 5 gpm (18.9 lpm). Note plane of mdel is at 839.65 m elevation which is near the contact between Units 2 and 3 (see Figure 14). Plume is elongated and converging, and is largely influenced by the forced-gradient due to pumping at B6.

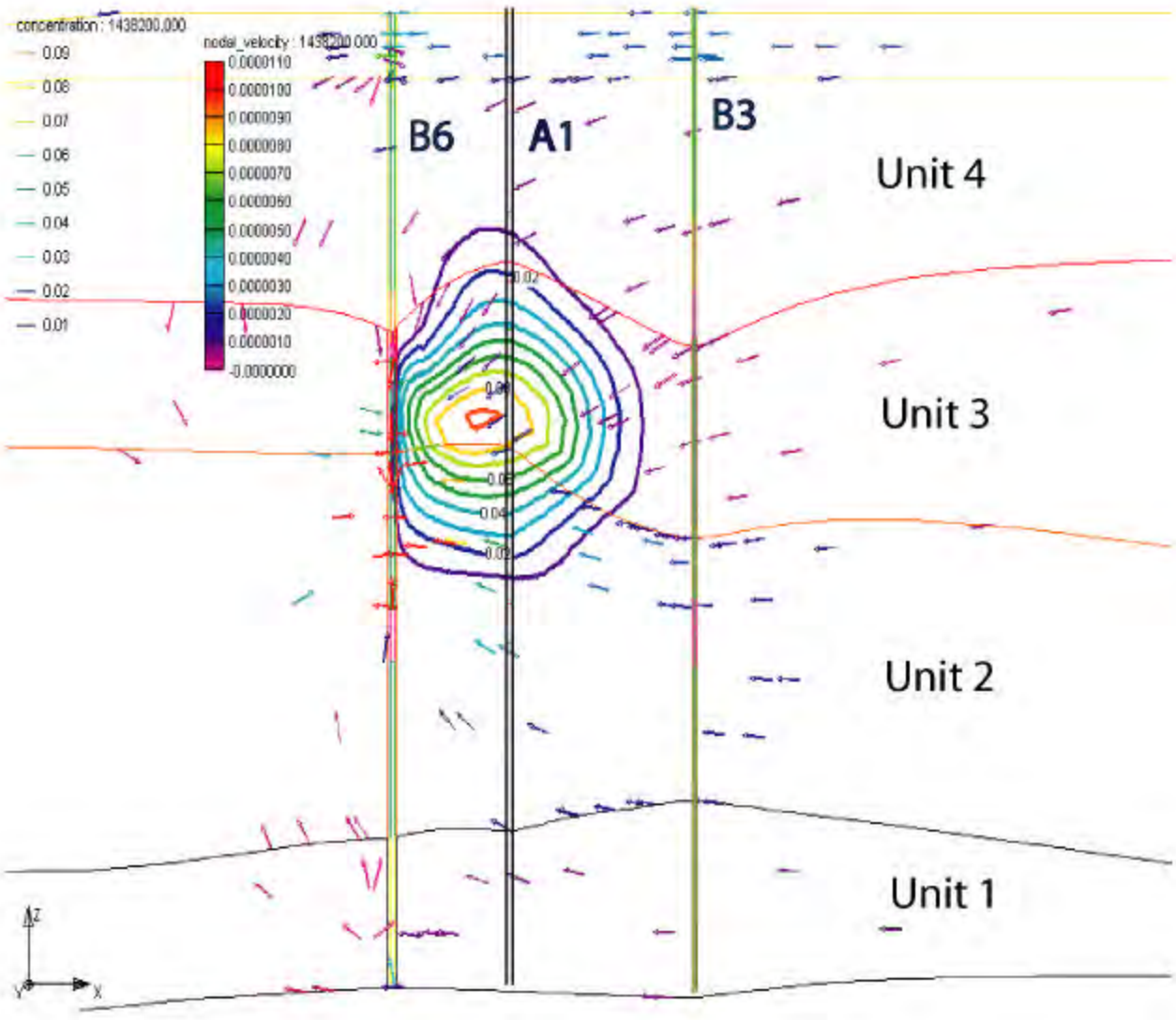

Figure 14. Cross-sectional view of pre-test 3D transport model with FEMWATER showing relative concentration distribution of bromide plume after ~16.6 days of pumping from B6 at 5 gpm (18.9 lpm). Plume is largely past A1.

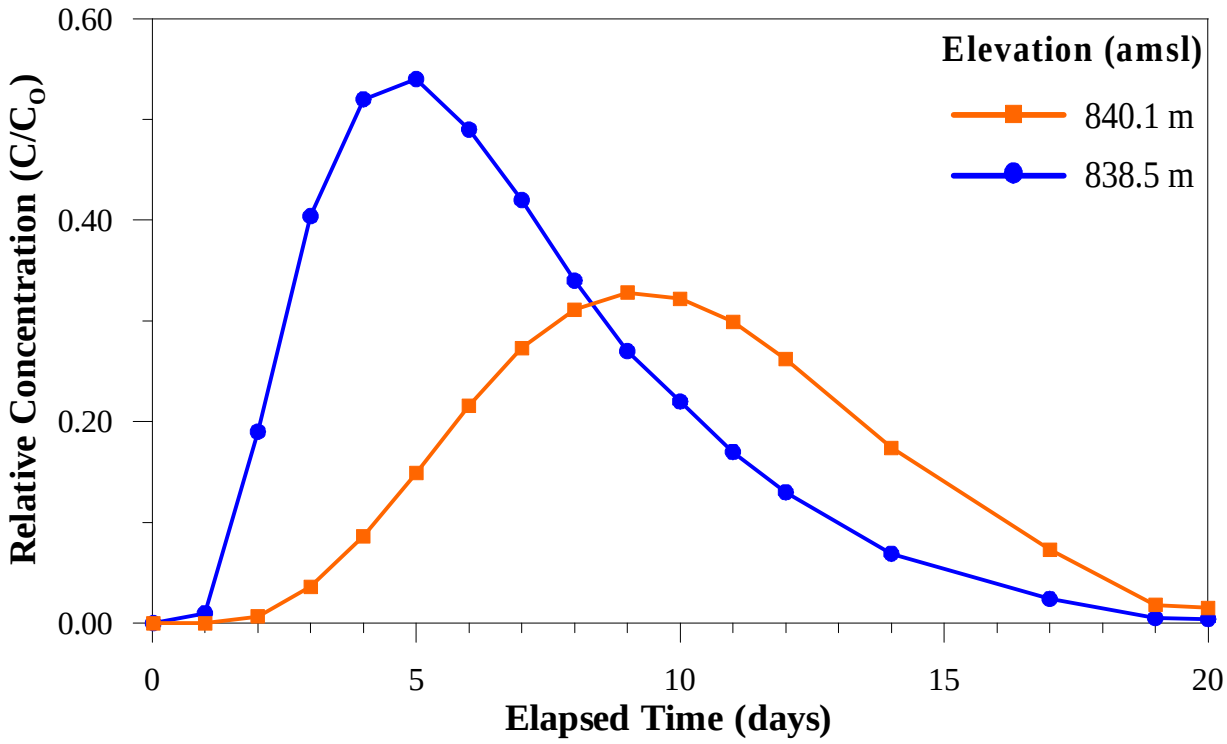

Figure 15. Model breakthrough curves of relative concentration of tracer at A1 at elevations near the plan view model section, which is close to the top of Unit 2.

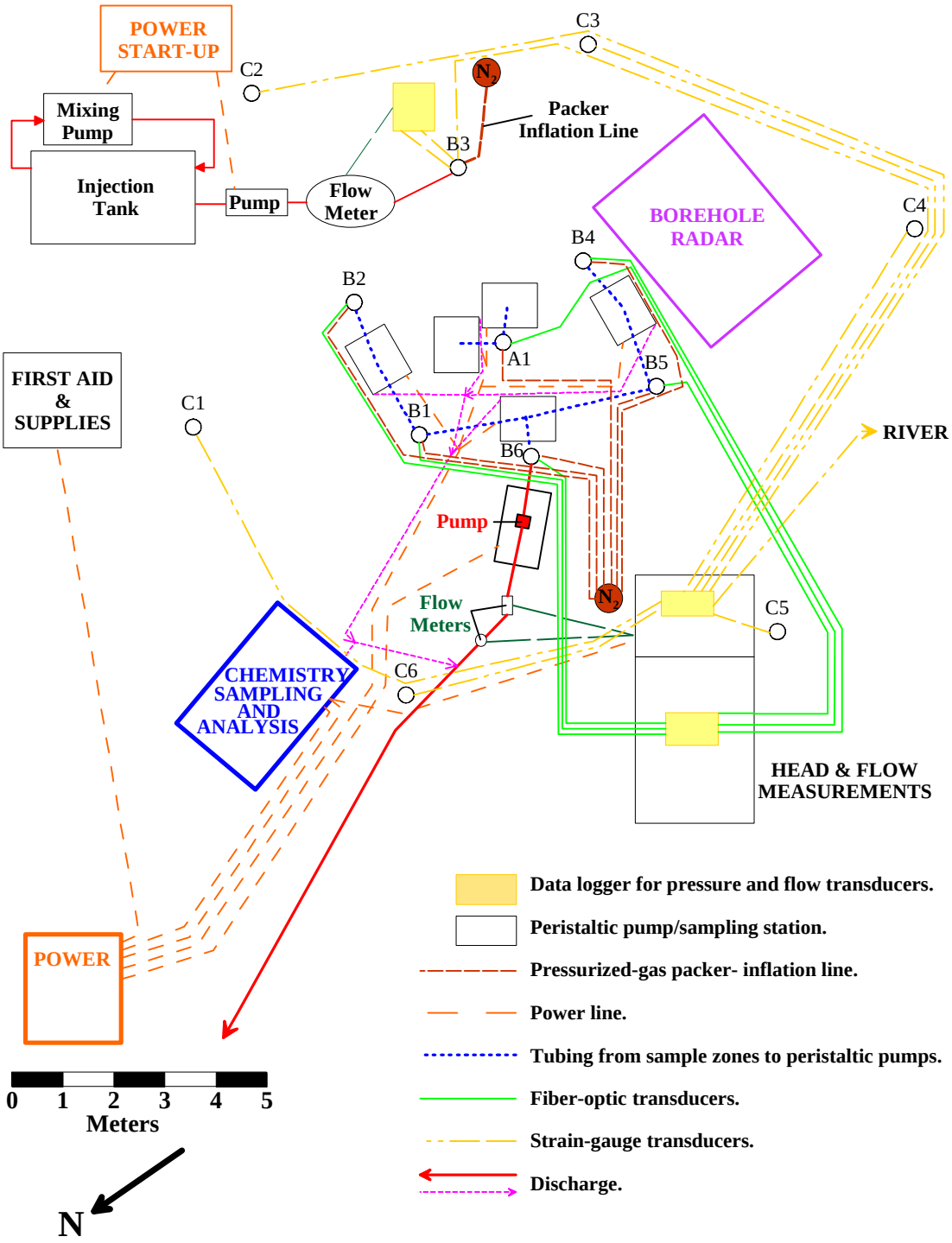

Figure 16. Schematic diagram of arrangement of logistical features at the BHRS for the TTLT.

Figure 17. Photograph from SH21 bridge of arrangement of logistical features at the BHRS for the TTLT. See Figure 16 for identification of features.

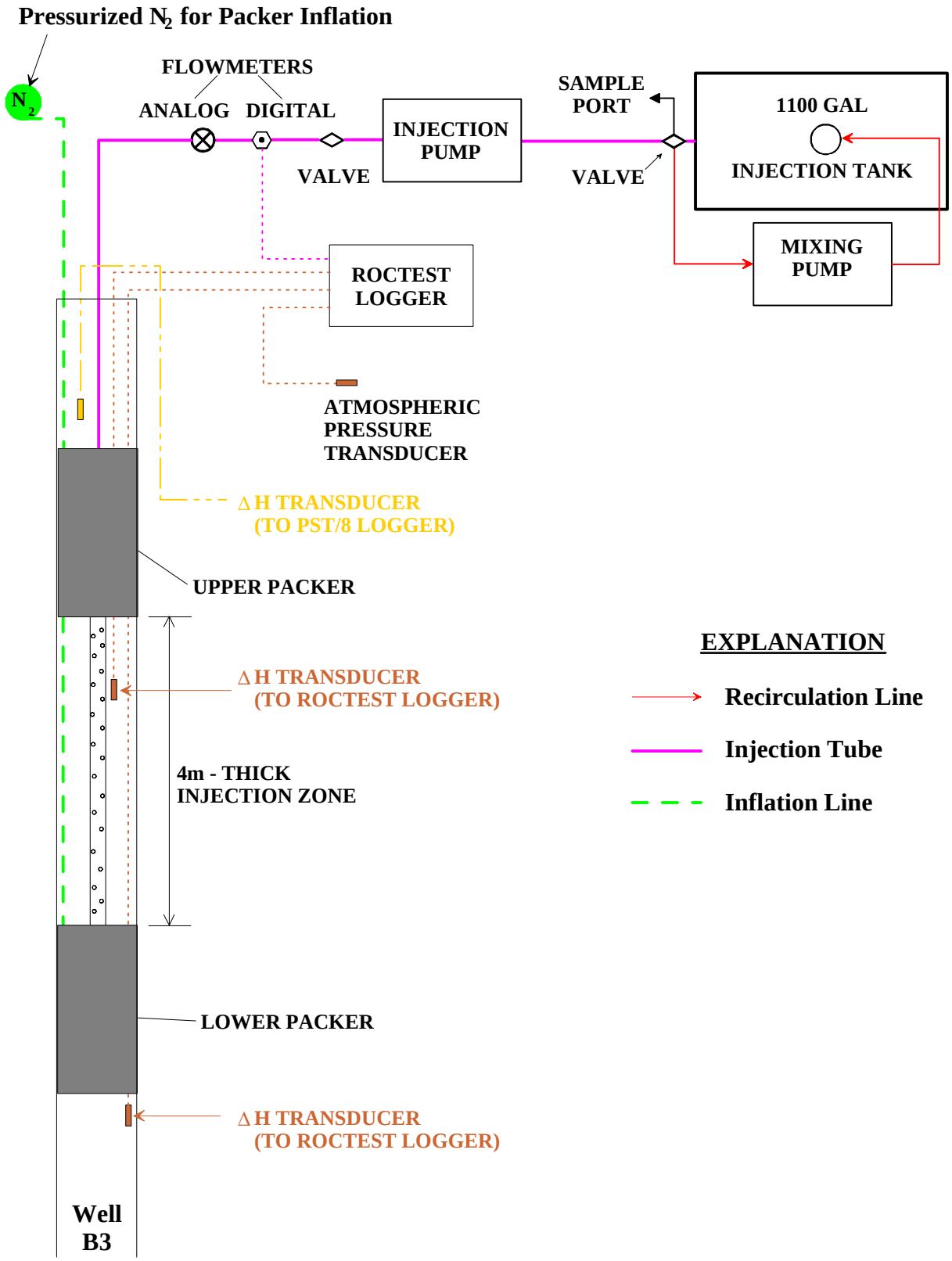

Figure 18. Schematic diagram of injection arrangement at the surface and through the straddle packer system in B3.

Figure 19. Photograph of straddle-packer being installed in well B3 showing upper portion of the injection zone and transducer for measuring head change within the injection zone.

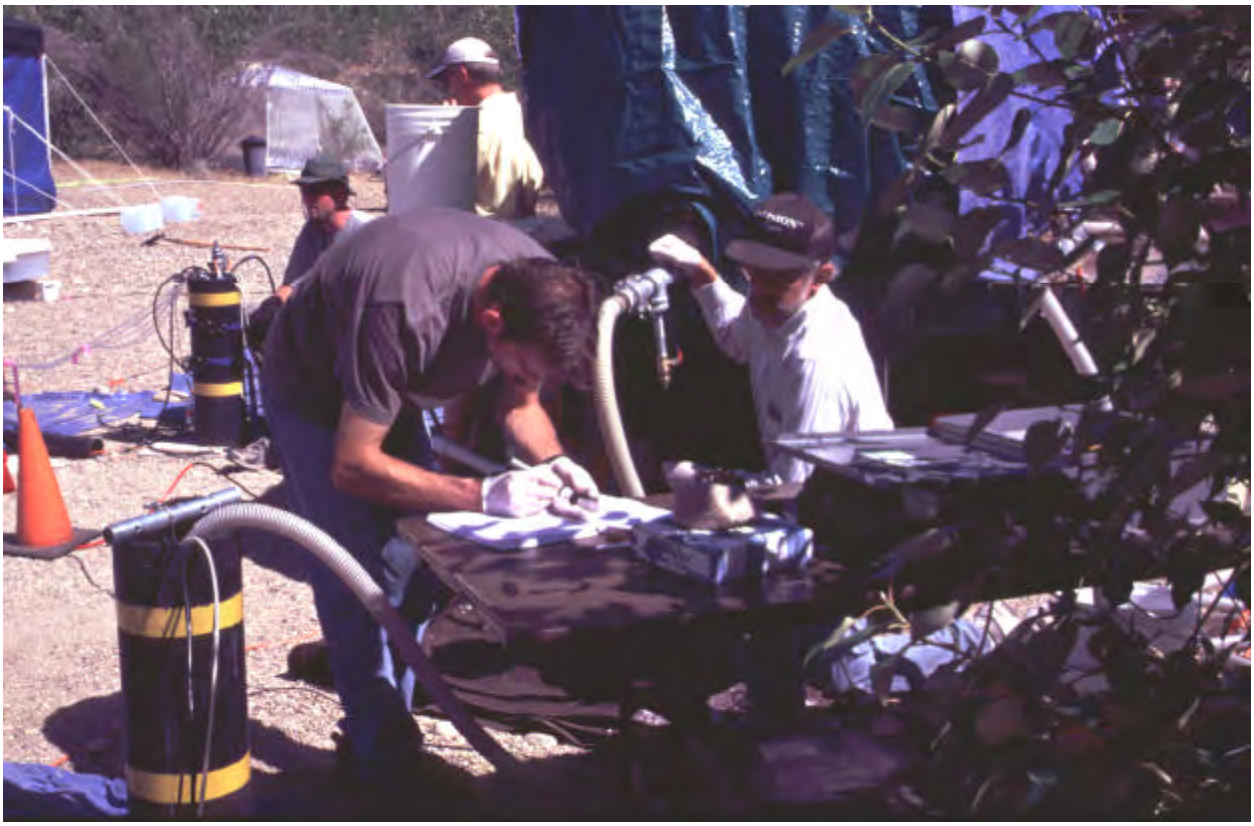

Figure 20. Photograph of sampling during injection on August 1, 2001. Note plastic cover on injection tank and collection of cross-hole radar data to image plume development during injection.

Figure 21. Photograph of custom log-through packer and port system with 1-m separations being assembled and installed in a well at the BHRS in preparation for the tracer/time-lapse imaging experiment in 2001.

Figure 22. Photograph of geophysical logging (i.e., radar tomography) inside custom log-through packer and port system in well B4 during tracer/time-lapse imaging experiment at the BHRS in 2001. Note two lines for sampling head change with fiber-optic transducers, six lines for water sampling through a peristaltic pump, and one line for packer inflation – all coming from outside the riser but within the well.

Figure 23. Photograph of sampling for water chemistry at well A1 in the middle of the radar imaging plane while radar tomography data are being collected through log-through packer and port systems in well B1 (near) and well B4 (far, under shade tent).

Figure 24. Photograph of custom packer and port system with twenty .25-m-long isolated zones.

A. System being assembled and installed in well A1.

B. Twenty water sampling lines, four head-change lines, and one packer inflation line coming from well A1 during tracer/time-lapse imaging experiment at the BHRS.

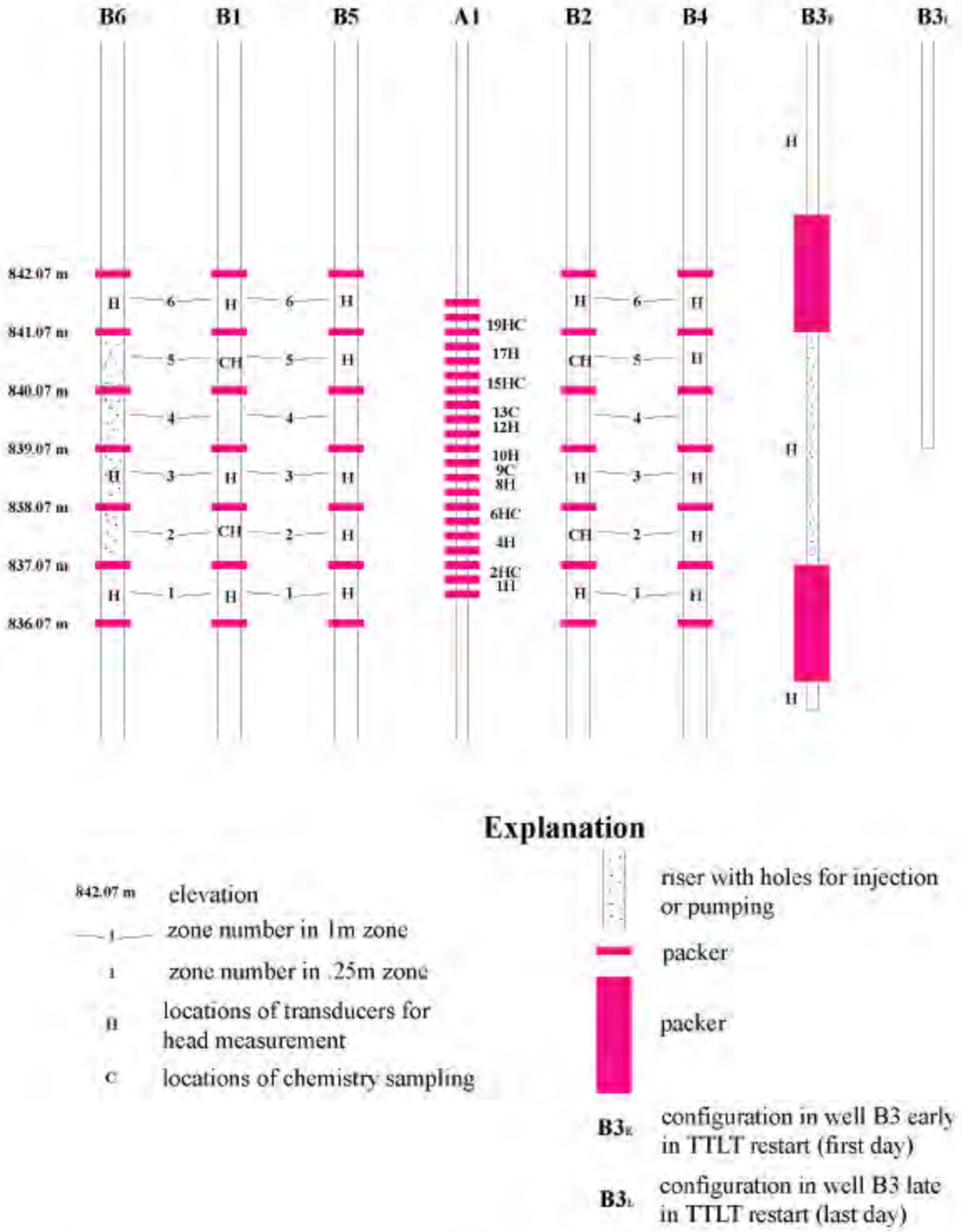

Figure 25. Schematic diagram of packer locations for the TTLT, and of head measurement and sampling zones for TTLT Restart in 2002.

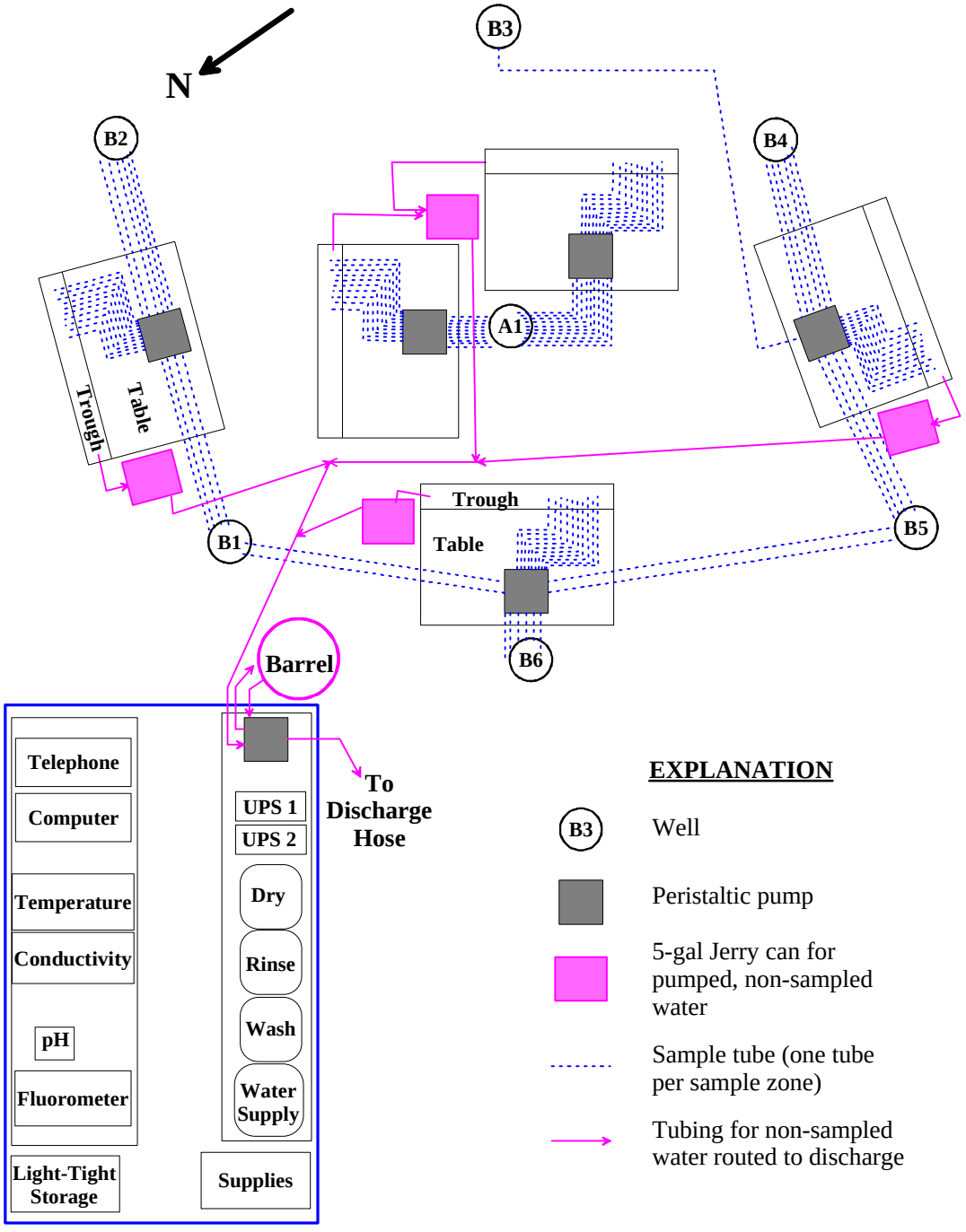

Figure 26. Schematic diagram of logistical arrangements for water chemistry sampling and analysis during the TTLT at the BHRS.

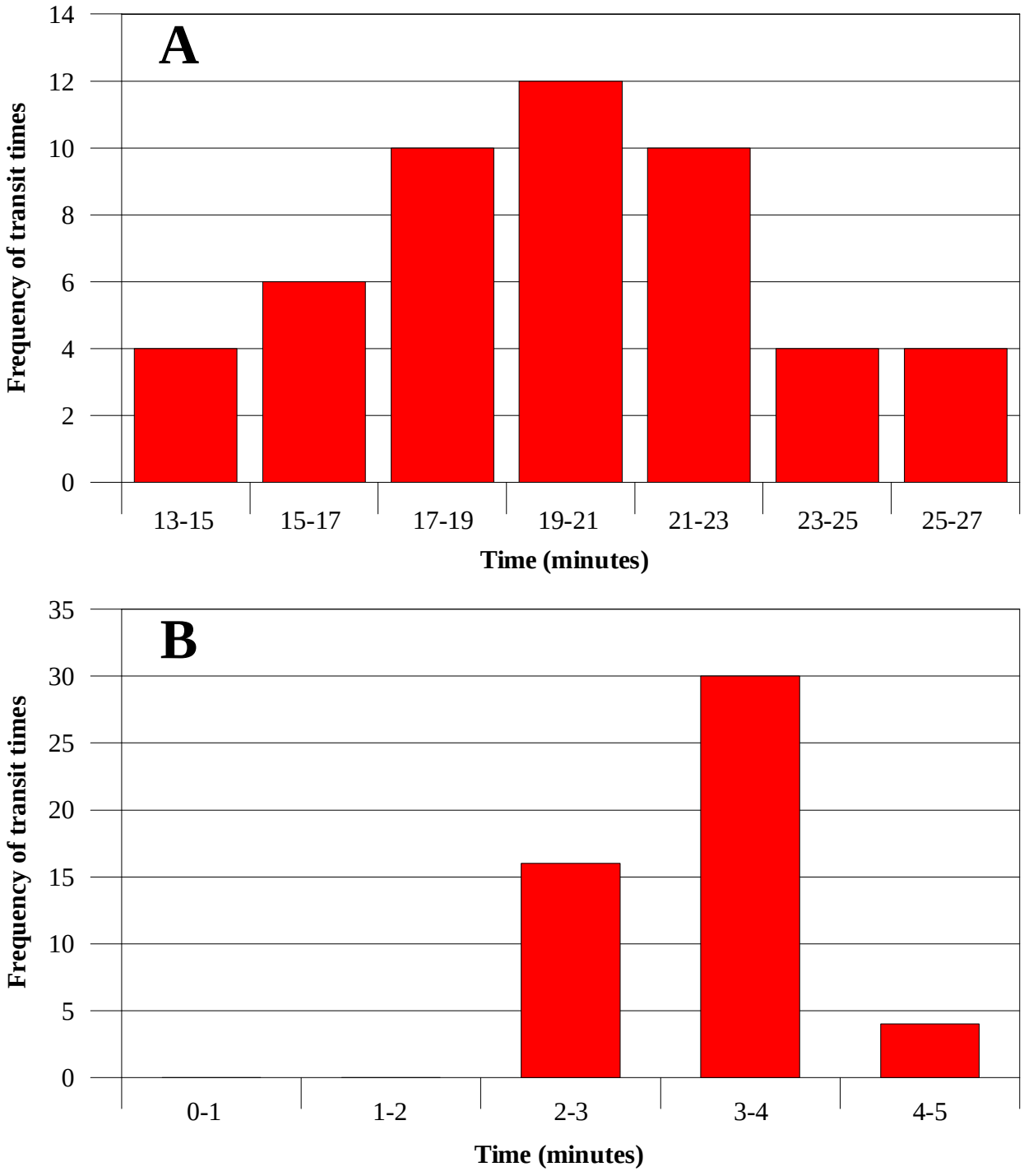

Figure 27. Transit time from sampling zone in the aquifer to sampling point at the surface. A. At 5 ml/min pumping with peristaltic pump. B. At 30 ml/min pumping with peristaltic pump.

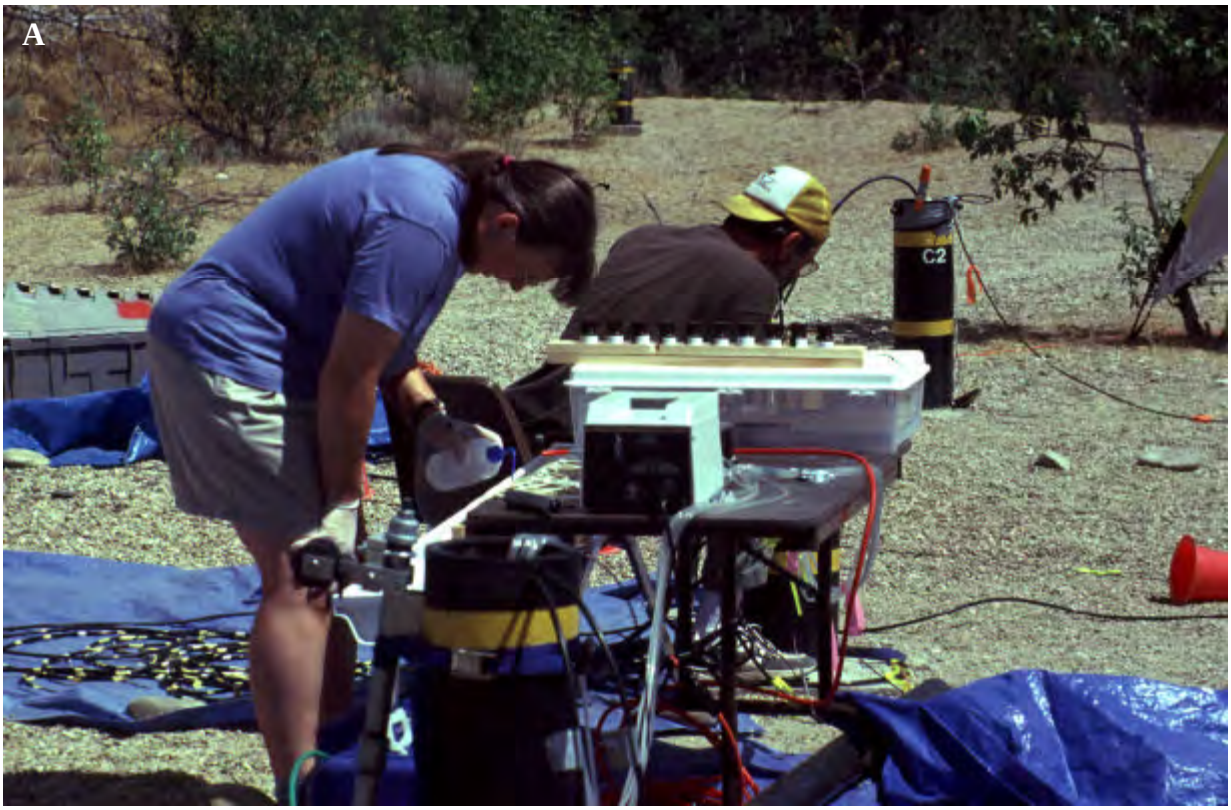

Figure 28. Photographs of sampling from a peristaltic pump drawing from 10 isolated zones in wells B1, B5, and B6.

A. Rinsing sampling lines with deionized water prior to sampling. Note placement of pre-labeled vials in sampling tray keyed to dedicated sampling lines. Amber vials are used to minimize exposure of samples to light.

B. Sampling of 10 zones simultaneously with pre-labeled vials in sampling tray keyed to dedicated sampling lines.

Figure 29. Photograph of discharge systems. Pumping from well B6 using log-through packer and port system with holes drilled into the center riser in zones of injection interval. Discharge was recorded with analogue and digital flow meters. Waste waters from continually-pumping peristaltic pumps and from the chemistry laboratory were collected in a drum (corner of field laboratory in background) and then pumped into the discharge line below flow meters.

Figure 30. Photograph of the field chemistry laboratory at the BHRS which was used to generate near realtime results on uranine concentration from fluorescence and conductivity as analogue for bromide concentration from samples from 50 locations in six wells during the tracer/time-lapse imaging experiment.

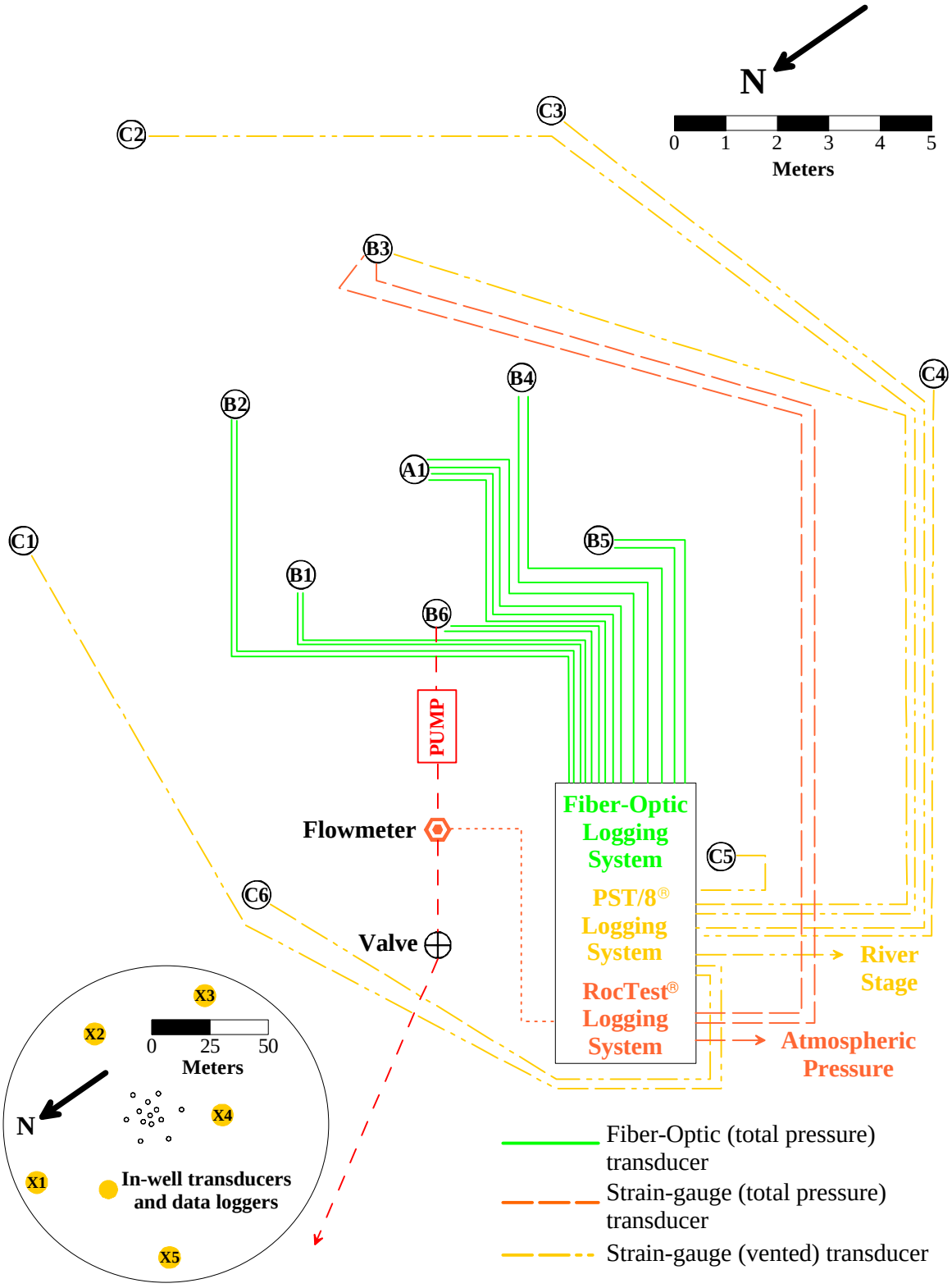

Figure 31. Schematic diagram of head-change and flow-rate measurement and logging systems.

Figure 32. Photograph of station for logging head-change data from strain-gauge and fiber-optic transducers.

Figure 33. Photograph of near-realtime review of radar data.

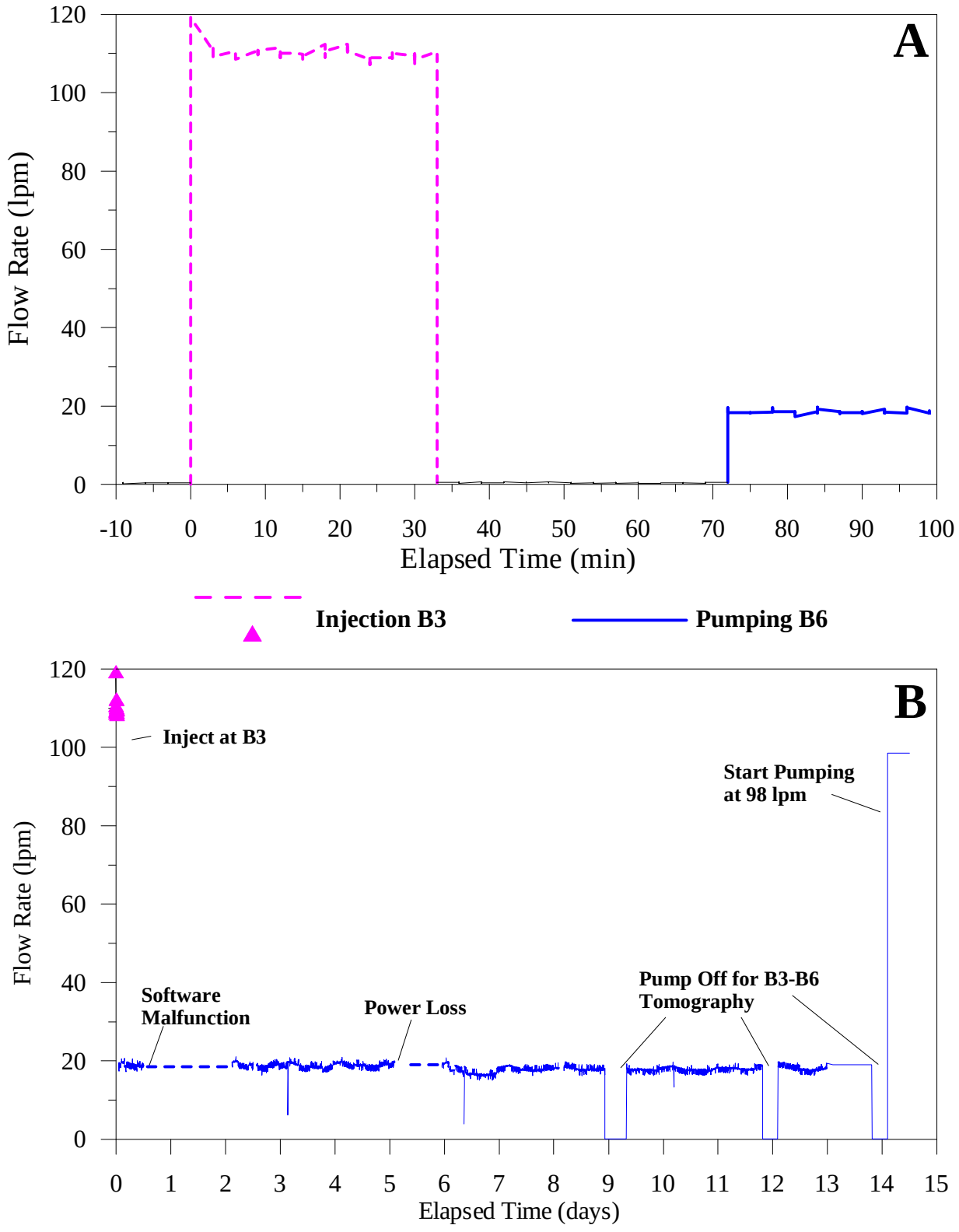

Figure 34. Record of injection and pumping rates. A. Injection and start of pumping at ~19 lpm (5 gpm) at B6. B. Full TTLT.

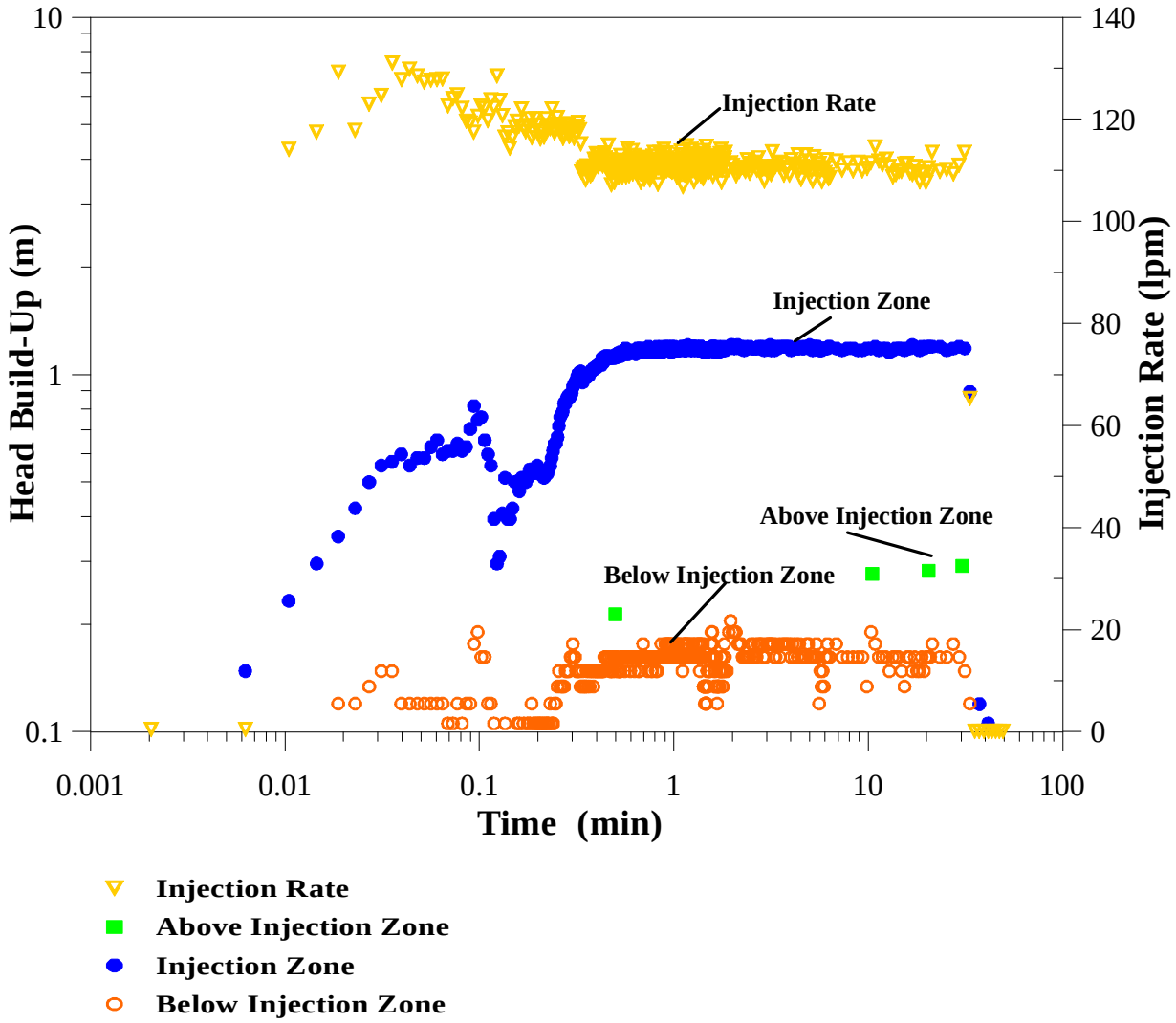

Figure 35. High-resolution record of injection rate and head-change at B3 during injection.

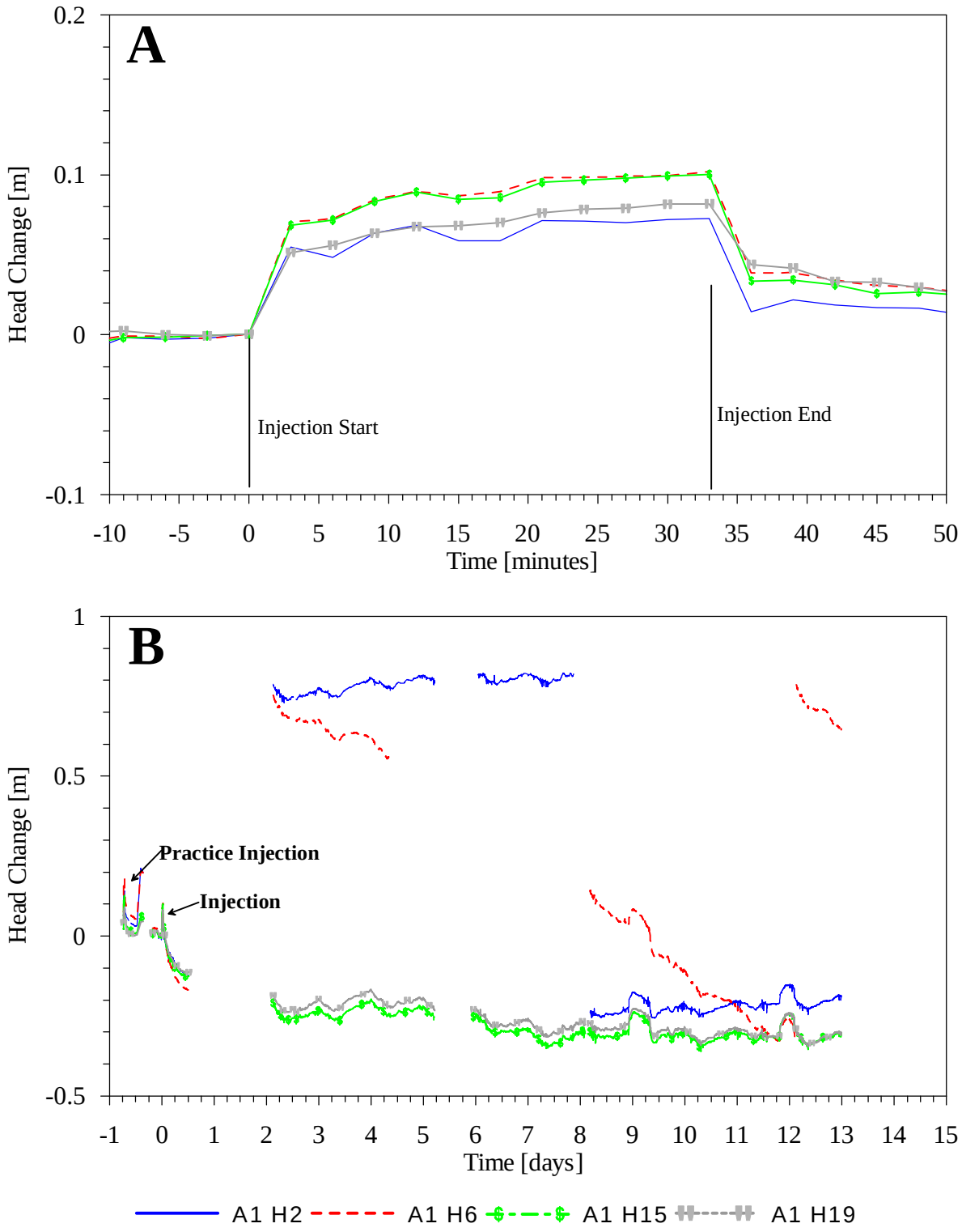

Figure 36. Record of head-changes (adjusted for atmospheric pressure) in zones in A1 during the TTLT measured with total-pressure fiber-optic transducers. A. Injection. B. Full TTLT. Note drift and offset problems with transducers in A1H2 and A1H6.

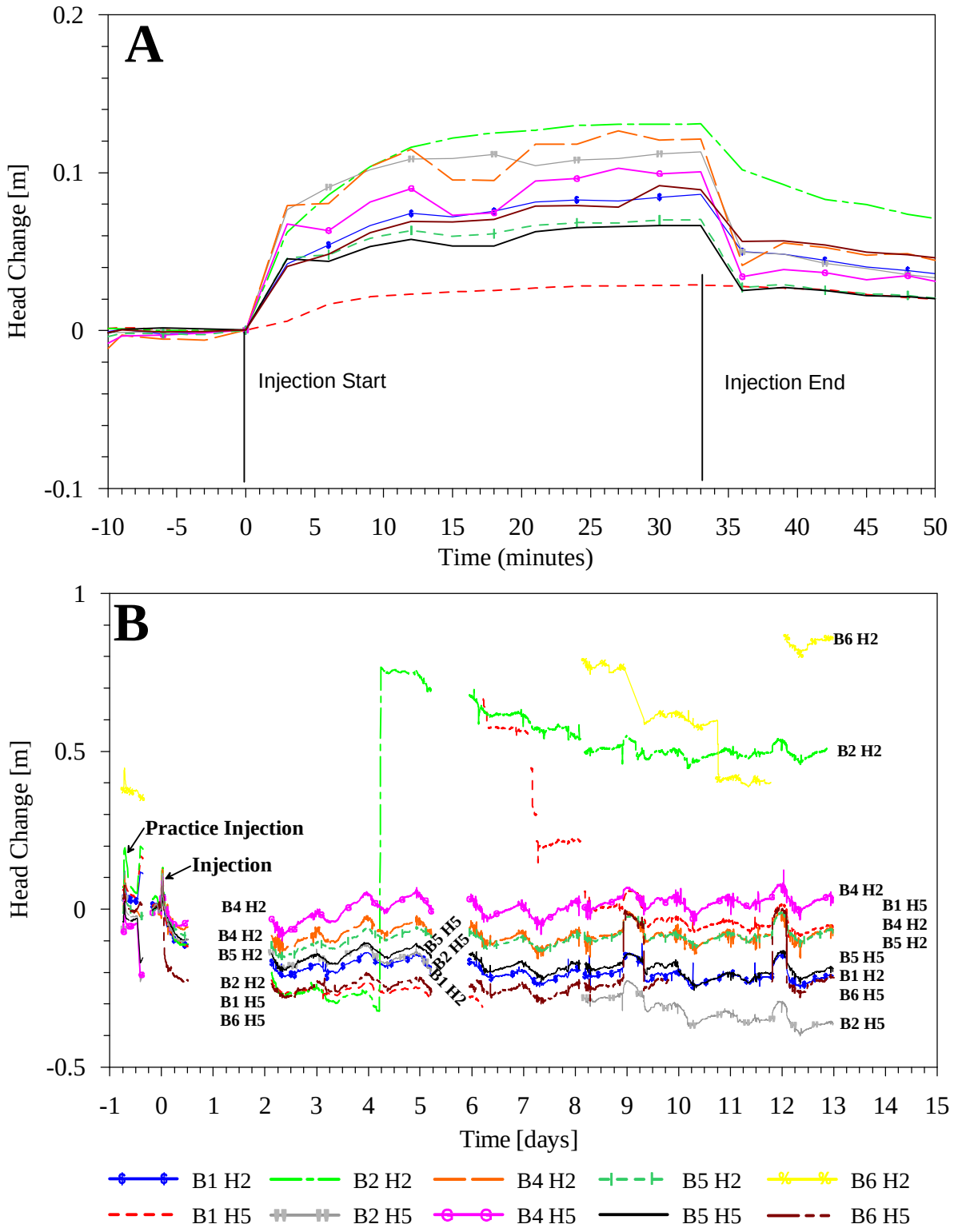

Figure 37. Record of head-changes (adjusted for atmospheric pressure) in zones in wells B1, B2, B4, B5, and B6 during the TTLT. A. Injection. B. Full TTLT. Note drift and offset problems with transducers in B1H5, B2H2, B2H5, and B6H2.

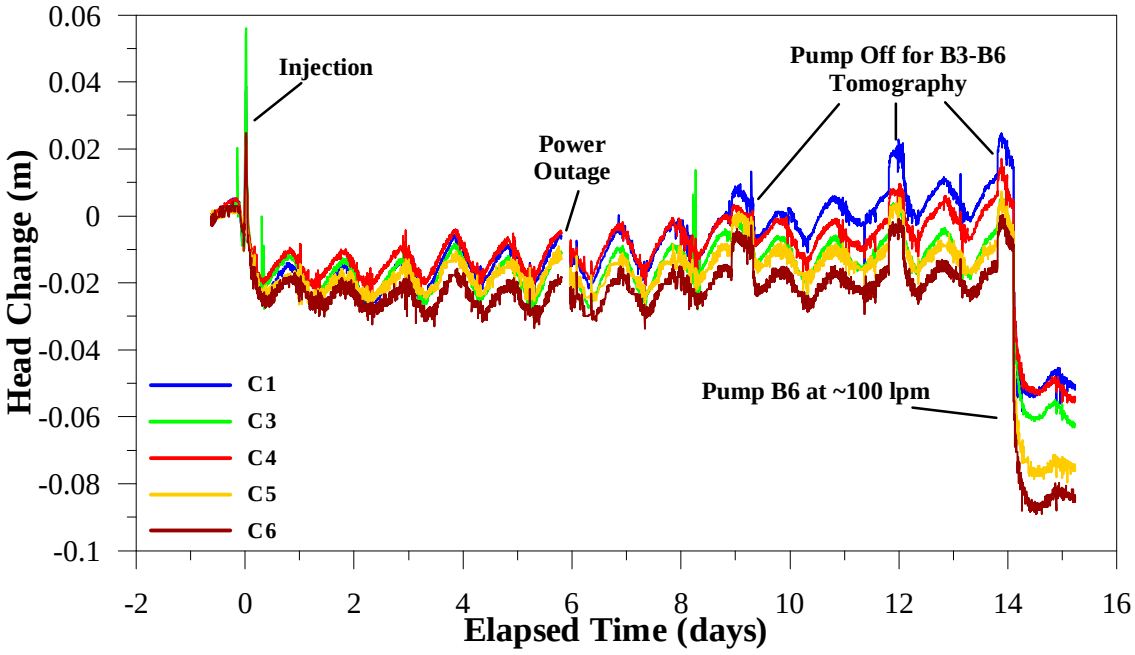

Figure 38. Record of head changes in wells C1, C3, C4, C5, and C6 measured with vented strain-gauge transducers during the TTLT to day 15 of the test. Periodicity is due to evapo-transpiration cycles. Overprinting of the cyclic head changes can be identified for injection and for pumping suspension during radar tomography between wells B3 and B6.

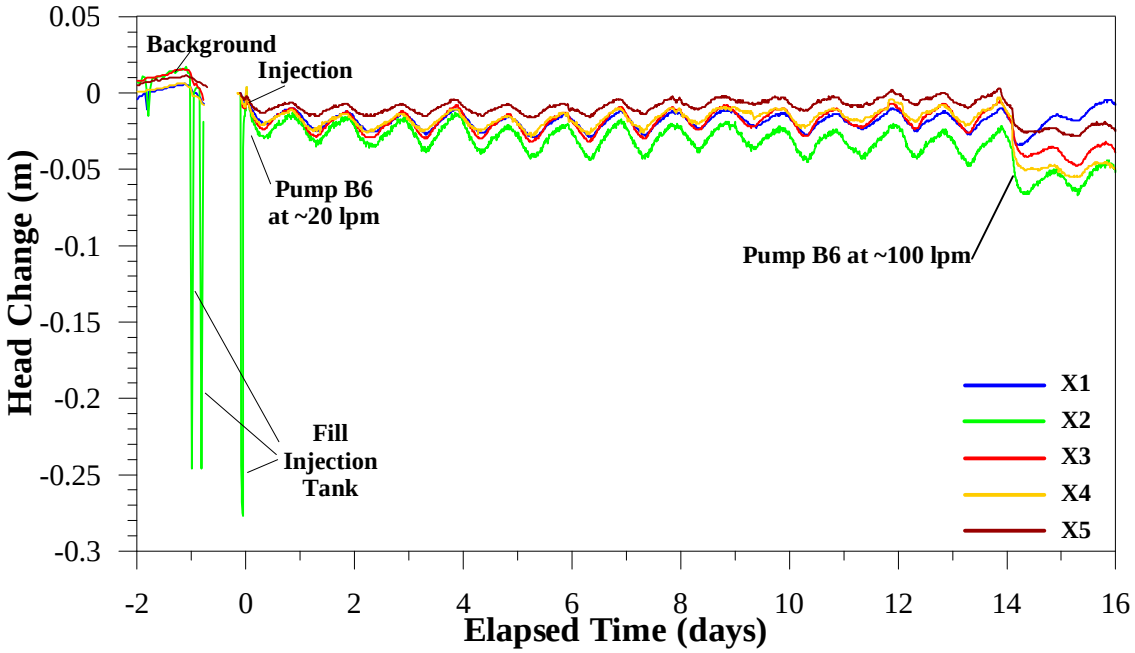

Figure 39. Record of head changes in wells X1, X2, X3, X4, and X5 measured with vented strain-gauge transducers during the TTLT to day 16 of the test. Periodicity is due to evapo-transpiration cycles.

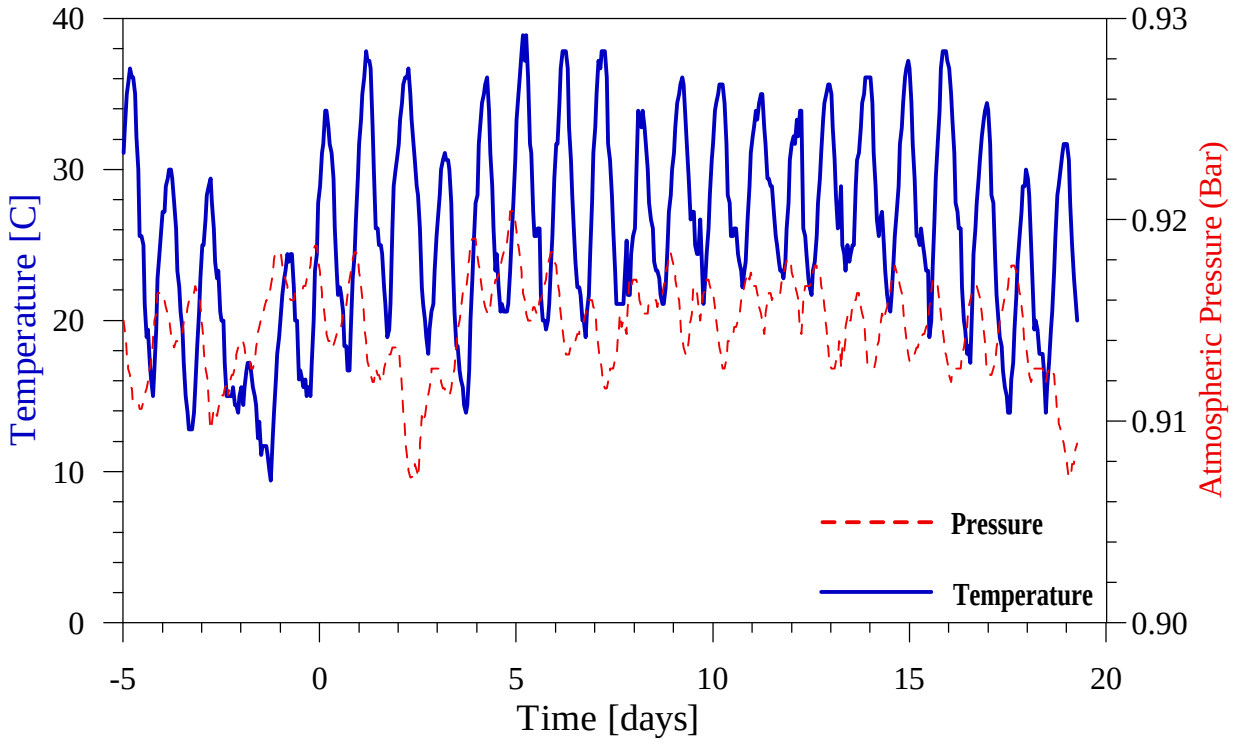

Figure 40. Atmospheric pressure and temperature recorded at the Boise Airport during the TTLT.

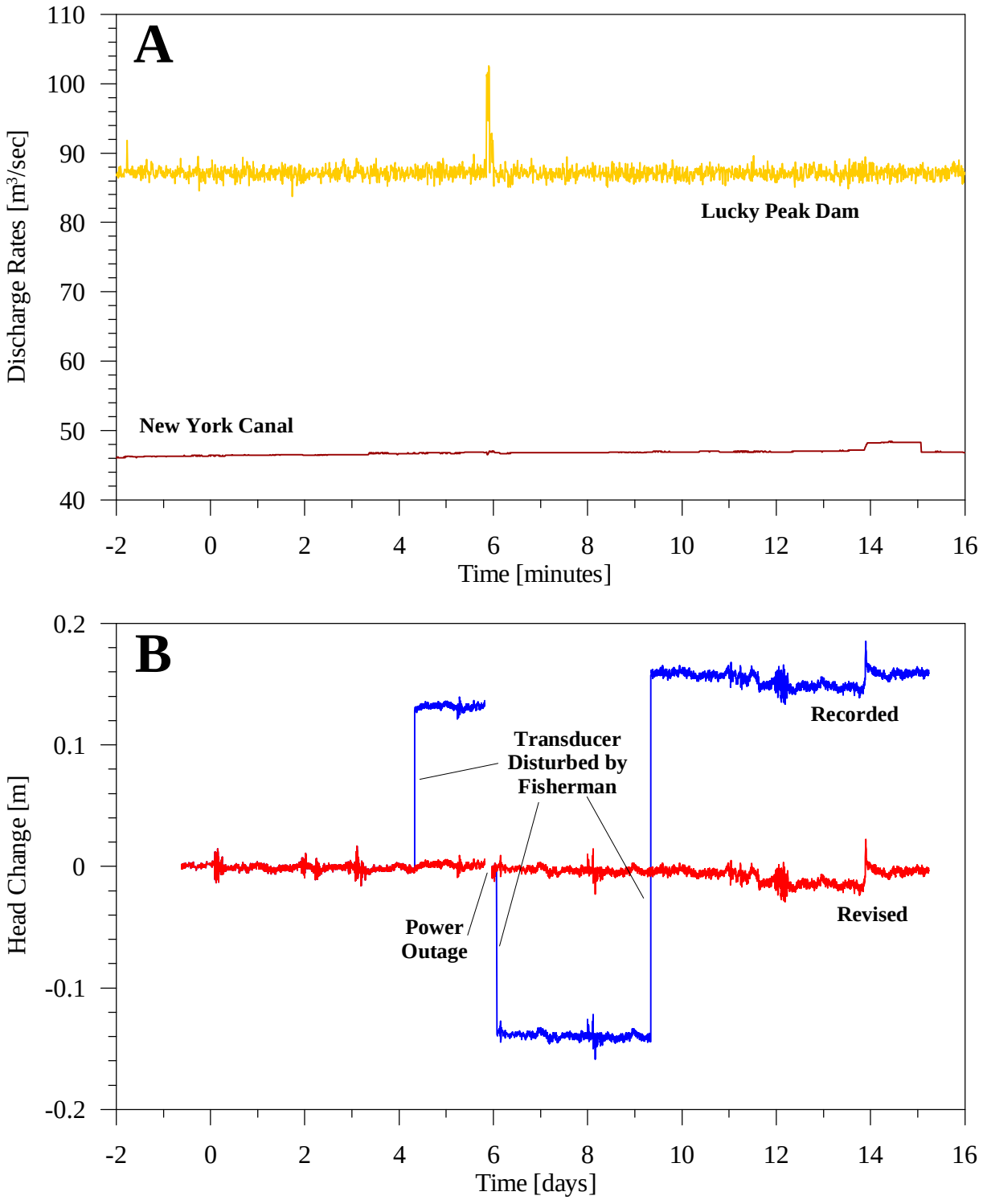

Figure 41. Record of flows and head change at the Boise River. A. Discharge from Lucky Peak Dam and into the New York Canal near the BHRS. Note trend in discharge to the New York Canal. B. Head change in the Boise River adjacent to the BHRS. Note trend in head change in Boise River.

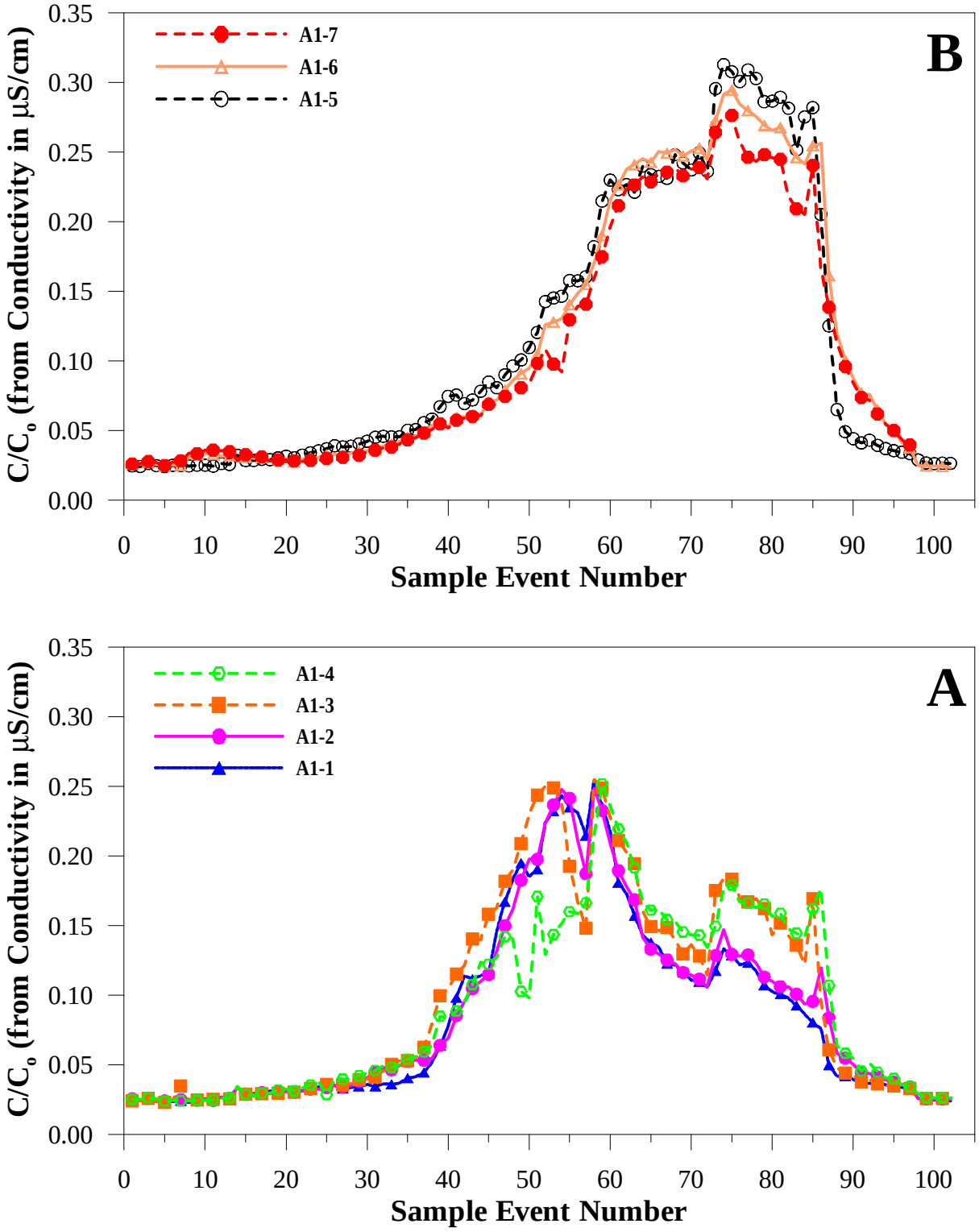

Figure 42. Breakthrough curves (adjusted for outliers) for conductivity in well A1.
A. Zones 1-4. B. Zones 5-7. C. Zones 8-14. D. Zones 15-20.

Note: Sampling events generally occur every 4 hours. See Appendix 1.

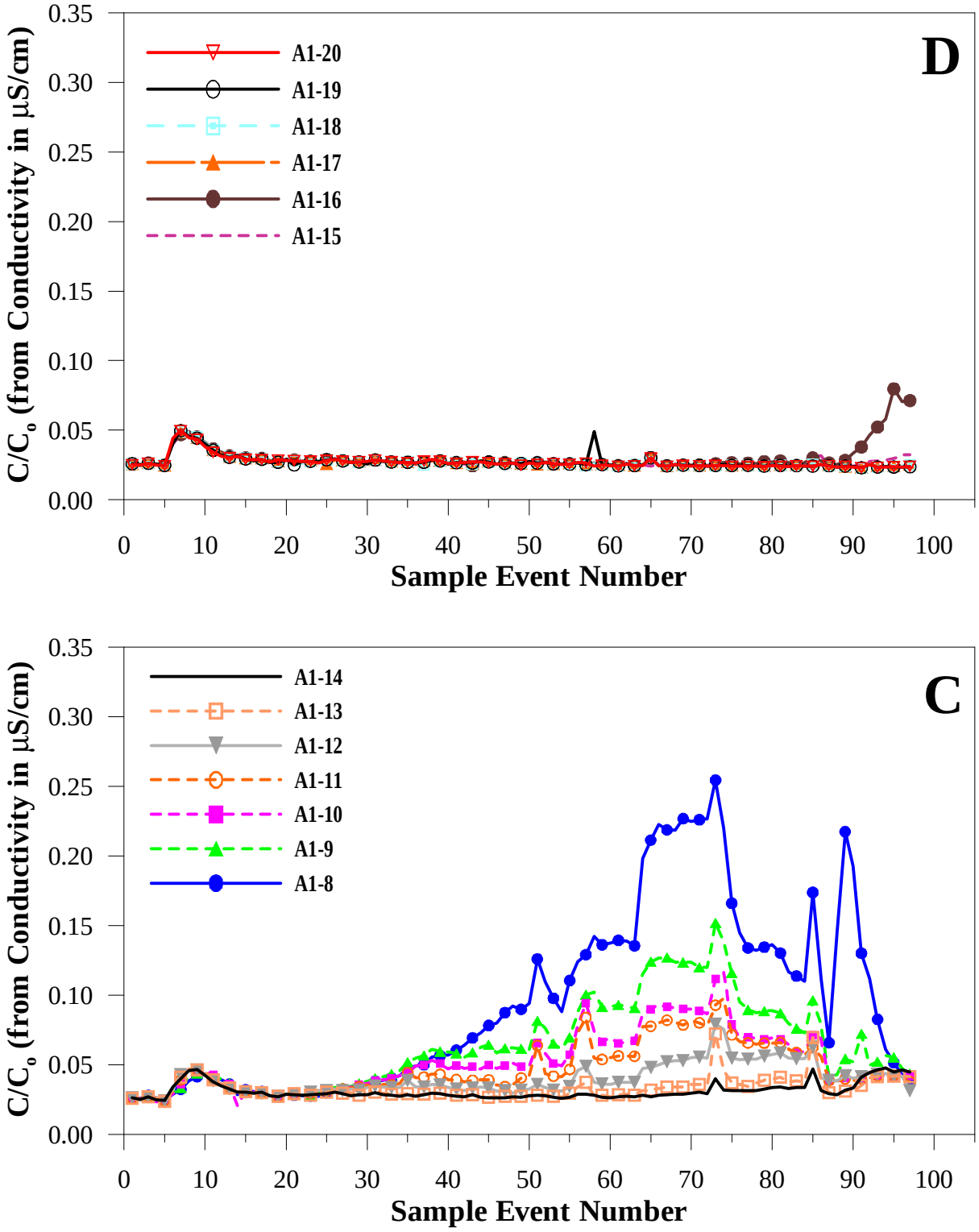

Figure 42. Breakthrough curves (adjusted for outliers) for conductivity in well A1.
A. Zones 1-4. B. Zones 5-7. C. Zones 8-14. D. Zones 15-20.

Note: Sampling events generally occur every 4 hours. See Appendix 1.

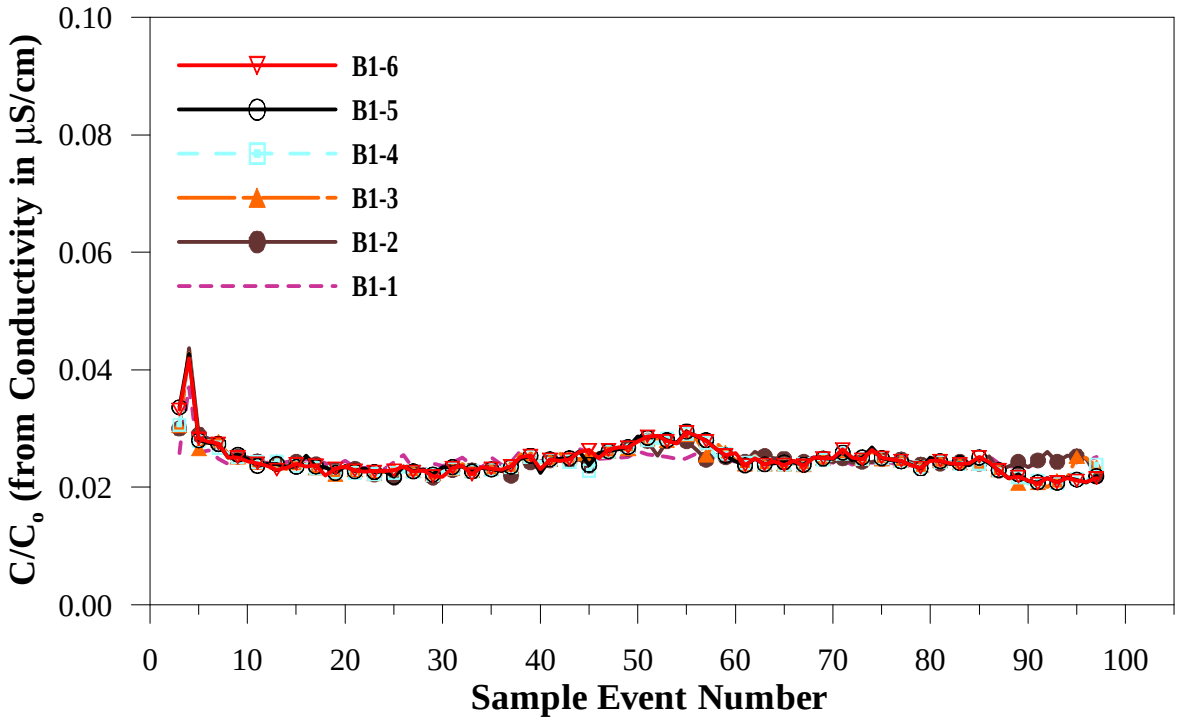

Figure 43. Breakthrough curves for conductivity in well B1.

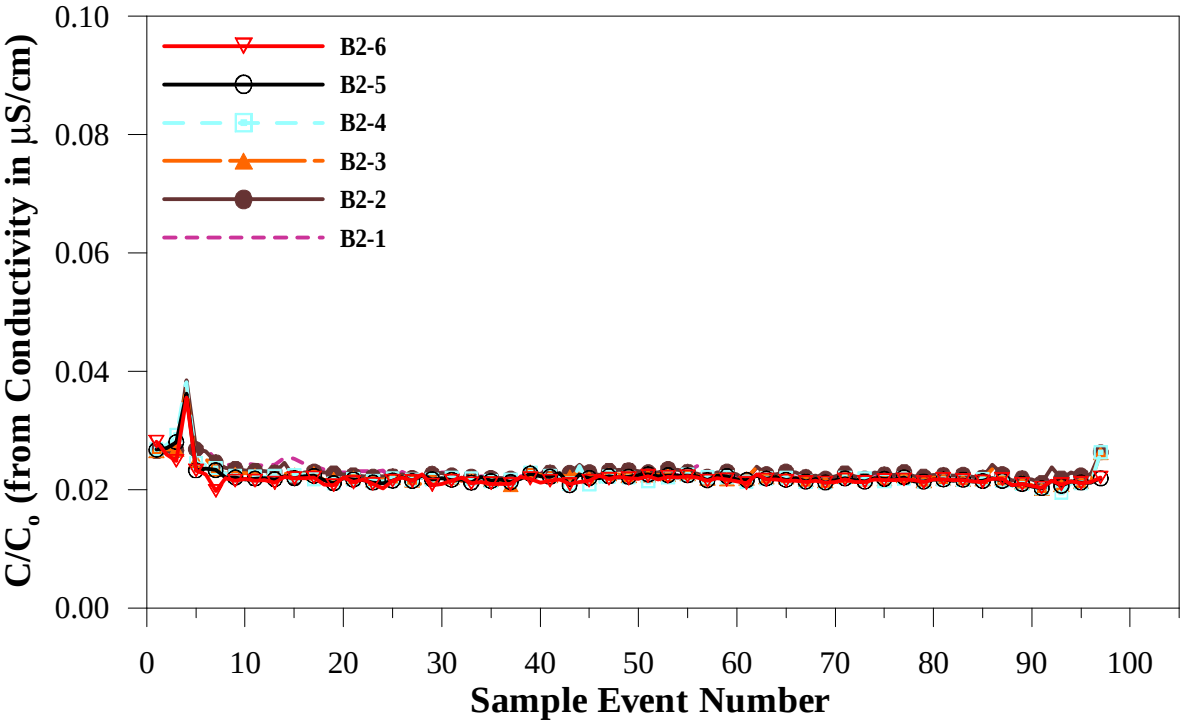

Figure 44. Breakthrough curves for conductivity in well B2.

Note: Sampling events generally occur every 4 hours. See Appendix 1.

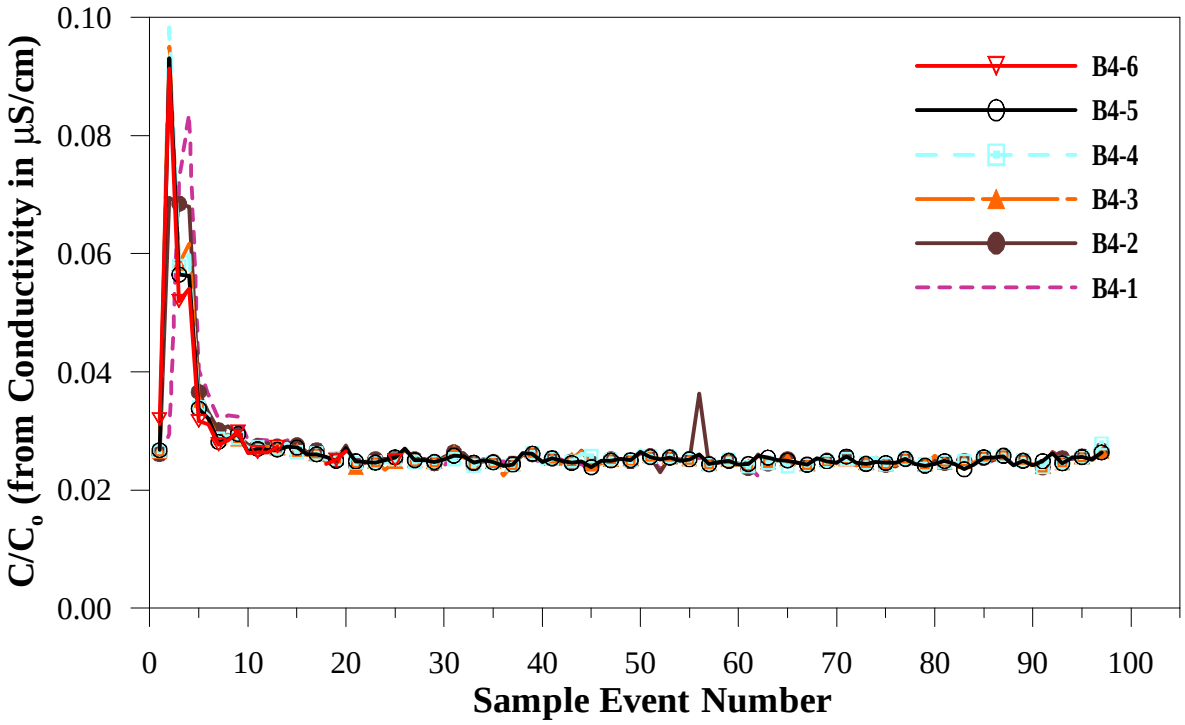

Figure 45. Breakthrough curves for conductivity in well B4.

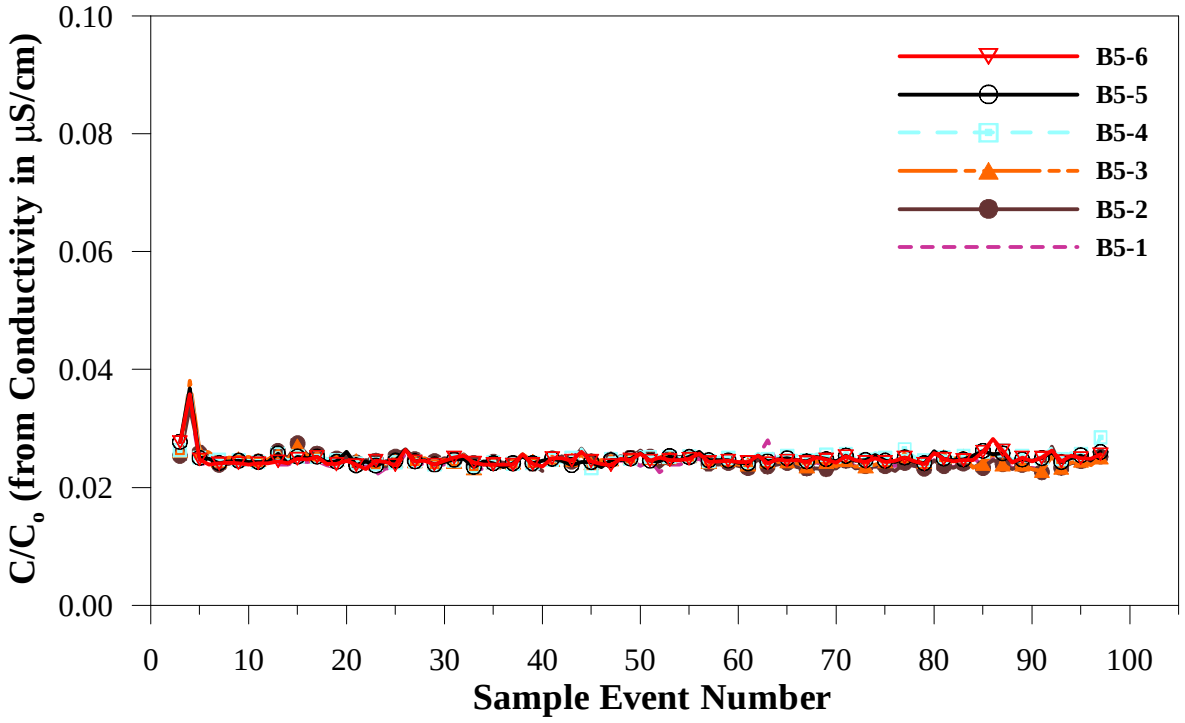

Figure 46. Breakthrough curves for conductivity in well B5.

Note: Sampling events generally occur every 4 hours. See Appendix 1.

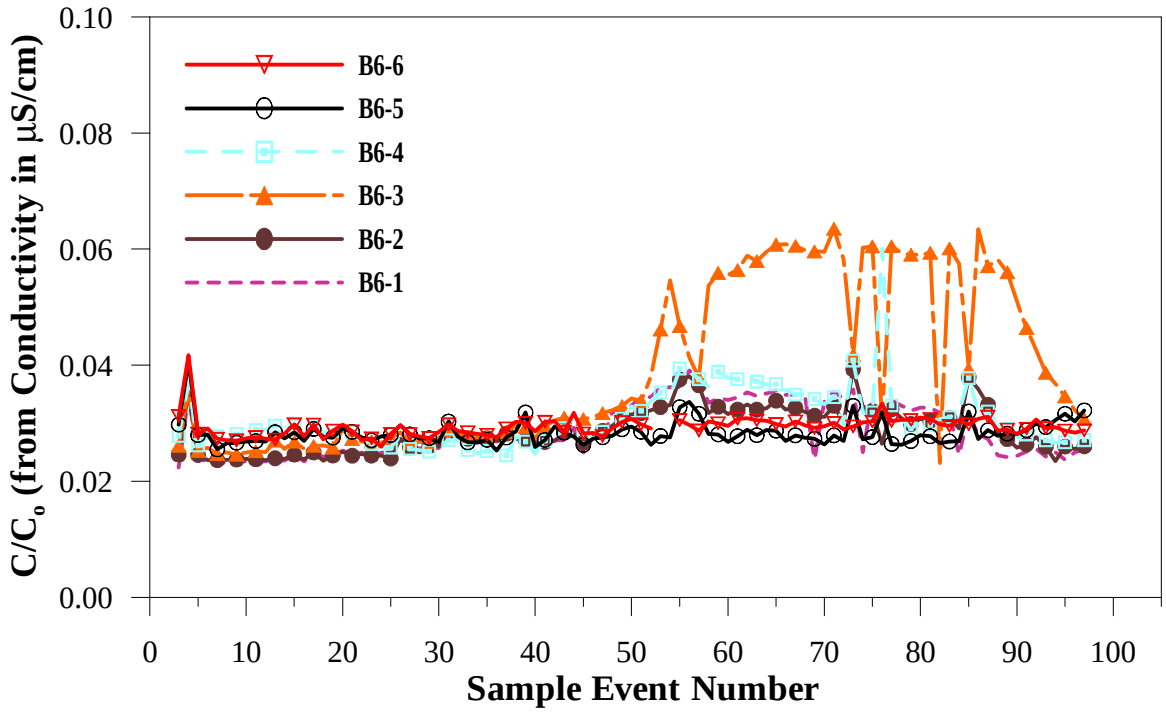

Figure 47. Breakthrough curves for conductivity in withdrawal well B6.

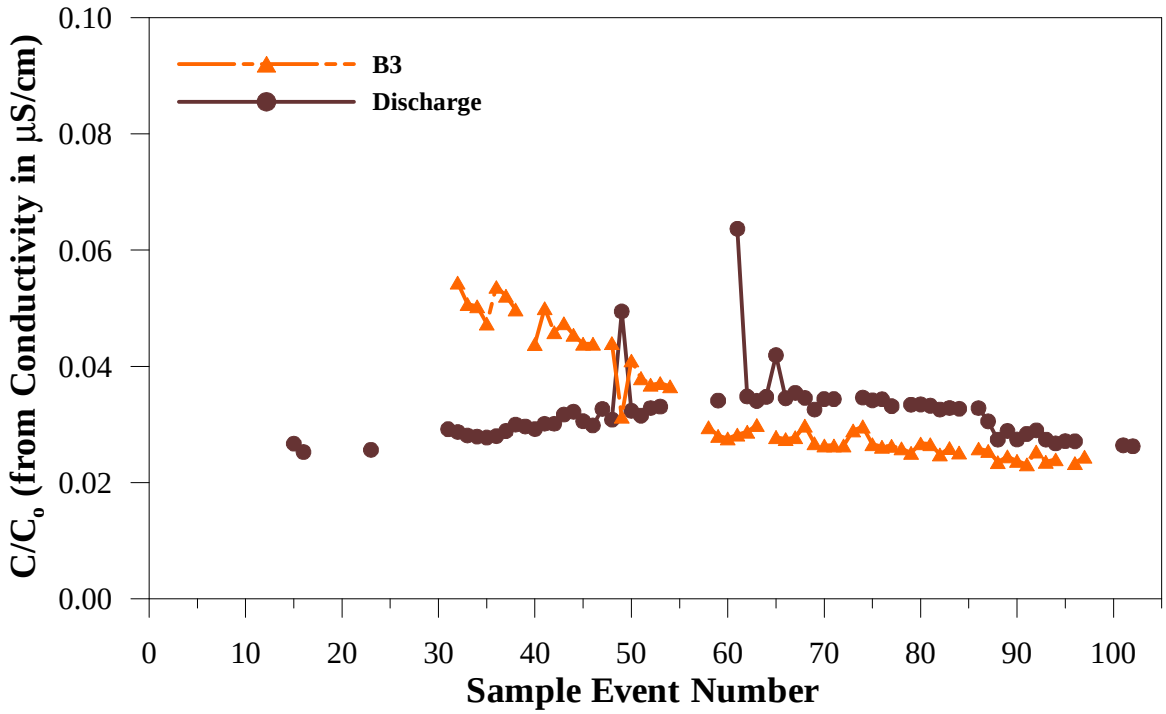

Figure 48. Breakthrough curves for conductivity in injection well B3 after the straddle packer was removed, and from the discharge line.

Note: Sampling events generally occur every 4 hours. See Appendix 1.

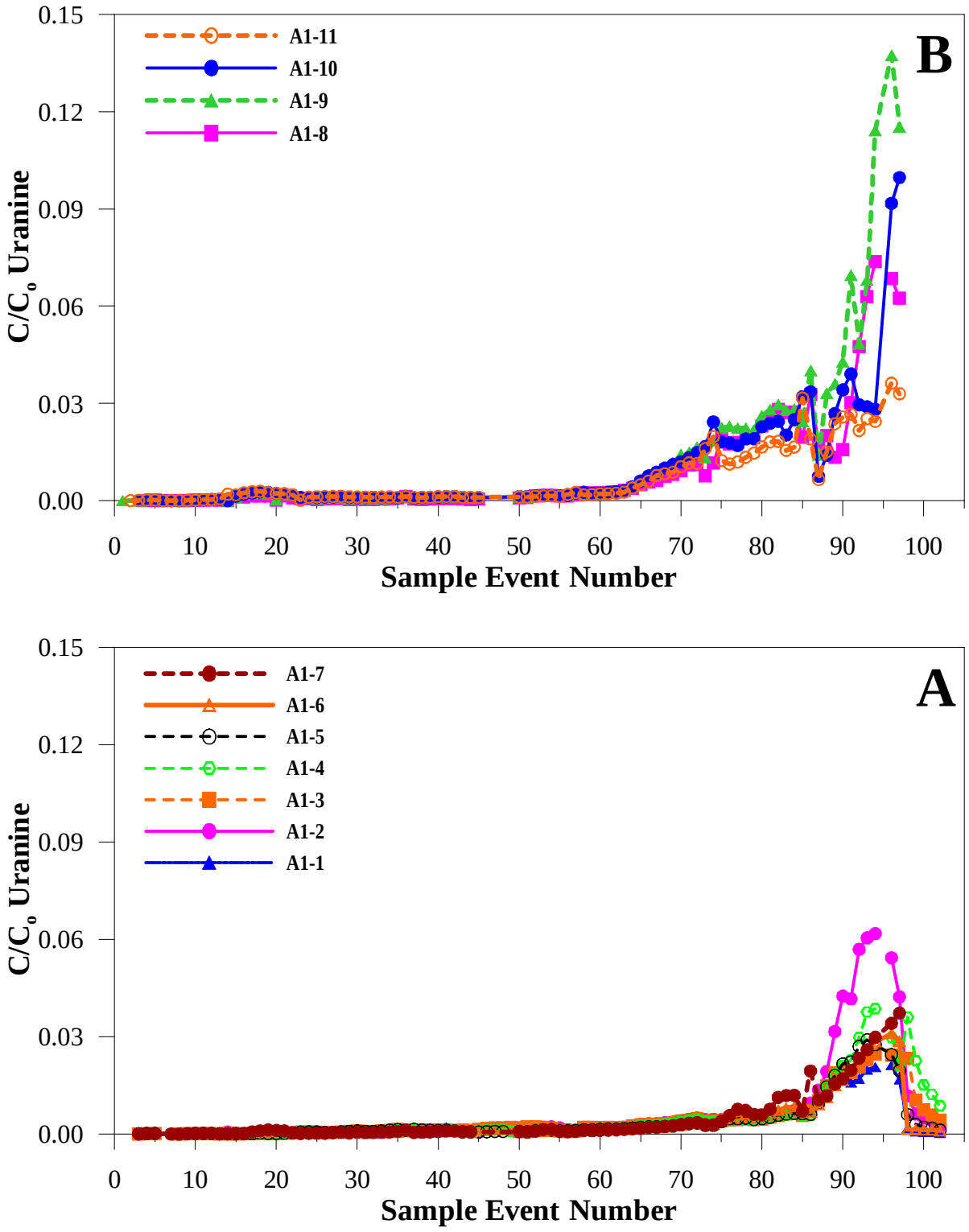

Figure 49. Breakthrough curves for uranine in well A1.
A. Zones 1-7. B. Zones 8-11. C. Zones 12-14. D. Zones 15-20.

Note: Sampling events generally occur every 4 hours. See Appendix 1.

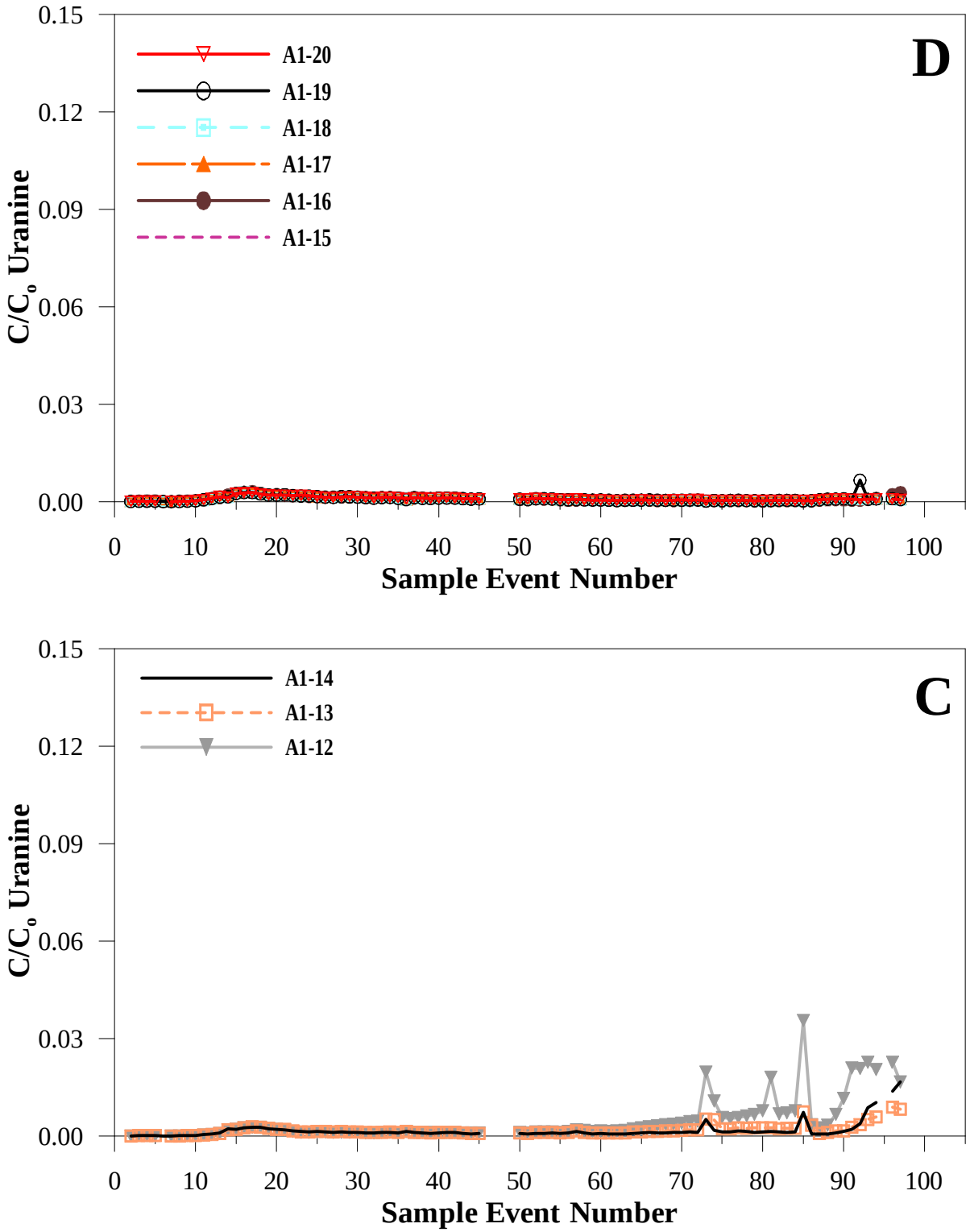

Figure 49. Breakthrough curves for uranine in well A1.
A. Zones 1-7. B. Zones 8-11. C. Zones 12-14. D. Zones 15-20.

Note: Sampling events generally occur every 4 hours. See Appendix 1.

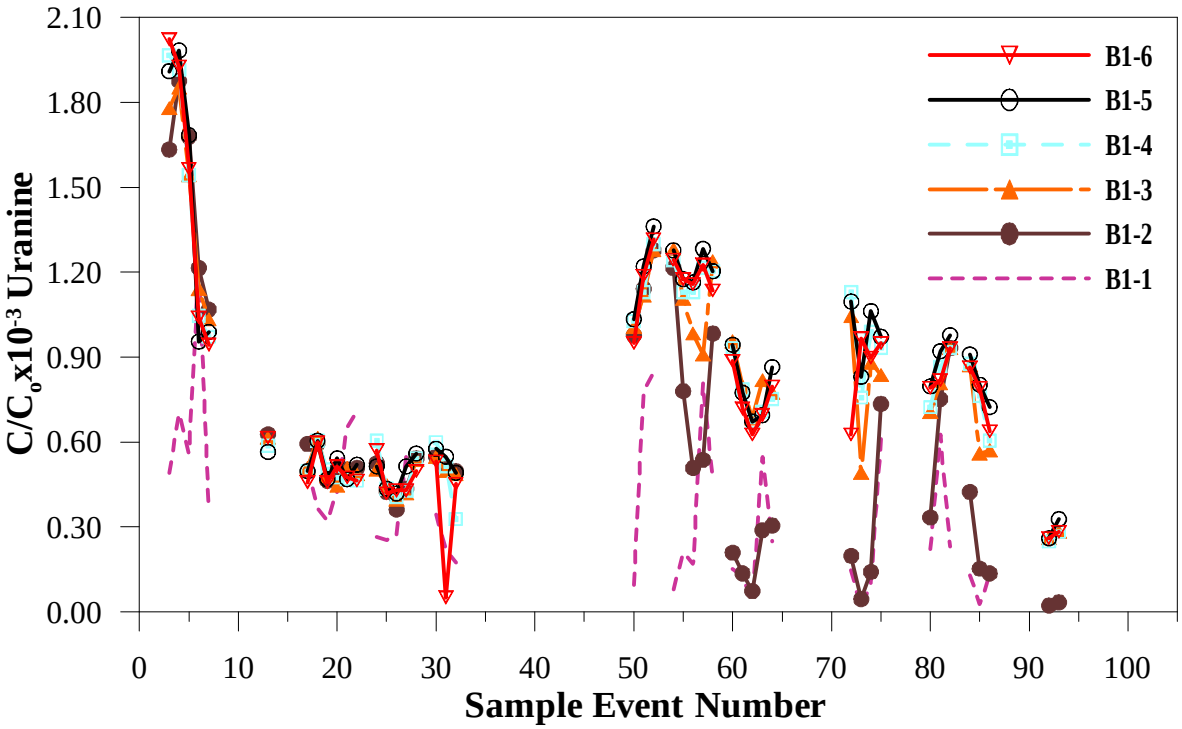

Figure 50. Breakthrough curves for uranine in well B1.

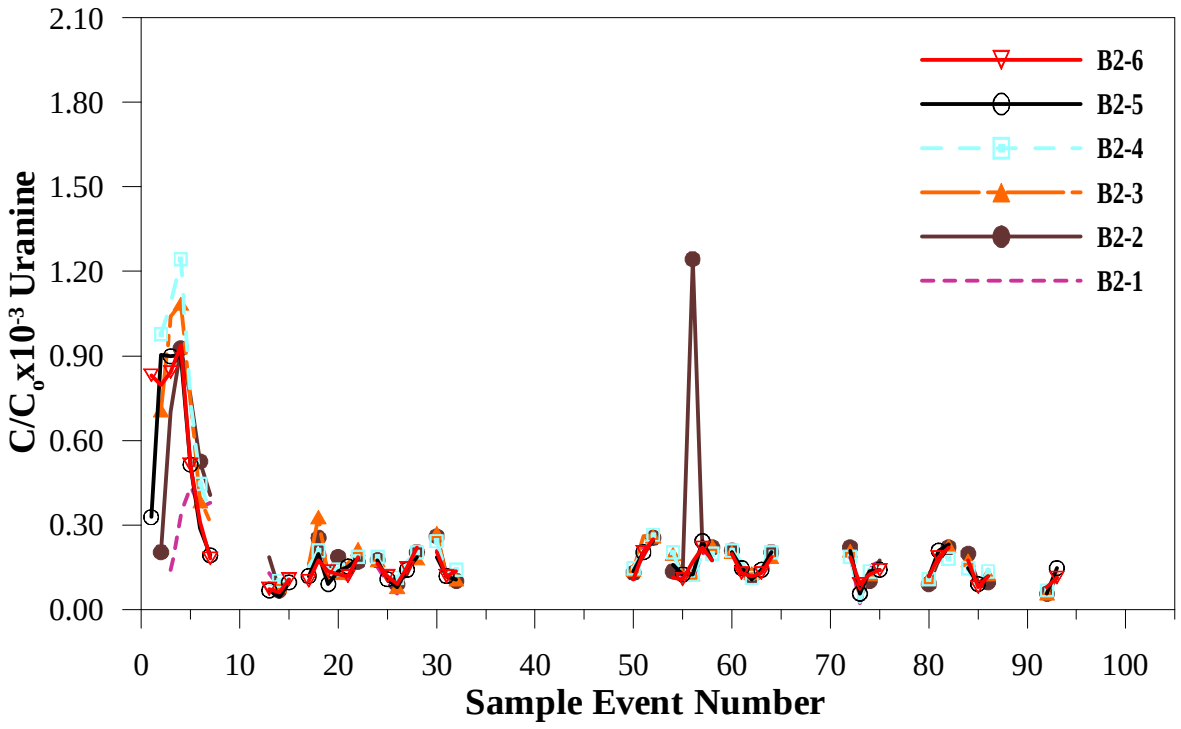

Figure 51. Breakthrough curves for uranine in well B2.

Note: Sampling events generally occur every 4 hours. See Appendix 1.

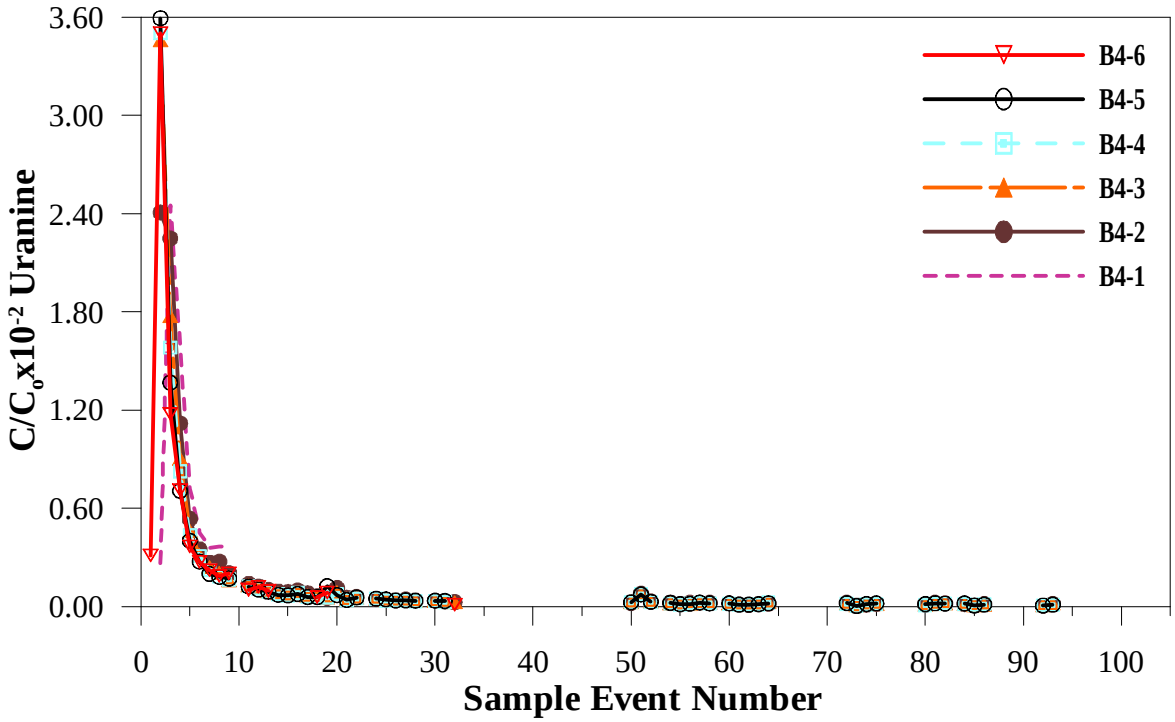

Figure 52. Breakthrough curves for uranine in well B4.

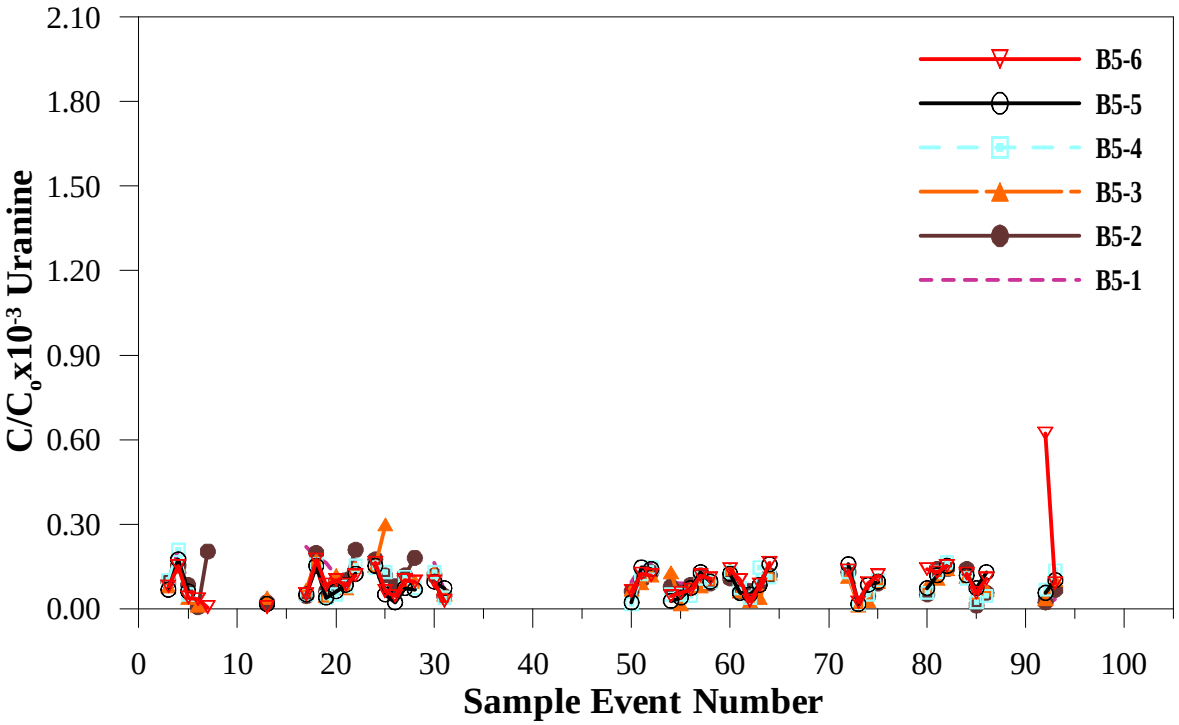

Figure 53. Breakthrough curves for uranine in well B5.

Note: Sampling events generally occur every 4 hours. See Appendix 1.

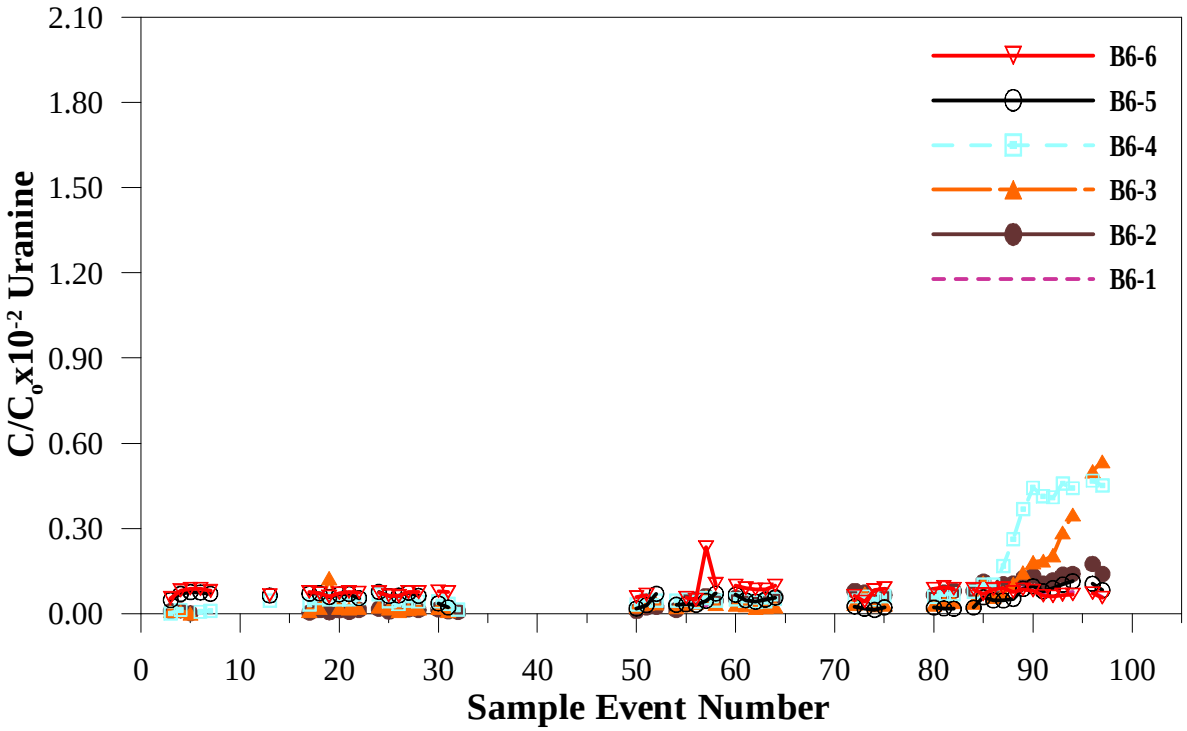

Figure 54. Breakthrough curves for uranine in withdrawal well B6.

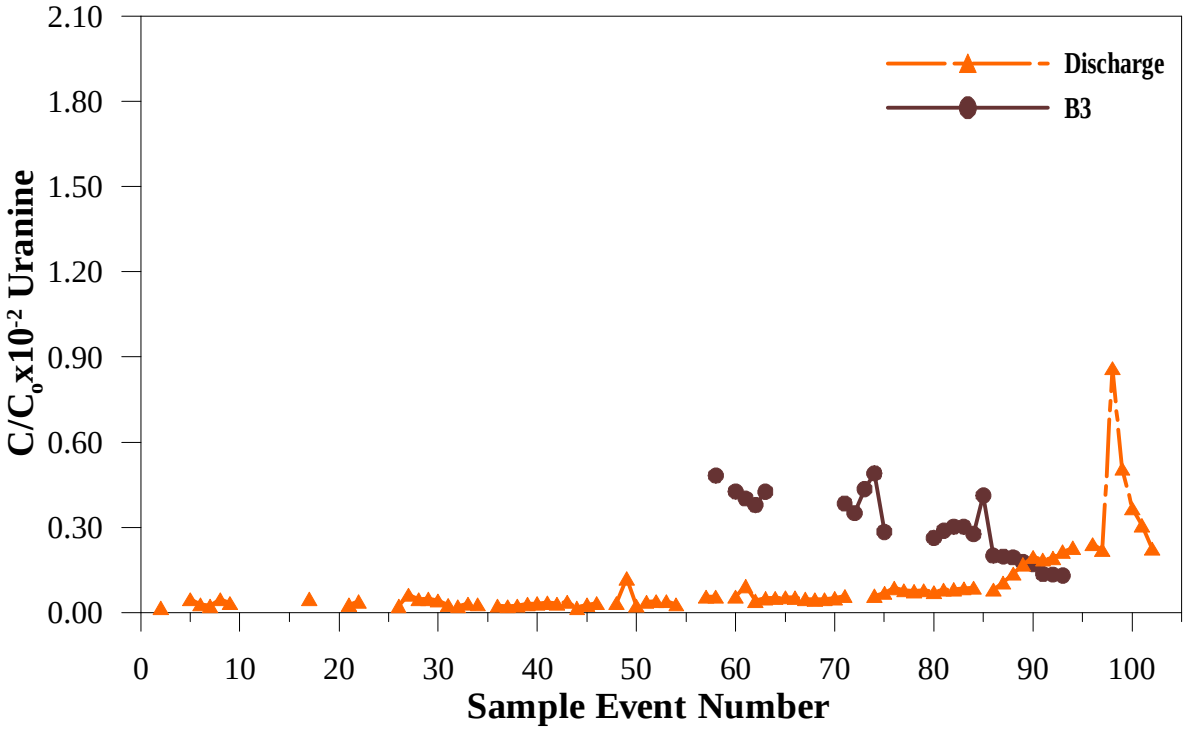

Figure 55. Breakthrough curves for uranine in injection well B3 after the straddle packer was removed, and from the discharge line.

Note: Sampling events generally occur every 4 hours. See Appendix 1.

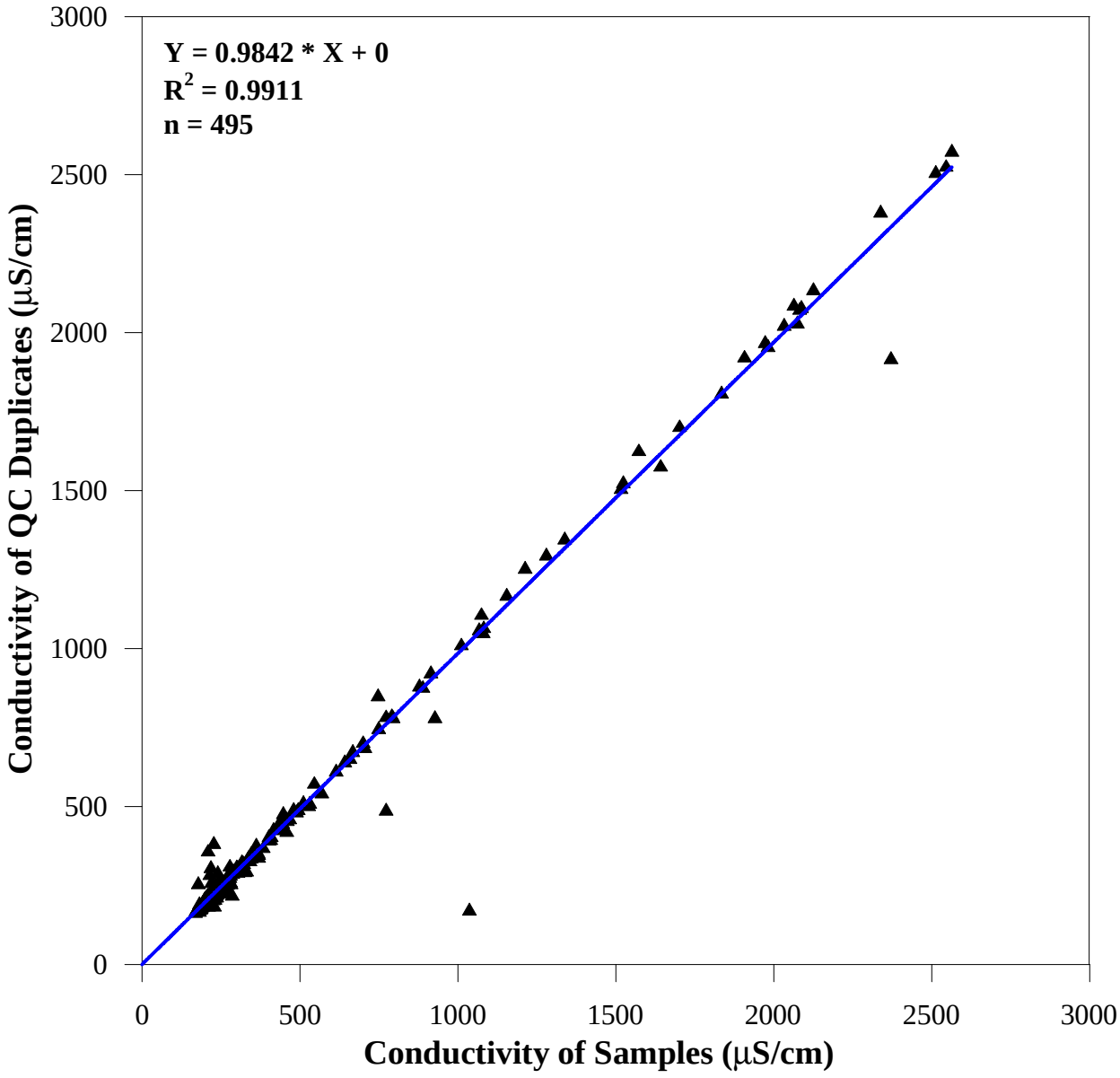

Figure 56. Comparison of 495 pairs of conductivity measurements for samples and QA/QC duplicates collected during the TTLT.

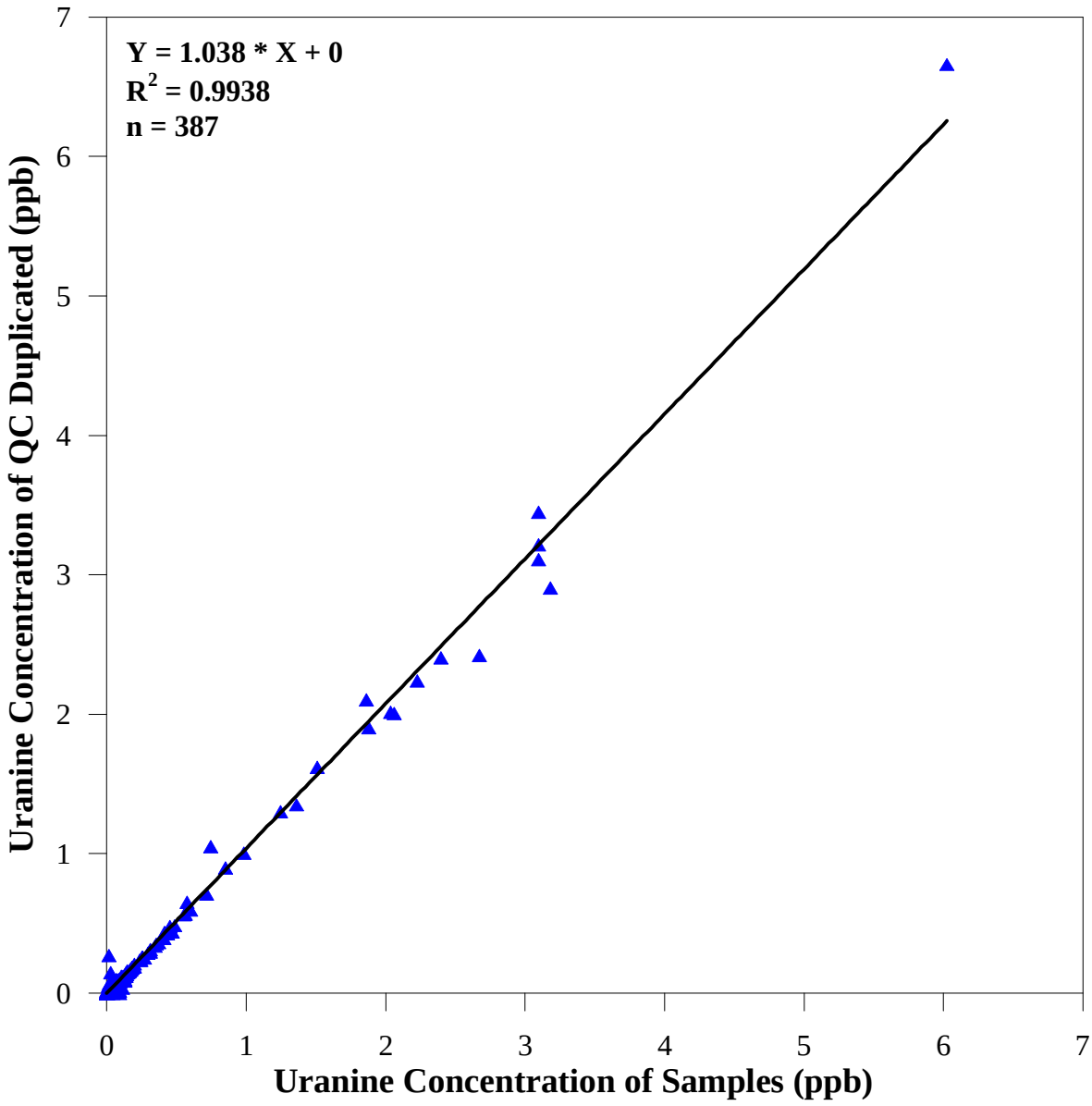

Figure 57. Comparison of 387 pairs of uranine concentration (fluorescence) measurements for samples and QA/QC duplicates collected during the TTLT.

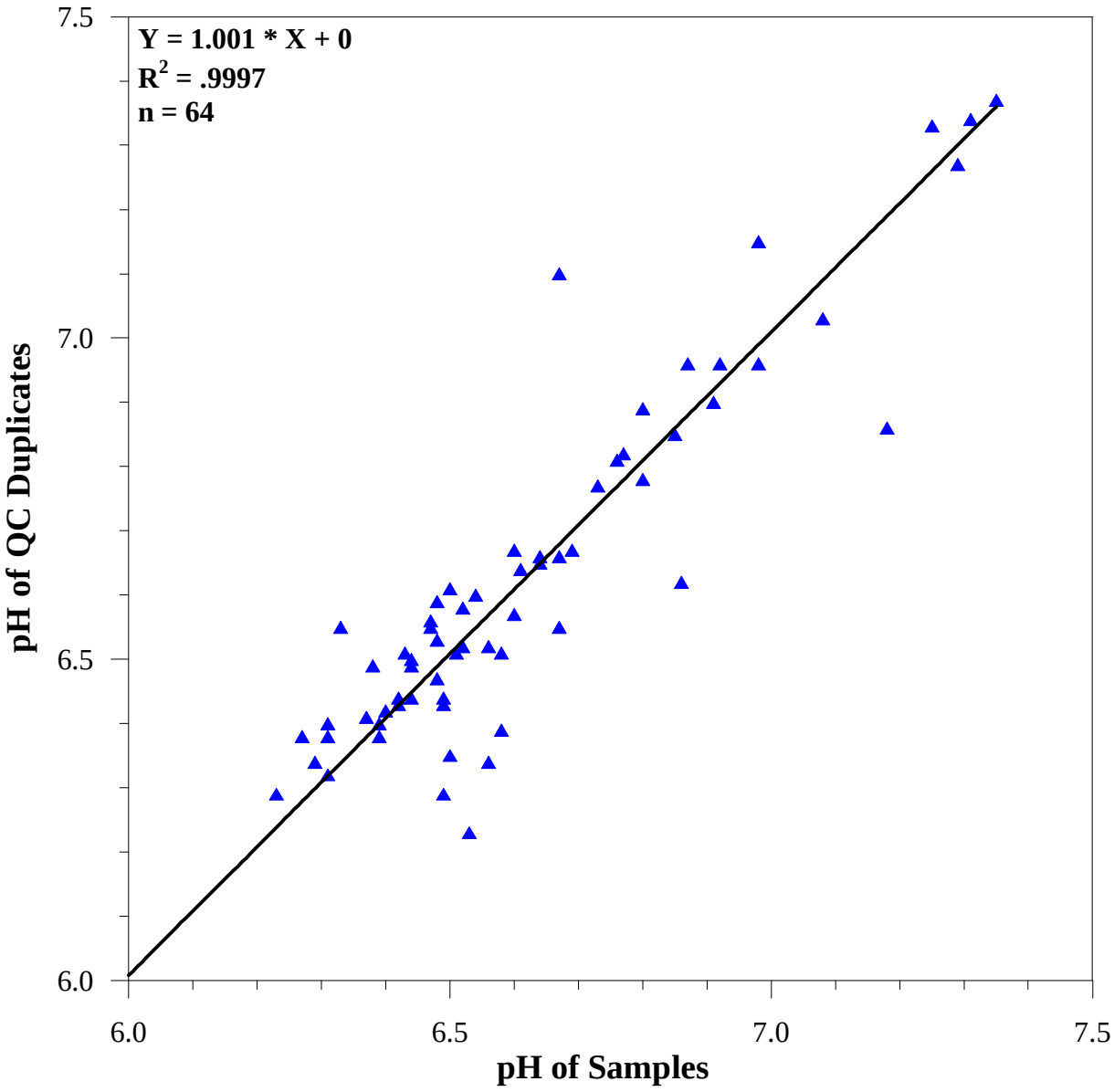

Figure 58. Comparison of 64 pairs of pH measurements for samples and QA/QC duplicates collected during the TTLT.

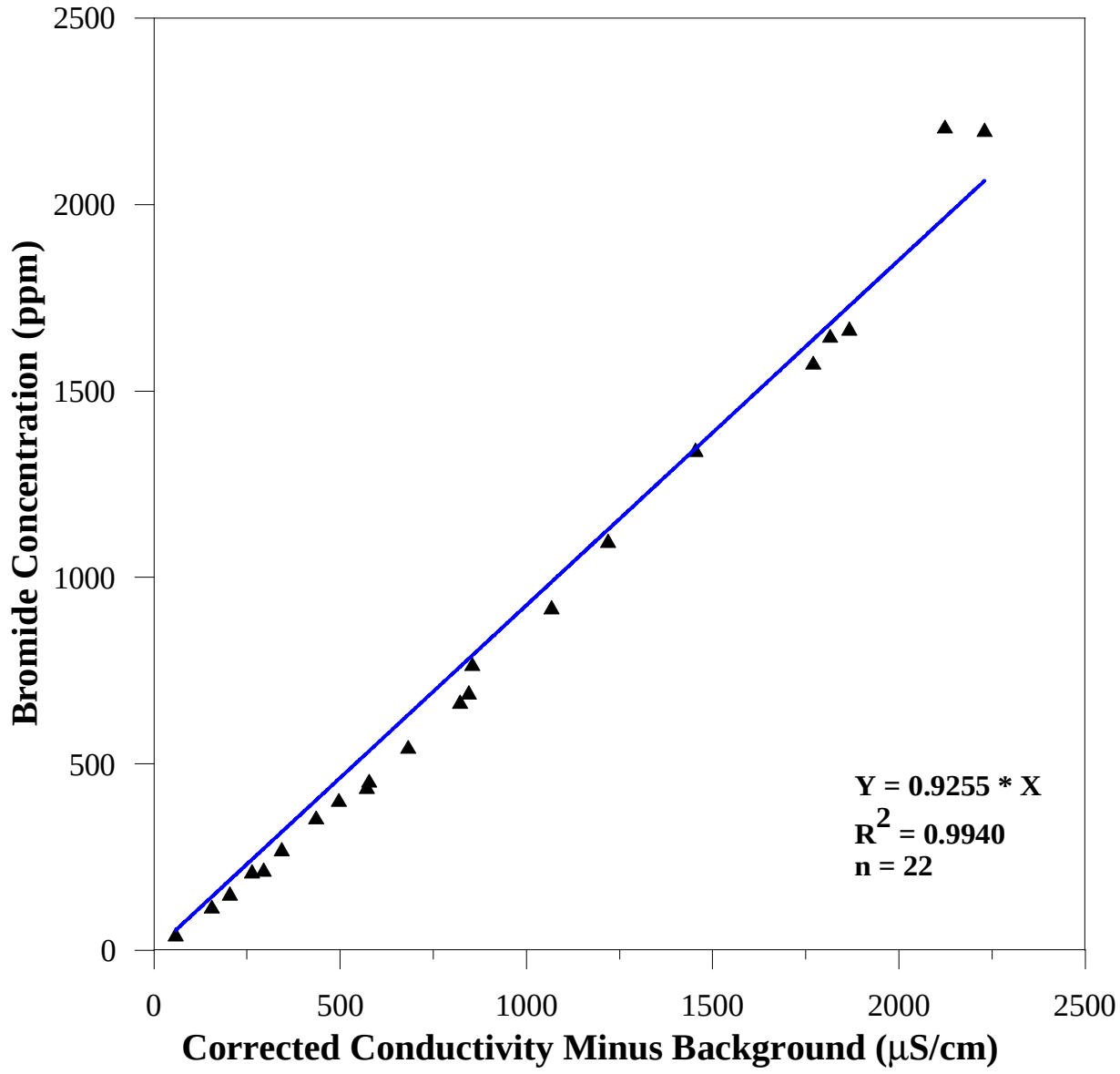

Figure 59. Relationship between conductivity (with probe measurements) and bromide concentration.

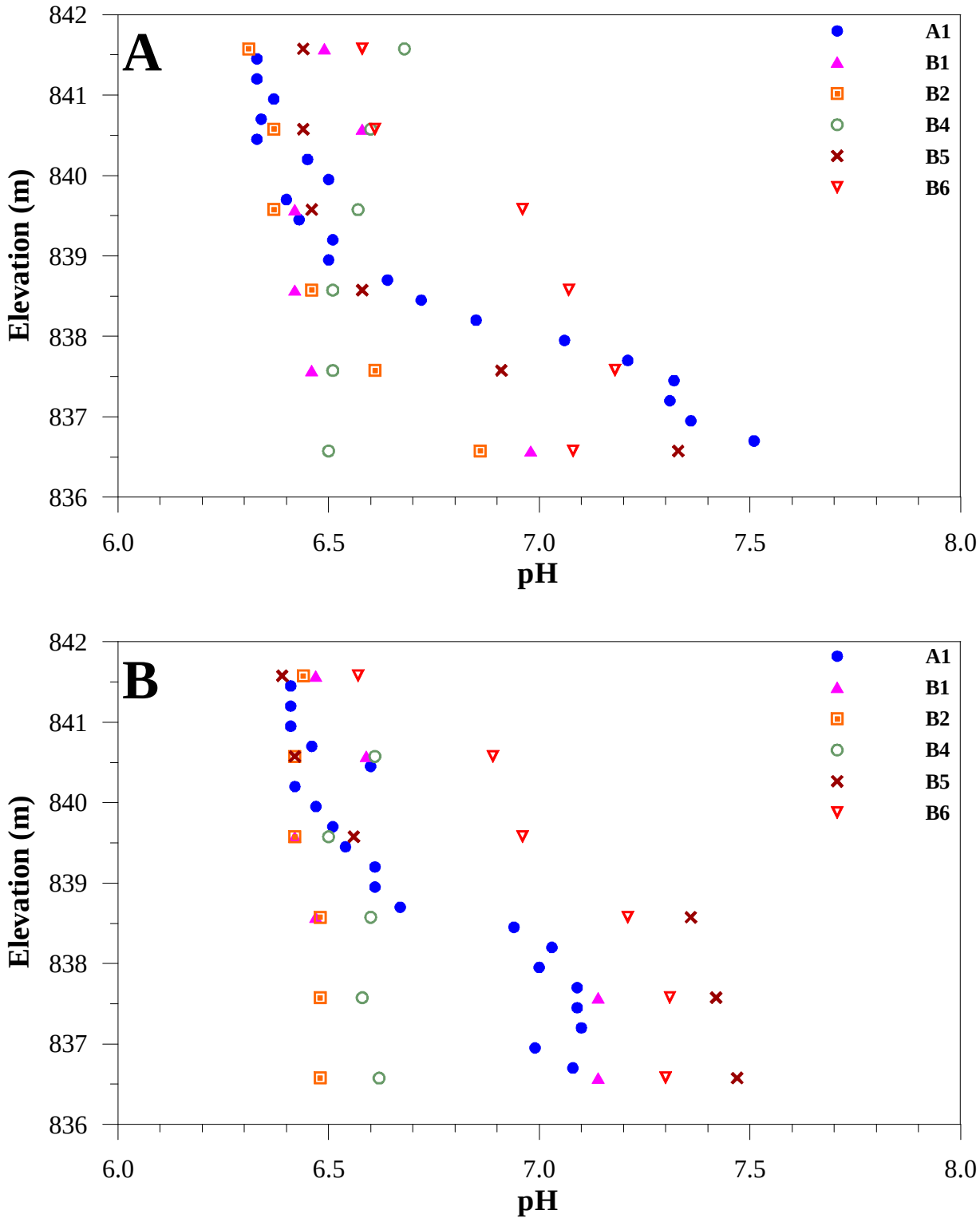

Figure 60. Typical pH profiles showing increase with depth. A. Sample event 5. B. Sample event 93.

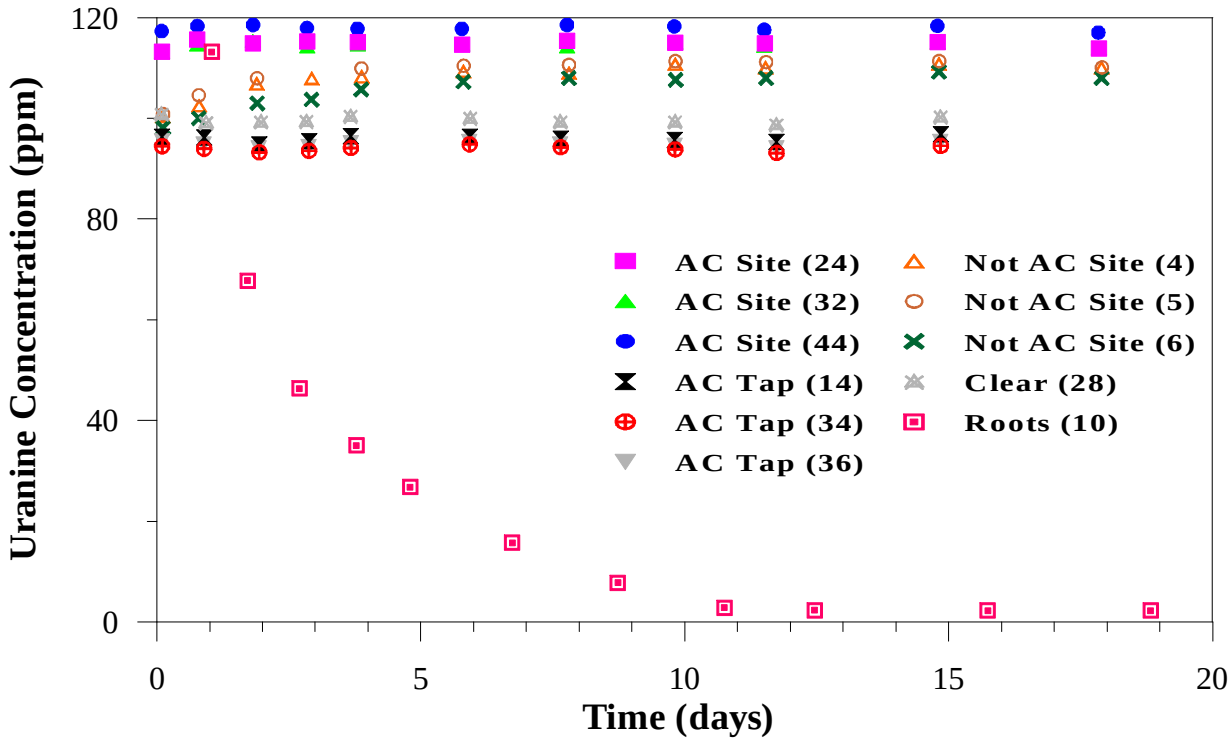

Figure 61. Changes in uranine concentration or fluorescence with time in microbiological experiment with 100 ppb uranine. No change in autoclaved (AC) site water and Boise tap water. Increase in uranine concentration of fluorescence over initial six days, then no further change in live site water without roots. Exponential decay in uranine concentration or fluorescence over 12 days in live site water with roots.

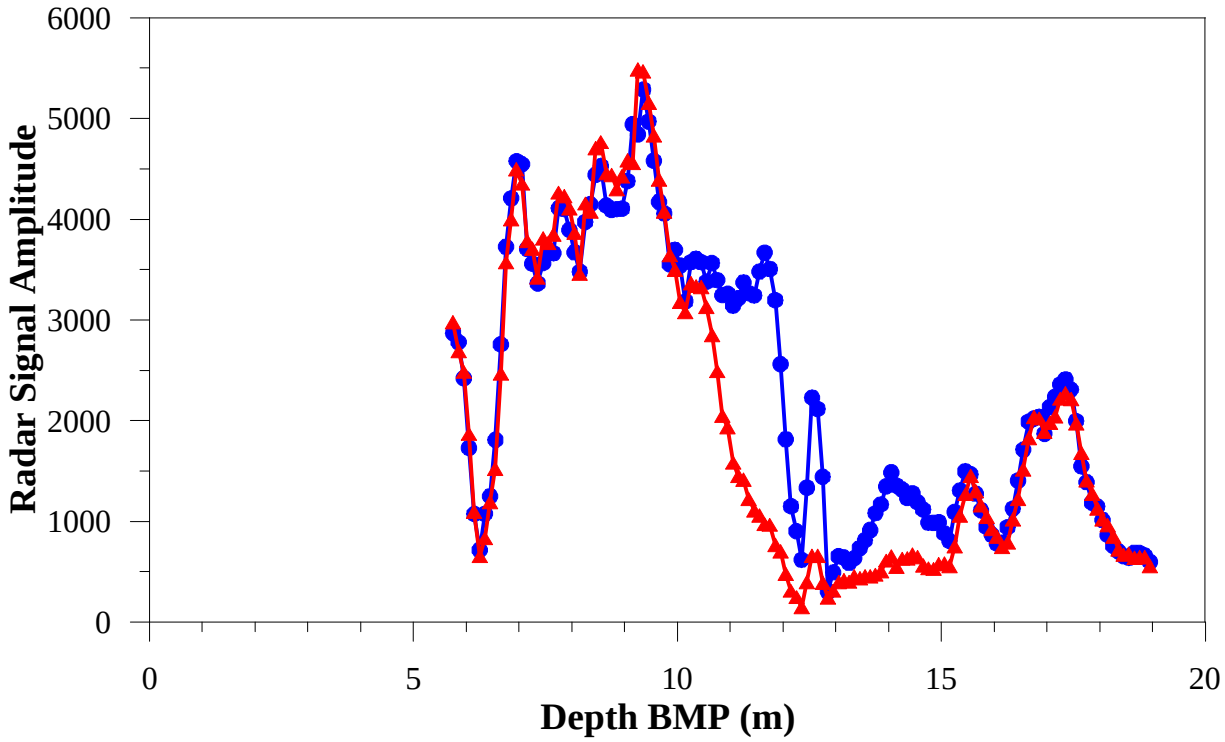

Figure 62. Radar level run data between wells B4 and B2 with 250 MHz antennas collected on the fourth and ninth days of the TTLT.

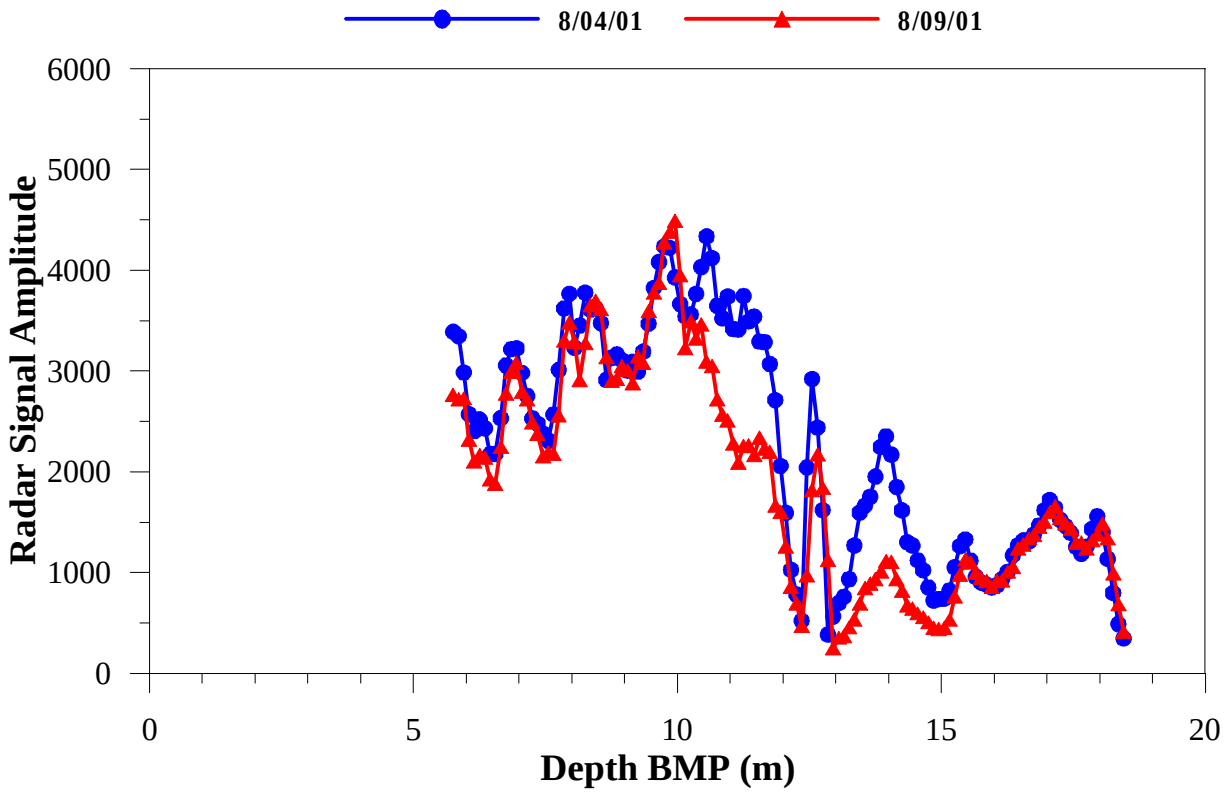

Figure 63. Radar level run data between wells B4 and B1 with 250 MHz antennas collected on the fourth and ninth days of the TTLT.

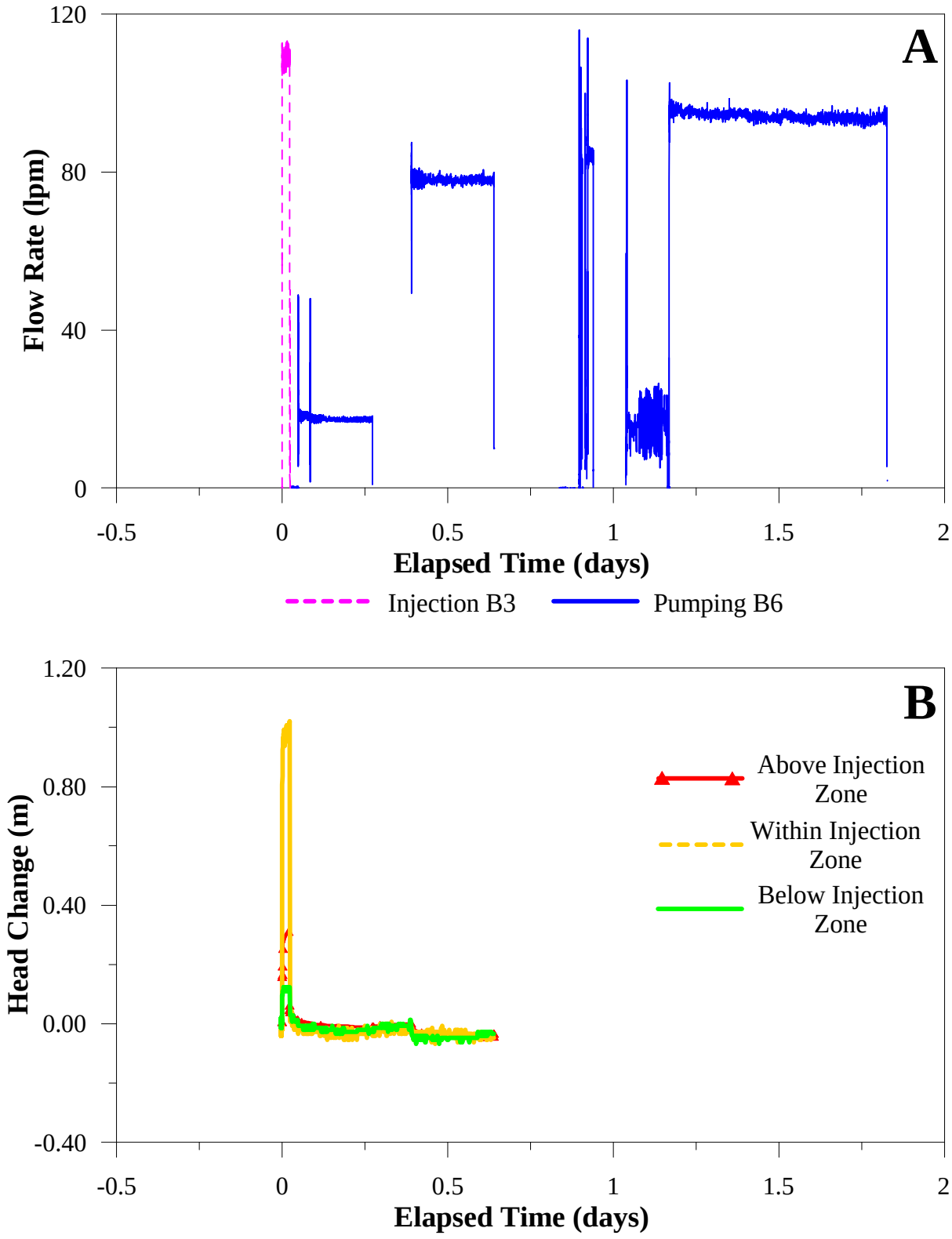

Figure 64. For test restart 2002: A. Record of flow rates (injection into B3, pumping from B6). B. Record of head change in B3.

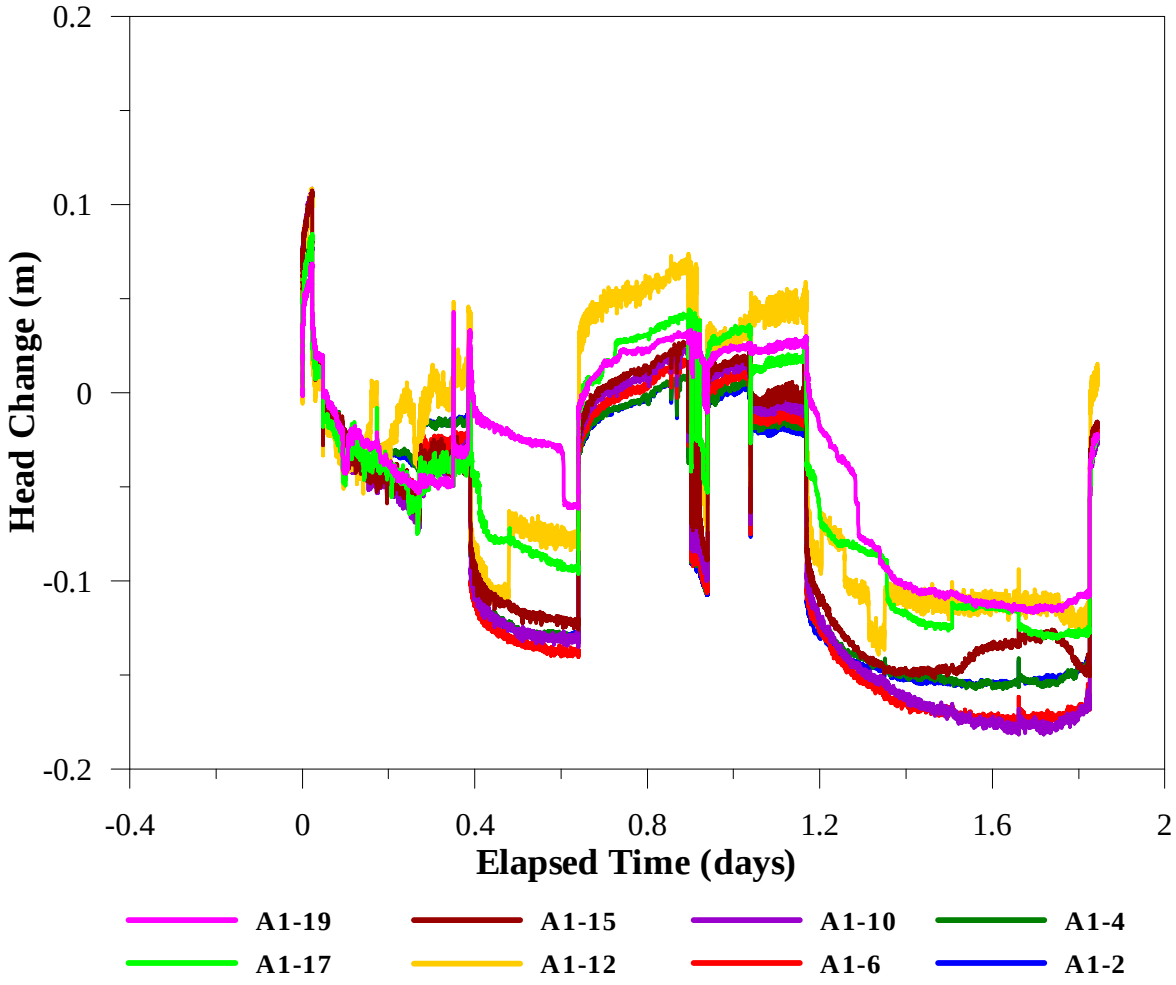

Figure 65. For test restart in 2002: Record of head change in zones in A1.

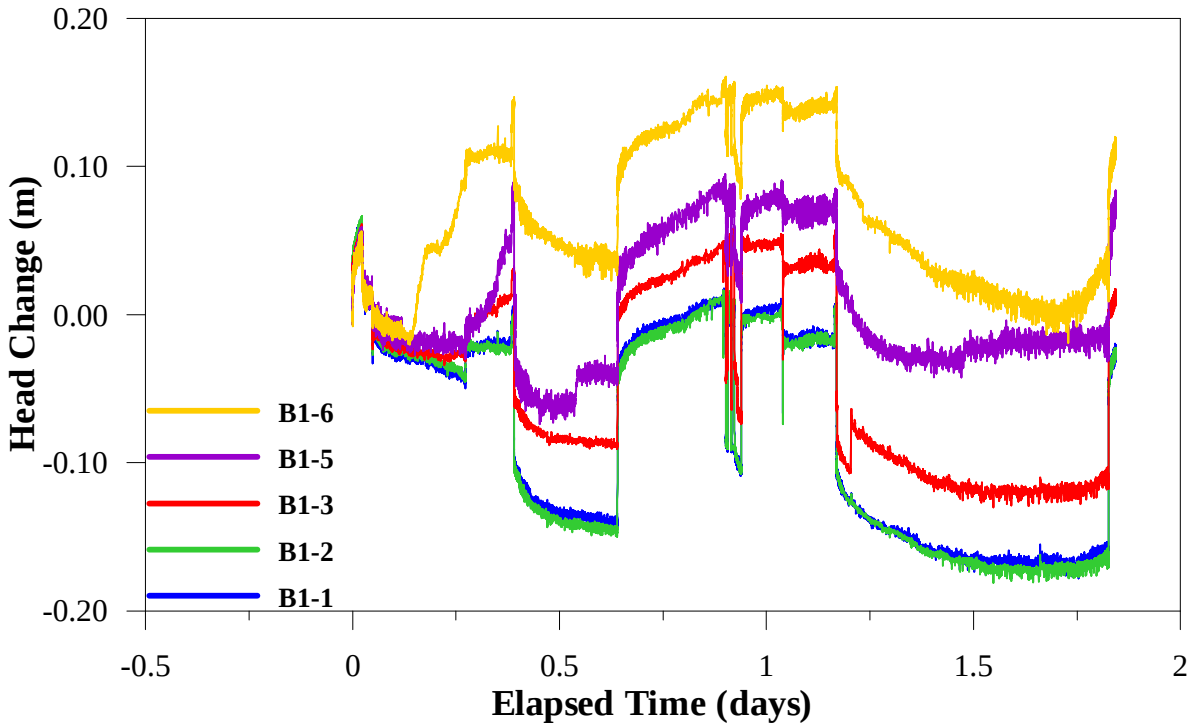

Figure 66. For test restart 2002: Record of head change in zones in B1.

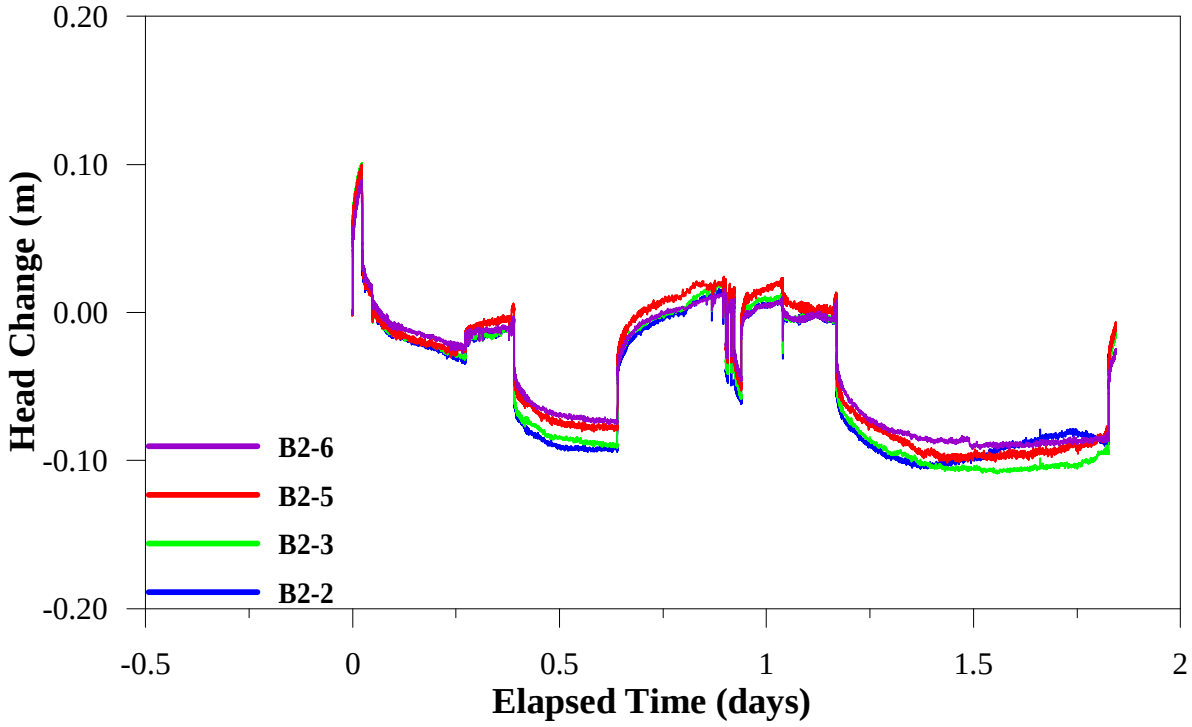

Figure 67. For test restart 2002: Record of head change in zones in B2.

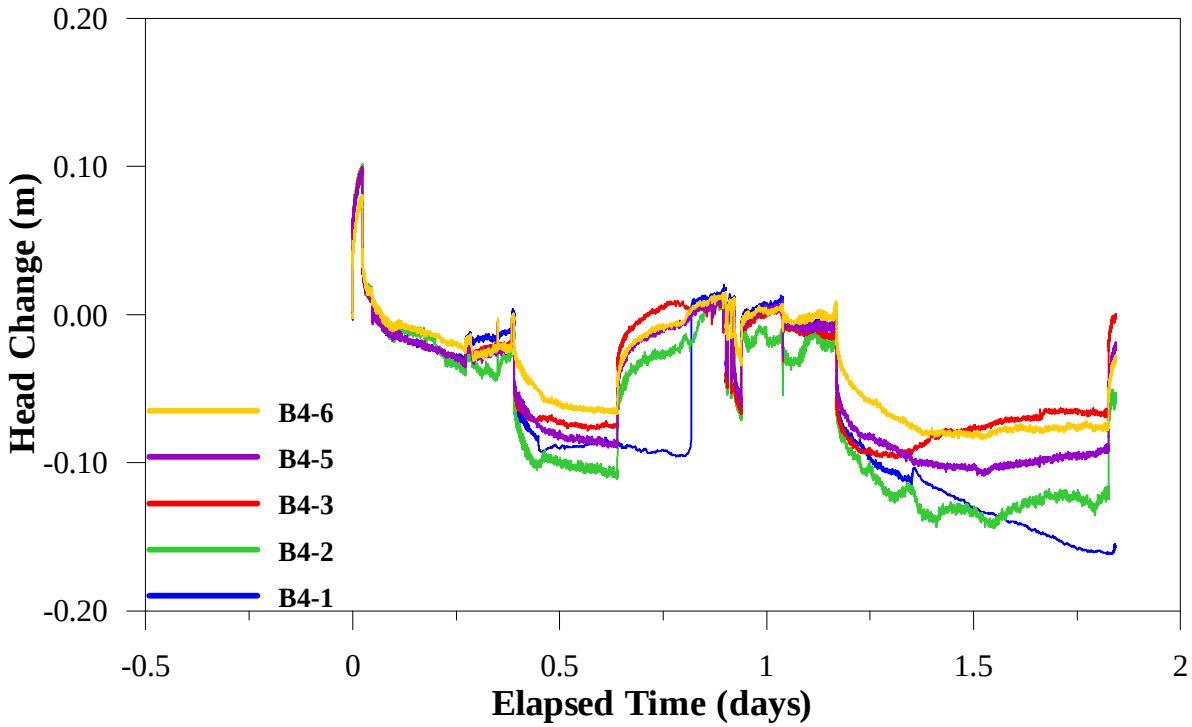

Figure 68. For test restart 2002: Record of head change in zones in B4.

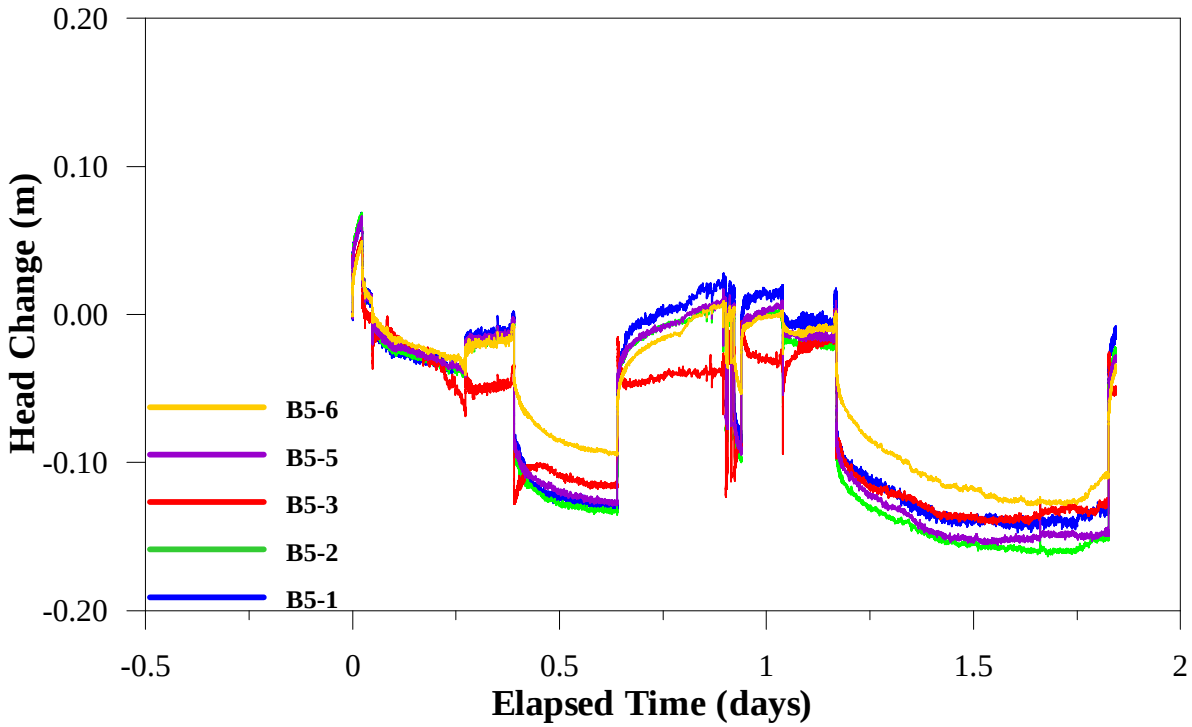

Figure 69. For test restart 2002: Record of head change in zones in B5.

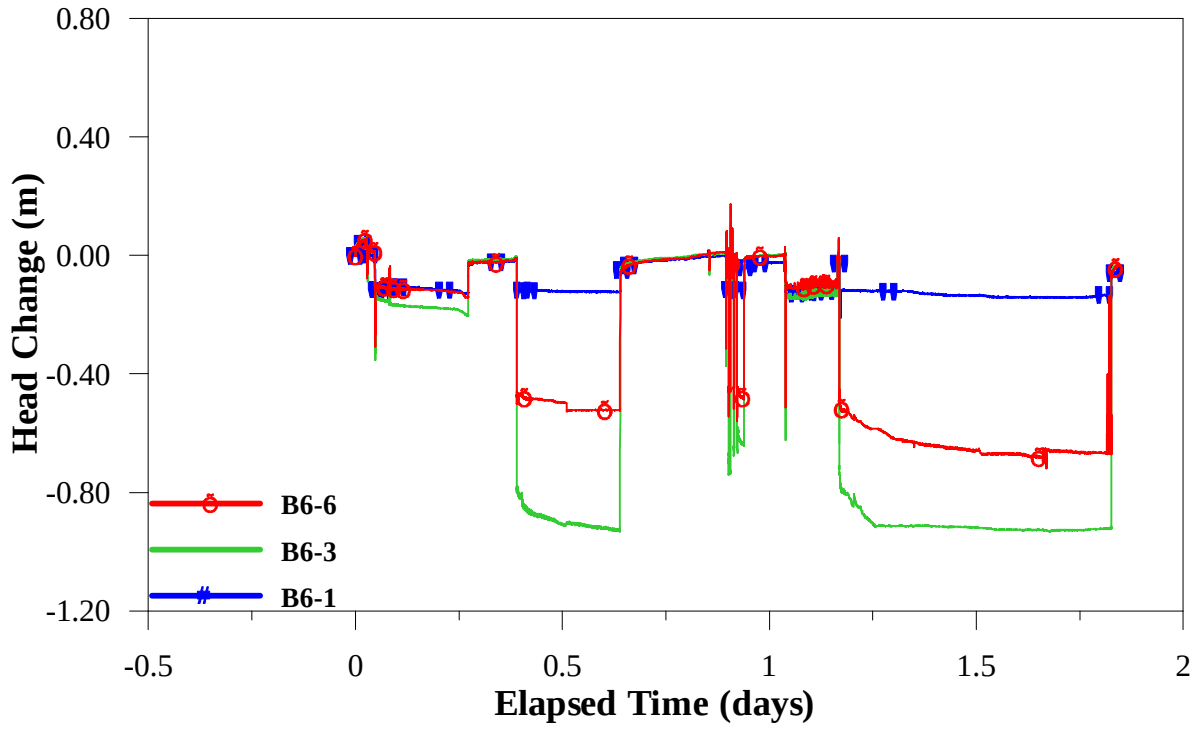

Figure 70. For test restart 2002: Record of head change in zones in B6.

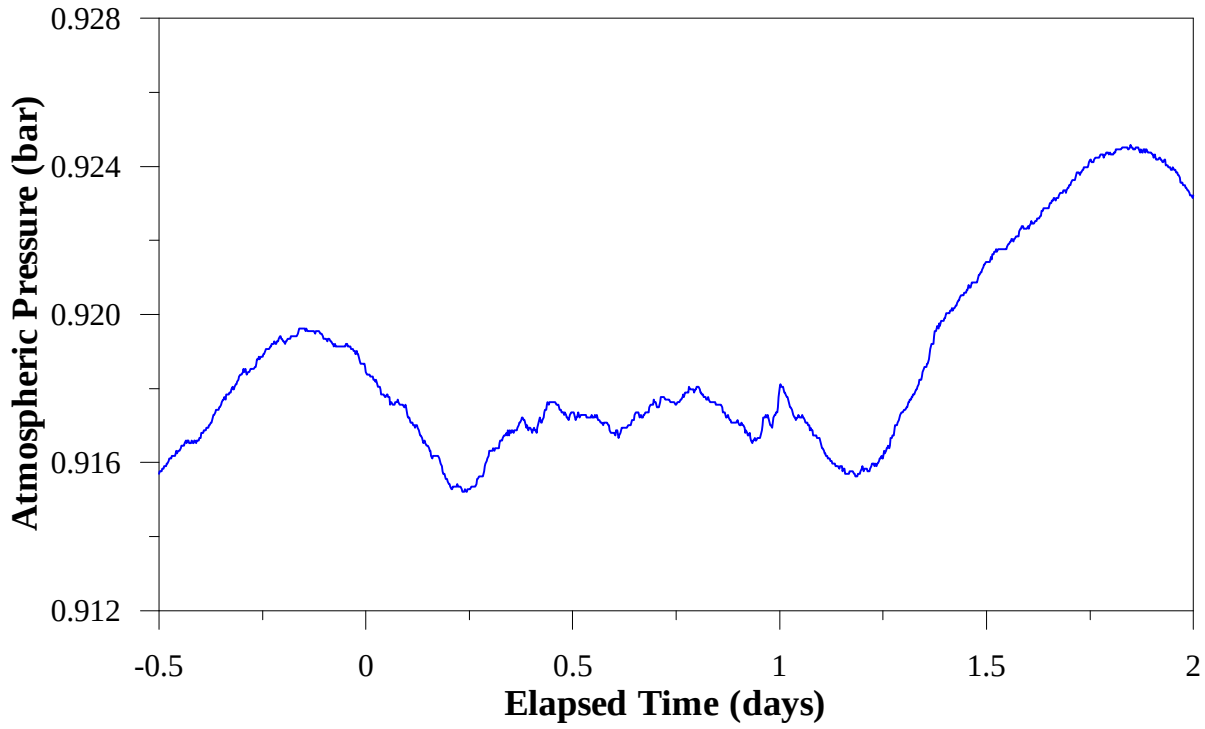

Figure 71. For test restart 2002: Record of atmospheric pressure.

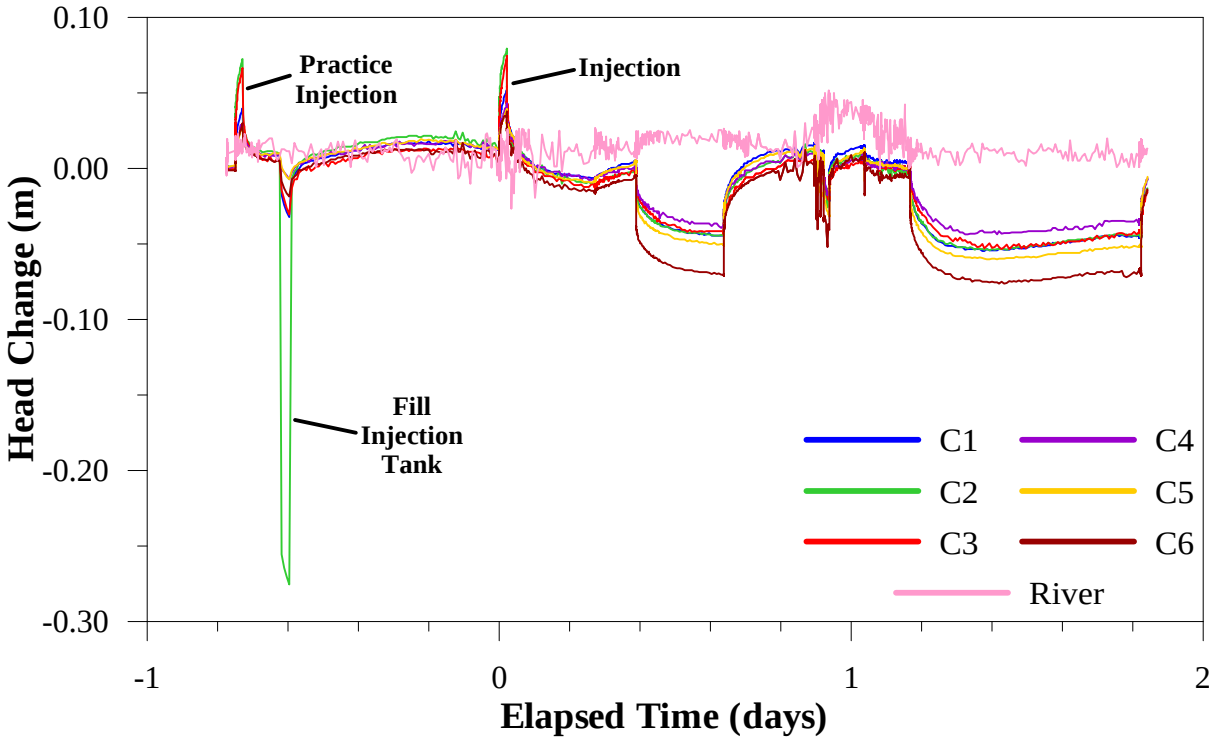

Figure 72. For test restart in 2002: Record of head change in C wells and the Boise River.

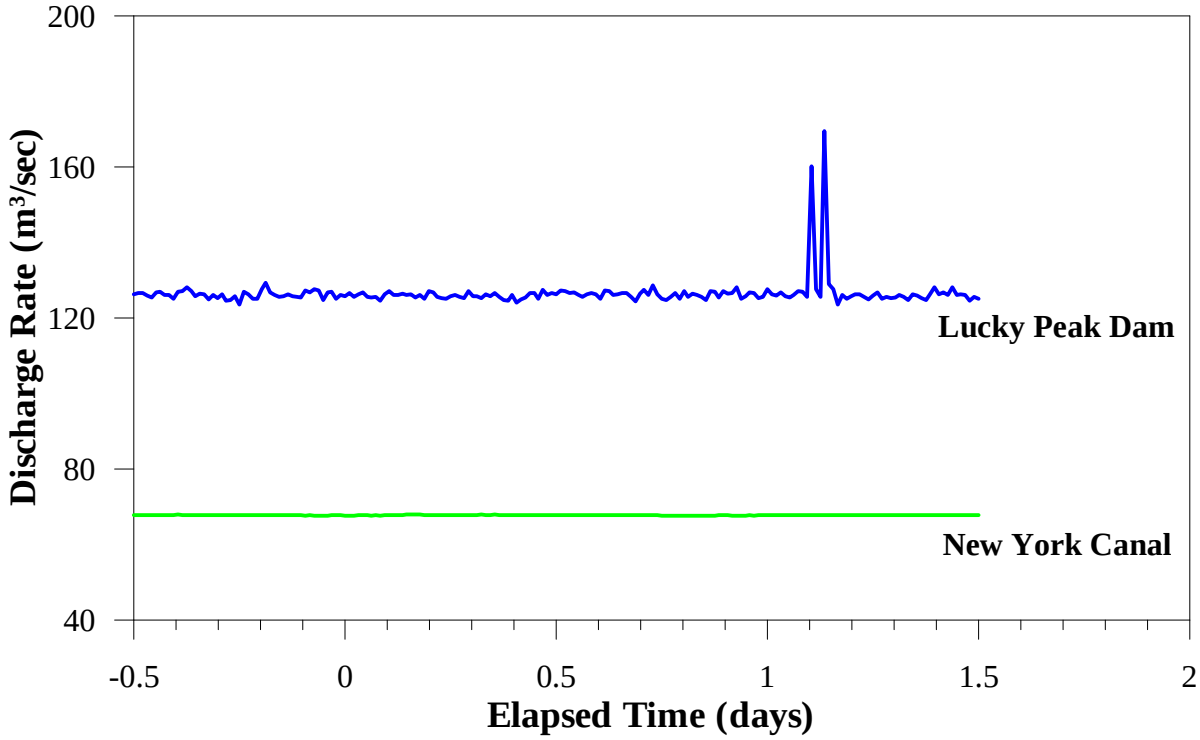

Figure 73. Record of discharge from Lucky Peak Dam to Boise River and discharge from Boise River to New York Canal nearby upstream of the BHRS.

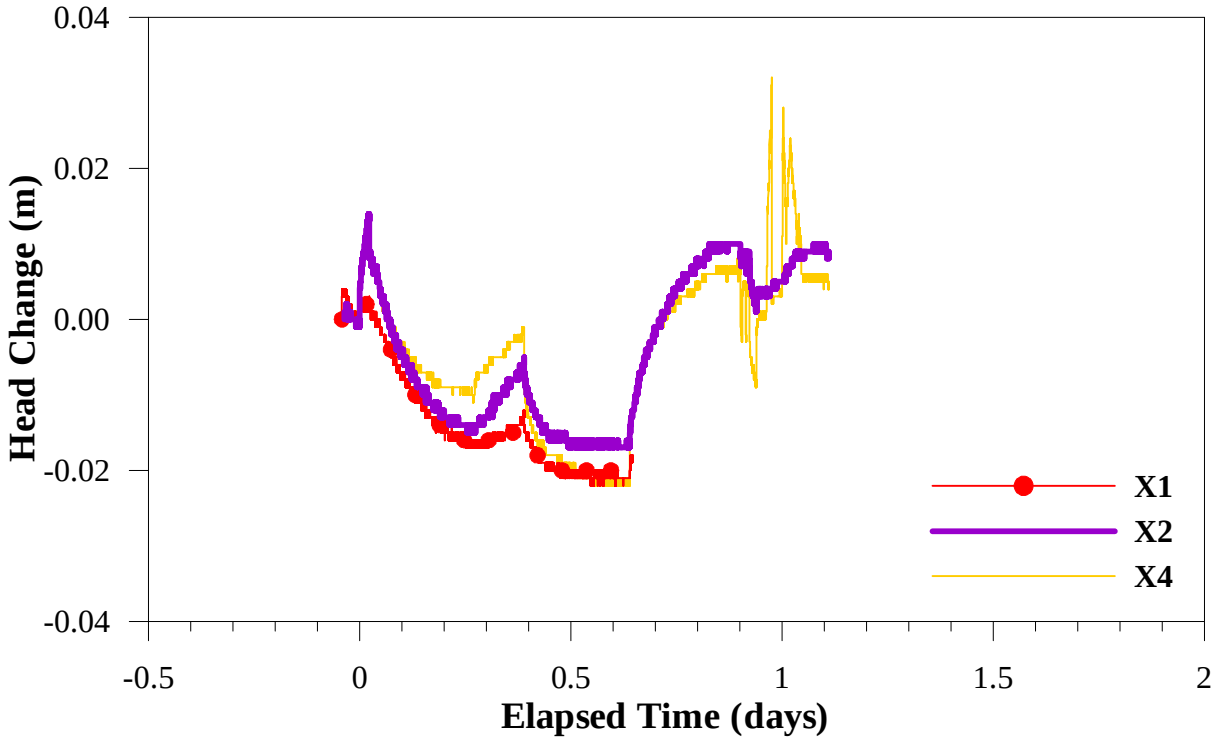

Figure 74. For test restart 2002: Record of head change in wells X1, X2, and X4.

Appendix 1. Sampling events and numbers and types of samples: Conductivity

			collected		analyzed					
Event	Date	Time	# samples	# QC	# samples	# QC	B3	B6(outflow)	Field	Lab
Bkgrd	31-Jul-2001	15:00	38	2	38	0	0	0	38	0
Bkgrd	01-Aug-2001	07:00	50	5	50	5	0	0	55	0
Inject	01-Aug-2001	11:40	13	0	13	0	0	0	13	0
1	01-Aug-2001	13:00	32	3	32	3	0	0	35	0
2	01-Aug-2001	16:00	34	6	32	6	0	2	40	0
3	01-Aug-2001	20:00	50	4	50	4	0	0	54	0
4	02-Aug-2001	00:14	50	5	50	5	0	0	55	0
5	02-Aug-2001	06:30	52	5	50	5	1	1	57	0
6	02-Aug-2001	11:00	51	5	50	5	0	1	56	0
7	02-Aug-2001	15:00	51	5	50	5	0	1	32	24
8	02-Aug-2001	19:00	51	5	50	5	0	1	25	31
9	02-Aug-2001	22:00	51	5	50	5	0	1	26	30
10	03-Aug-2001	01:00	51	5	50	5	0	1	21	35
11	03-Aug-2001	04:00	51	5	50	5	0	1	26	30
12	03-Aug-2001	07:00	50	5	50	5	0	0	28	27
13	03-Aug-2001	10:00	50	5	50	5	0	0	55	0
14	03-Aug-2001	14:00	51	5	50	5	0	1	32	24
15	03-Aug-2001	17:00	50	5	49	5	0	1	31	24
16	03-Aug-2001	20:00	50	4	49	4	0	1	25	29
17	03-Aug-2001	23:00	50	6	49	6	0	1	56	0
18	04-Aug-2001	07:00	50	6	50	6	0	0	56	0
19	04-Aug-2001	11:00	50	6	50	6	0	0	56	0
20	04-Aug-2001	15:00	50	5	50	5	0	0	55	0
21	04-Aug-2001	19:00	50	5	49	5	0	1	55	0
22	04-Aug-2001	23:00	50	5	49	5	0	1	55	0
23	05-Aug-2001	03:00	50	5	49	5	0	1	20	35
24	05-Aug-2001	07:00	49	6	49	6	0	0	55	0
25	05-Aug-2001	11:00	50	7	50	7	0	0	57	0
26	05-Aug-2001	15:00	50	6	49	6	0	1	56	0
27	05-Aug-2001	19:00	50	5	49	5	0	1	55	0
28	05-Aug-2001	23:00	50	5	49	5	0	1	55	0
29	06-Aug-2001	03:00	50	6	49	6	0	1	27	29
30	06-Aug-2001	07:00	50	5	49	5	0	1	55	0
31	06-Aug-2001	11:00	50	5	49	5	0	1	55	0
32	06-Aug-2001	15:00	51	5	49	5	1	1	56	0
33	06-Aug-2001	19:00	51	5	49	5	1	1	56	0
34	06-Aug-2001	23:00	51	5	49	5	1	1	56	0
35	07-Aug-2001	04:00	51	5	49	5	1	1	22	34

Appendix 1. Sampling events and numbers and types of samples: Conductivity (continued)

			collected		analyzed					
Event	Date	Time	# samples	# QC	# samples	# QC	B3	B6(outflow)	Field	Lab
36	07-Aug-2001	07:00	51	5	49	5	1	1	56	0
37	07-Aug-2001	11:00	51	5	49	5	1	1	56	0
38	07-Aug-2001	15:00	51	5	49	5	1	1	56	0
39	07-Aug-2001	19:00	50	5	49	5	0	1	55	0
40	07-Aug-2001	23:00	51	5	49	5	1	1	56	0
41	08-Aug-2001	03:00	51	5	49	5	1	1	25	31
42	08-Aug-2001	07:00	51	5	49	5	1	1	56	0
43	08-Aug-2001	11:00	51	5	49	5	1	1	56	0
44	08-Aug-2001	15:00	51	5	49	5	1	1	56	0
45	08-Aug-2001	19:00	51	5	49	5	1	1	56	0
46	08-Aug-2001	23:00	51	5	49	5	1	1	56	0
47	09-Aug-2001	03:00	51	5	49	5	1	1	21	35
48	09-Aug-2001	07:00	51	7	49	7	1	1	58	0
49	09-Aug-2001	11:00	51	6	49	6	1	1	57	0
50	09-Aug-2001	15:00	51	5	49	5	1	1	56	0
51	09-Aug-2001	19:00	51	5	49	5	1	1	56	0
52	09-Aug-2001	23:00	51	5	49	5	1	1	56	0
53	10-Aug-2001	03:00	51	5	49	5	1	1	28	28
54	10-Aug-2001	07:00	52	5	49	5	2	1	57	0
55	10-Aug-2001	11:00	49	5	49	5	0	0	54	0
56	10-Aug-2001	15:00	49	5	49	5	0	0	54	0
57	10-Aug-2001	19:00	50	4	49	4	0	1	54	0
58	10-Aug-2001	23:00	51	5	49	5	1	1	56	0
59	11-Aug-2001	03:00	51	5	49	5	1	1	20	36
60	11-Aug-2001	07:00	51	6	49	6	1	1	57	0
61	11-Aug-2001	11:00	51	5	49	5	1	1	56	0
62	11-Aug-2001	15:00	51	5	49	5	1	1	56	0
63	11-Aug-2001	19:00	51	5	49	5	1	1	56	0
64	11-Aug-2001	23:00	50	5	49	5	0	1	55	0
65	12-Aug-2001	03:00	52	5	49	5	2	1	21	36
66	12-Aug-2001	07:00	51	5	49	5	1	1	56	0
67	12-Aug-2001	11:00	51	5	49	5	1	1	56	0
68	12-Aug-2001	15:00	51	5	49	5	1	1	56	0
69	12-Aug-2001	19:00	52	4	49	4	2	1	56	0
70	12-Aug-2001	23:00	51	5	49	5	1	1	56	0
71	13-Aug-2001	03:00	51	5	49	5	1	1	27	29
72	13-Aug-2001	07:00	50	5	49	5	1	0	55	0

Appendix 1. Sampling events and numbers and types of samples: Conductivity (continued)

			collected		analyzed					
Event	Date	Time	# samples	# QC	# samples	# QC	B3	B6(outflow)	Field	Lab
73	13-Aug-2001	11:00	50	5	49	5	1	0	55	0
74	13-Aug-2001	15:00	51	5	49	5	1	1	56	0
75	13-Aug-2001	19:00	52	4	49	4	2	1	56	0
76	13-Aug-2001	23:00	51	5	49	5	1	1	56	0
77	14-Aug-2001	03:00	51	5	49	5	1	1	27	29
78	14-Aug-2001	07:00	52	4	49	4	2	1	56	0
79	14-Aug-2001	11:00	51	5	49	5	1	1	56	0
80	14-Aug-2001	15:00	51	5	49	5	1	1	56	0
81	14-Aug-2001	19:00	51	5	49	5	1	1	56	0
82	14-Aug-2001	23:00	51	5	49	5	1	1	56	0
83	15-Aug-2001	03:00	52	4	49	4	2	1	27	29
84	15-Aug-2001	07:00	51	4	49	4	1	1	55	0
85	15-Aug-2001	11:00	50	5	49	5	1	0	55	0
86	15-Aug-2001	15:00	51	5	49	5	1	1	56	0
87	15-Aug-2001	19:00	51	5	49	5	1	1	56	0
88	15-Aug-2001	23:00	51	5	49	5	1	1	56	0
89	16-Aug-2001	03:00	51	5	49	5	1	1	33	23
90	16-Aug-2001	07:00	52	4	49	4	2	1	56	0
91	16-Aug-2001	11:00	52	4	49	4	2	1	56	0
92	16-Aug-2001	15:00	51	5	49	5	1	1	56	0
93	16-Aug-2001	19:00	51	5	49	5	1	1	56	0
94	16-Aug-2001	23:00	51	5	49	5	1	1	27	29
95	17-Aug-2001	03:00	51	4	49	4	1	1	24	31
96	17-Aug-2001	07:00	51	5	49	5	1	1	56	0
97	17-Aug-2001	11:00	51	5	49	5	1	1	27	29
98	17-Aug-2001	19:00	7	1	6	1	0	1	8	0
99	17-Aug-2001	23:00	7	1	6	1	0	1	8	0
100	18-Aug-2001	03:00	7	1	6	1	0	1	8	0
101	18-Aug-2001	07:00	7	1	6	1	0	1	8	0
102	18-Aug-2001	11:00	7	1	6	1	0	1	8	0
	Total		5024	497	4866	495	70	88	4802	717

Appendix 2. Sampling events and numbers and types of samples: Uranine

			collected		analyzed					
Event	Date	Time	# samples	# QC	# samples	# QC	B3	B6(outflow)	Field	Lab
Bkgrd	31-Jul-2001	15:00	38	2	38	2	0	0	40	0
Bkgrd	01-Aug-2001	07:00	50	5	50	5	0	0	55	0
Inject	01-Aug-2001	11:40	13	0	13	0	0	0	13	0
1	01-Aug-2001	13:00	32	3	32	3	0	0	35	0
2	01-Aug-2001	16:00	34	6	32	3	0	0	35	0
3	01-Aug-2001	20:00	50	4	50	4	0	0	54	0
4	02-Aug-2001	00:14	50	5	50	5	0	0	55	0
5	02-Aug-2001	06:30	52	5	50	5	1	1	57	0
6	02-Aug-2001	11:00	51	5	50	5	0	0	55	0
7	02-Aug-2001	15:00	51	5	50	5	0	1	56	0
8	02-Aug-2001	19:00	51	5	26	0	0	1	27	0
9	02-Aug-2001	22:00	51	5	26	0	0	1	27	0
10	03-Aug-2001	01:00	51	5	20	0	0	0	20	0
11	03-Aug-2001	04:00	51	5	26	0	0	0	26	0
12	03-Aug-2001	07:00	50	5	26	2	0	0	28	0
13	03-Aug-2001	10:00	50	5	50	5	0	0	55	0
14	03-Aug-2001	14:00	51	5	31	0	0	0	31	0
15	03-Aug-2001	17:00	50	5	30	0	0	0	30	0
16	03-Aug-2001	20:00	50	4	25	0	0	0	25	0
17	03-Aug-2001	23:00	50	6	49	5	0	1	55	0
18	04-Aug-2001	07:00	50	6	50	6	0	0	56	0
19	04-Aug-2001	11:00	50	6	50	6	0	0	56	0
20	04-Aug-2001	15:00	50	5	50	5	0	0	55	0
21	04-Aug-2001	19:00	50	5	49	5	0	1	55	0
22	04-Aug-2001	23:00	50	5	49	5	0	1	55	0
23	05-Aug-2001	03:00	50	5	20	0	0	0	20	0
24	05-Aug-2001	07:00	49	6	49	5	0	0	54	0
25	05-Aug-2001	11:00	50	7	49	5	0	0	54	0
26	05-Aug-2001	15:00	50	6	47	6	0	1	54	0
27	05-Aug-2001	19:00	50	5	49	6	0	1	56	0
28	05-Aug-2001	23:00	50	5	49	5	0	1	55	0
29	06-Aug-2001	03:00	50	6	20	5	0	1	26	0
30	06-Aug-2001	07:00	50	5	49	5	0	1	55	0
31	06-Aug-2001	11:00	50	5	49	5	0	1	55	0
32	06-Aug-2001	15:00	51	5	49	5	2	1	57	0
33	06-Aug-2001	19:00	51	5	49	5	1	1	56	0
34	06-Aug-2001	23:00	51	5	49	5	1	1	56	0
35	07-Aug-2001	04:00	51	5	20	2	0	0	22	0

Appendix 2. Sampling events and numbers and types of samples: Uranine (continued)

			collected		analyzed					
Event	Date	Time	# samples	# QC	# samples	# QC	B3	B6(outflow)	Field	Lab
36	07-Aug-2001	07:00	51	5	49	5	1	1	56	0
37	07-Aug-2001	11:00	51	5	49	5	1	1	56	0
38	07-Aug-2001	15:00	51	5	49	5	1	1	56	0
39	07-Aug-2001	19:00	50	5	49	5	0	1	55	0
40	07-Aug-2001	23:00	51	5	49	5	1	1	56	0
41	08-Aug-2001	03:00	51	5	20	2	1	1	24	0
42	08-Aug-2001	07:00	51	5	49	5	1	1	56	0
43	08-Aug-2001	11:00	51	5	49	5	1	1	56	0
44	08-Aug-2001	15:00	51	5	49	5	1	1	56	0
45	08-Aug-2001	19:00	51	5	49	5	1	1	56	0
46	08-Aug-2001	23:00	51	5	49	5	1	1	56	0
47	09-Aug-2001	03:00	51	5	20	0	1	0	21	0
48	09-Aug-2001	07:00	51	7	49	7	1	1	58	0
49	09-Aug-2001	11:00	51	6	49	5	1	1	56	0
50	09-Aug-2001	15:00	51	5	49	5	1	1	56	0
51	09-Aug-2001	19:00	51	5	49	5	1	1	56	0
52	09-Aug-2001	23:00	51	5	49	4	1	1	55	0
53	10-Aug-2001	03:00	51	5	20	5	1	1	27	0
54	10-Aug-2001	07:00	52	5	48	5	2	1	56	0
55	10-Aug-2001	11:00	49	5	49	5	0	0	54	0
56	10-Aug-2001	15:00	49	5	49	5	0	0	54	0
57	10-Aug-2001	19:00	50	4	49	4	0	1	54	0
58	10-Aug-2001	23:00	51	5	49	5	1	1	56	0
59	11-Aug-2001	03:00	51	5	20	0	0	0	20	0
60	11-Aug-2001	07:00	51	6	49	6	1	1	57	0
61	11-Aug-2001	11:00	51	5	49	5	1	1	56	0
62	11-Aug-2001	15:00	51	5	49	4	1	1	55	0
63	11-Aug-2001	19:00	51	5	49	4	1	1	55	0
64	11-Aug-2001	23:00	50	5	49	4	1	1	55	0
65	12-Aug-2001	03:00	52	5	20	0	0	1	21	0
66	12-Aug-2001	07:00	51	5	49	5	1	1	56	0
67	12-Aug-2001	11:00	51	5	49	5	1	1	56	0
68	12-Aug-2001	15:00	51	5	49	5	1	1	56	0
69	12-Aug-2001	19:00	52	4	49	4	2	1	56	0
70	12-Aug-2001	23:00	51	5	49	4	1	1	55	0
71	13-Aug-2001	03:00	51	5	20	4	1	1	26	0
72	13-Aug-2001	07:00	50	5	49	5	1	0	55	0
73	13-Aug-2001	11:00	50	5	49	5	1	0	55	0
74	13-Aug-2001	15:00	51	5	49	5	1	1	56	0

Appendix 2. Sampling events and numbers and types of samples: Uranine (continued)

			collected		analyzed					
Event	Date	Time	# samples	# QC	# samples	# QC	B3	B6(outflow)	Field	Lab
75	13-Aug-2001	19:00	52	4	49	4	2	1	56	0
76	13-Aug-2001	23:00	51	5	49	4	1	1	55	0
77	14-Aug-2001	03:00	51	5	20	4	1	1	26	0
78	14-Aug-2001	07:00	52	4	49	4	2	1	56	0
79	14-Aug-2001	11:00	51	5	49	5	1	1	56	0
80	14-Aug-2001	15:00	51	5	49	5	1	1	56	0
81	14-Aug-2001	19:00	51	5	49	5	1	1	56	0
82	14-Aug-2001	23:00	51	5	49	4	1	1	55	0
83	15-Aug-2001	03:00	52	4	20	4	2	1	27	0
84	15-Aug-2001	07:00	51	4	49	4	1	1	55	0
85	15-Aug-2001	11:00	50	5	49	5	1	0	55	0
86	15-Aug-2001	15:00	51	5	49	5	1	1	56	0
87	15-Aug-2001	19:00	51	5	49	5	1	1	56	0
88	15-Aug-2001	23:00	51	5	49	4	1	1	55	0
89	16-Aug-2001	03:00	51	5	26	4	1	1	32	0
90	16-Aug-2001	07:00	52	4	49	4	2	1	56	0
91	16-Aug-2001	11:00	52	4	49	4	2	1	56	0
92	16-Aug-2001	15:00	51	5	49	5	1	1	56	0
93	16-Aug-2001	19:00	51	5	49	5	1	1	56	0
94	16-Aug-2001	23:00	51	5	26	0	0	1	27	0
95	17-Aug-2001	03:00	51	4	0	0	0	0	0	0
96	17-Aug-2001	07:00	51	5	49	5	1	1	56	0
97	17-Aug-2001	11:00	51	5	26	1	0	1	28	0
98	17-Aug-2001	19:00	7	1	6	1	0	1	8	0
99	17-Aug-2001	23:00	7	1	6	1	0	1	8	0
100	18-Aug-2001	03:00	7	1	6	1	0	1	8	0
101	18-Aug-2001	07:00	7	1	6	1	0	1	8	0
102	18-Aug-2001	11:00	7	1	6	1	0	1	8	0
	Total		5024	497	4237	402	65	75	4779	0

Appendix 3. Sampling events and numbers and types of samples: pH

			collected		analyzed					
Event	Date	Time	# samples	# QC	# samples	# QC	B3	B6(outflow)	Field	Lab
Bkgrd	31-Jul-2001	15:00	38	2	37	0	0	0	37	0
Bkgrd	01-Aug-2001	07:00	50	5	8	5	0	0	13	0
Inject	01-Aug-2001	11:40	13	0	13	1	0	0	14	0
1	01-Aug-2001	13:00	32	3	6	0	0	0	6	0
2	01-Aug-2001	16:00	34	6	5	0	0	0	5	0
3	01-Aug-2001	20:00	50	4	6	0	0	0	6	0
4	02-Aug-2001	00:14	50	5	5	0	0	0	5	0
5	02-Aug-2001	06:30	52	5	50	5	1	1	57	0
6	02-Aug-2001	11:00	51	5	50	5	0	1	56	0
7	02-Aug-2001	15:00	51	5	49	5	0	1	55	0
8	02-Aug-2001	19:00	51	5	18	0	0	0	18	0
9	02-Aug-2001	22:00	51	5	0	0	0	0	0	0
10	03-Aug-2001	01:00	51	5	0	0	0	0	0	0
11	03-Aug-2001	04:00	51	5	0	0	0	0	0	0
12	03-Aug-2001	07:00	50	5	0	0	0	0	0	0
13	03-Aug-2001	10:00	50	5	0	0	0	0	0	0
14	03-Aug-2001	14:00	51	5	18	0	0	0	18	0
15	03-Aug-2001	17:00	50	5	29	0	0	0	29	0
16	03-Aug-2001	20:00	50	4	24	0	0	0	24	0
17	03-Aug-2001	23:00	50	6	0	0	0	0	0	0
18	04-Aug-2001	07:00	50	6	0	0	0	0	0	0
19	04-Aug-2001	11:00	50	6	0	0	0	0	0	0
20	04-Aug-2001	15:00	50	5	0	0	0	0	0	0
21	04-Aug-2001	19:00	50	5	0	0	0	0	0	0
22	04-Aug-2001	23:00	50	5	0	0	0	0	0	0
23	05-Aug-2001	03:00	50	5	0	0	0	0	0	0
24	05-Aug-2001	07:00	49	6	0	0	0	0	0	0
25	05-Aug-2001	11:00	50	7	0	0	0	0	0	0
26	05-Aug-2001	15:00	50	6	0	0	0	0	0	0
27	05-Aug-2001	19:00	50	5	0	0	0	0	0	0
28	05-Aug-2001	23:00	50	5	0	0	0	0	0	0
29	06-Aug-2001	03:00	50	6	0	0	0	0	0	0
30	06-Aug-2001	07:00	50	5	0	0	0	0	0	0
31	06-Aug-2001	11:00	50	5	0	0	0	0	0	0
32	06-Aug-2001	15:00	51	5	15	1	2	1	19	0
33	06-Aug-2001	19:00	51	5	11	0	0	1	12	0
34	06-Aug-2001	23:00	51	5	16	2	1	0	19	0
35	07-Aug-2001	04:00	51	5	0	0	0	0	0	0

Appendix 3. Sampling events and numbers and types of samples: pH (continued)

			collected		analyzed					
Event	Date	Time	# samples	# QC	# samples	# QC	B3	B6(outflow)	Field	Lab
36	07-Aug-2001	07:00	51	5	0	0	0	0	0	0
37	07-Aug-2001	11:00	51	5	0	0	0	0	0	0
38	07-Aug-2001	15:00	51	5	11	1	1	0	13	0
39	07-Aug-2001	19:00	50	5	11	1	0	0	12	0
40	07-Aug-2001	23:00	51	5	11	0	1	1	13	0
41	08-Aug-2001	03:00	51	5	4	2	1	1	8	0
42	08-Aug-2001	07:00	51	5	11	1	0	0	12	0
43	08-Aug-2001	11:00	51	5	23	4	1	1	29	0
44	08-Aug-2001	15:00	51	5	49	5	1	1	56	0
45	08-Aug-2001	19:00	51	5	49	5	1	1	56	0
46	08-Aug-2001	23:00	51	5	11	0	0	0	11	0
47	09-Aug-2001	03:00	51	5	0	0	0	0	0	0
48	09-Aug-2001	07:00	51	7	0	0	0	0	0	0
49	09-Aug-2001	11:00	51	6	0	0	0	0	0	0
50	09-Aug-2001	15:00	51	5	14	0	1	0	15	0
51	09-Aug-2001	19:00	51	5	13	1	1	0	15	0
52	09-Aug-2001	23:00	51	5	7	0	0	0	7	0
53	10-Aug-2001	03:00	51	5	3	0	0	0	3	0
54	10-Aug-2001	07:00	52	5	6	0	0	0	6	0
55	10-Aug-2001	11:00	49	5	7	0	0	0	7	0
56	10-Aug-2001	15:00	49	5	49	5	0	0	54	0
57	10-Aug-2001	19:00	50	4	49	4	0	1	54	0
58	10-Aug-2001	23:00	51	5	7	0	0	0	7	0
59	11-Aug-2001	03:00	51	5	0	0	0	0	0	0
60	11-Aug-2001	07:00	51	6	0	0	0	0	0	0
61	11-Aug-2001	11:00	51	5	0	0	0	0	0	0
62	11-Aug-2001	15:00	51	5	0	0	0	0	0	0
63	11-Aug-2001	19:00	51	5	3	0	0	0	3	0
64	11-Aug-2001	23:00	50	5	20	0	0	0	20	0
65	12-Aug-2001	03:00	52	5	6	0	0	0	6	0
66	12-Aug-2001	07:00	51	5	8	0	0	0	8	0
67	12-Aug-2001	11:00	51	5	9	0	1	0	10	0
68	12-Aug-2001	15:00	51	5	9	0	0	0	9	0
69	12-Aug-2001	19:00	52	4	10	2	2	0	14	0
70	12-Aug-2001	23:00	51	5	12	0	1	0	13	0
71	13-Aug-2001	03:00	51	5	5	1	1	1	8	0
72	13-Aug-2001	07:00	50	5	8	0	0	0	8	0
73	13-Aug-2001	11:00	50	5	12	0	1	0	13	0

Appendix 3. Sampling events and numbers and types of samples: pH (continued)

			collected		analyzed					
Event	Date	Time	# samples	# QC	# samples	# QC	B3	B6(outflow)	Field	Lab
74	13-Aug-2001	15:00	51	5	10	1	0	0	11	0
75	13-Aug-2001	19:00	52	4	10	1	0	1	12	0
76	13-Aug-2001	23:00	51	5	25	3	1	1	30	0
77	14-Aug-2001	03:00	51	5	0	0	0	0	0	0
78	14-Aug-2001	07:00	52	4	6	1	0	0	7	0
79	14-Aug-2001	11:00	51	5	7	0	1	0	8	0
80	14-Aug-2001	15:00	51	5	9	1	1	0	11	0
81	14-Aug-2001	19:00	51	5	12	2	1	0	15	0
82	14-Aug-2001	23:00	51	5	26	0	1	0	27	0
83	15-Aug-2001	03:00	52	4	6	3	2	1	12	0
84	15-Aug-2001	07:00	51	4	7	0	1	0	8	0
85	15-Aug-2001	11:00	50	5	7	0	1	0	8	0
86	15-Aug-2001	15:00	51	5	17	4	1	1	23	0
87	15-Aug-2001	19:00	51	5	9	1	1	1	12	0
88	15-Aug-2001	23:00	51	5	20	0	1	0	21	0
89	16-Aug-2001	03:00	51	5	8	0	1	0	9	0
90	16-Aug-2001	07:00	52	4	7	0	1	0	8	0
91	16-Aug-2001	11:00	52	4	6	0	1	1	8	0
92	16-Aug-2001	15:00	51	5	20	5	1	1	27	0
93	16-Aug-2001	19:00	51	5	49	5	1	1	56	0
94	16-Aug-2001	23:00	51	5	0	0	0	0	0	0
95	17-Aug-2001	03:00	51	4	0	0	0	0	0	0
96	17-Aug-2001	07:00	51	5	8	0	1	1	10	0
97	17-Aug-2001	11:00	51	5	2	0	0	0	2	0
98	17-Aug-2001	19:00	7	1	2	1	0	1	4	0
99	17-Aug-2001	23:00	7	1	6	1	0	0	7	0
100	18-Aug-2001	03:00	7	1	6	1	0	1	8	0
101	18-Aug-2001	07:00	7	1	6	0	0	0	6	0
102	18-Aug-2001	11:00	7	1	6	0	0	0	6	0
	Total		5024	497	1094	86	36	23	1239	0

Appendix 4. Tracer/Time-Lapse Test chronology: July 29-August 18, 2001

Month/Day	Military Time	Event
7/29	0730	measure C and X wells
	1132	start recording background in PST8 (note river level drop)
	1500	start recording in X wells, measure X wells
	~1600	peristaltic pumps at ~10-20 ml/min
	1804	stop recording PST8
7/30	0700	measure C and X wells
	0948	start recording new background in PST8
	1750	set up fiber-optic transducer system, start recording at 5 min interval
7/31	1630	pump from X2 (16.5-17 gpm) to top off 1000 gal water tank (pump ~20 min)
	1735	stop background recording in PST8
	1738	stop background in fiber-optic transducer system
	~1745	set straddle packer in B3
	~1808	start practice injection test
	~1832	stop practice injection test
	2028	pump with low-flow-rate sample pump from X1 for site water
	2040	stop collecting from practice injection test with PST8
	2105	start recording with PST8; transducer has been added to B3 upper zone
	2115	stop recording with fiber-optic transducer system
	2128	start recording with fiber-optic transducer system
8/01	0725	stop recording with fiber-optic transducer system
	0725	add flowmeter to fiber-optic transducer data logging system
	0728	start recording with fiber-optic transducer system (same settings)
	0 730 to 0830	extract files from in-well loggers in X wells, start recording again
	0730 to 0830	measure X wells
	0930	start filling tank from well X2, add tracers, mix
	1015	tank water temperature is 14.8 ^{o}C
	1030	stop filling tank
	1115	tank water temperature is 16.3 ^{o}C
	1122	stop mixing
	1128	start priming
	1139	start recording straddle packer data
	1140	start injecting into target zone in B3 *elapsed time for test = 0*
	1213	stop injecting after 33 min and 20 sec; water temperature is 19.8 C
	1248	start pumping from B6 at ~5 gpm
	1320	remove transducer from C2 (it was disturbing radar tomography)
	1530	decrease pumping rate at B6 from ~5.25-5.3 gpm to ~5 gpm
	1600	readjust pumping rate at B6

Appendix 4. Tracer/Time-Lapse Test chronology: July 29-August 18, 2001 (continued)

Month/Day	Military Time	Event
8/02	0830	decrease pumping rate at B6 from ~5.35 to 5 gpm
	1215	peristaltic pumps: turn down from 30 to 15
	1500	peristaltic pumps: turn down from 15 to 5
8/03	1620	put transducer back in C2
	~1630	peristaltic pumps: turn up from 5 to 30
	~1730	peristaltic pumps: turn down to 5
8/04	1200	measure C and X wells
	~1430	peristaltic pumps: turn up from 5 to 30
	~1530	peristaltic pumps: turn down to 5
	~1830	peristaltic pumps: turn up from 5 to 30
	~1930	peristaltic pumps: turn down to 5
8/05	~0500	peristaltic pumps: turn up from 5 to 30
	~0600	peristaltic pumps: turn down to 5
	~1430	peristaltic pumps: turn up from 5 to 30
	~1530	peristaltic pumps: turn down to 5
	~1830	peristaltic pumps: turn up from 5 to 30
	~1930	peristaltic pumps: turn down to 5
8/06	~0630	peristaltic pumps: turn up from 5 to 30
	~0730	peristaltic pumps: turn down to 5
	~1030	peristaltic pumps: turn up from 5 to 30
	~1130	peristaltic pumps: turn down to 5
		replace B4-6 with B3 at B4-B5 peristaltic pump
	~1500??	peristaltic pumps: turn up from 5 to 30
	~1700??	peristaltic pumps: turn down to 5
	1715	measure C and X wells
8/07	~0700	power failure, PST8 stopped ~700
	1036	restart fiber-optic transducer system with straddle packer and atmospheric pressure transducers added
	1103	restart PST8
	1343	stop pumping at B6, small pump quit
	1400	start pumping at B6, use red pump
	1050	measure A, B, C and X wells
	~2010	generator out, stop pumping at B6
	~2017	start red pump again
8/08	1315	measure C and X wells

Appendix 4. Tracer/Time-Lapse Test chronology: July 29-August 18, 2001 (continued)

Month/Day	Military Time	Event
8/09	1215	measure C and X wells
8/10		remove packers from B3
	1000	stop pump, start B3-B6 tomography
	1315	measure A, B, C and X wells
	1930	start pump after tomography
8/11	0225	peristaltic pumps: turn up to 30
8/12	1345	measure C and X wells
8/13	0710	stop pump, start B3-B6 tomography
	~1345	start pump after tomography
	1610	measure C and X wells
8/14	2140	tripped valve, pumping rate spike to 15 gpm at B6 for ~30 sec
8/15	0700	stop pump, start B3-B6 tomography
	1400	start red pump at 26 +/- 1 gpm in B6 after tomography
	~1415	move discharge point to slough NE of X1
	~1430	peristaltic pumps: down to 10 ml/min
	1445	measure C and X wells
8/16	1720	stop recording in PST8
8/17	12-1400	remove in-well loggers from X wells
	~1400	radar tomography completed, pull A1 and B6, put B6 string in A1
	~1600	start pumping from A1 ~26 gpm

Appendix 5. Schedule of cross-hole radar measurements during the TTLT.

Date	Tx well	Rx well	Freq (MHz)	System	Start time	End time	Tx step size (m)	Rx step size (m)	Packers installed	Calibration	Survey type
7/26/2001	B4	B1	100	Mala	14:00	19:30	0.05	0.20	no	SW, airwave	tomo
7/27/2001	B4	B1	100	Mala	8:00	14:00	0.05	0.20	yes	SW, airwave	tomo
7/27/2001	B4	B1	250	Mala	14:40	18:45	0.05	0.20	yes	SW, airwave	tomo
7/28/2001	B4	B1	100	Mala	11:00	15:30	0.05	0.20	yes	SW, airwave	tomo
7/28/2001	B4	B1	250	Mala	16:30	20:15	0.05	0.20	yes	SW, airwave	tomo
7/29/2001	B4	B1	250	Mala	8:50	14:36	0.05	0.20	yes	SW, airwave	tomo
7/29/2001	B4	B1	200	Sensors	16:00	21:30	0.25	0.50	yes	SW	tomo
7/30/2001	B3	B6	100	Mala	8:45	15:00	0.05	0.20	yes	SW, airwave	tomo
7/30/2001	B4	B2	250	Mala	16:45	19:45	0.05	0.20	yes	SW, airwave	tomo
7/30/2001	B4	B1	200	Sensors	12:30	15:20	0.25	0.25	yes	SW	tomo
7/31/2001	C3	B2	200	Sensors	10:00	11:30	n/a	n/a	yes	SW	noise test/stacks
8/1/2001	C2	B4	100	Mala	9:50	12:40	0.05	5.00/16.80	yes	SW, airwave	fans
8/1/2001	C2	B4	100	Mala	13:40	17:00	0.05	0.20	yes	SW, airwave	tomo
8/1/2001	C3	B2	100	Sensors	7:30	12:52	0.25	0.25	yes	SW	LR
8/1/2001	C3	B2	100	Sensors	18:30	20:48	0.25	0.50	yes	SW	tomo
8/1/2001	B4	B2	100	Sensors	21:00	23:00	0.25	0.50	yes	SW, airwave	tomo
8/2/2001	B5	B1	250	Mala	9:30	15:40	0.05	0.20	yes	SW, airwave	tomo
8/2/2001	B4	B1	100	Mala	16:30	21:40	0.05	0.20	yes	SW, airwave	tomo
8/2/2001	B4	B2	100	Sensors	8:00	12:30	0.25	0.25	yes	SW, airwave	tomo

Appendix 5. Schedule of cross-hole radar measurements during the TTLT. (continued)

Date	Tx well	Rx well	Freq (MHz)	System	Start time	End time	Tx step size (m)	Rx step size (m)	Packers installed	Calibration	Survey type
8/3/2001	B4	B1	100	Mala	14:40	20:02	0.05	0.20	yes	SW, airwave	tomo
8/3/2001	B4	B2	250	Mala	7:45	13:20	0.05	0.20	yes	SW, airwave	tomo
8/3/2001	B5	B1	250	Mala	13:30	14:40	n/a	n/a	yes	SW, airwave	noise test
8/3/2001	B5	B2	200	Sensors	13:30	14:40	n/a	n/a	yes	n/a	noise test
8/4/2001	B4	B2	250	Mala	7:50	13:50	0.05	0.20	yes	SW, airwave	tomo
8/4/2001	B4	B2	100	Mala	14:30	15:00	0.10	0.10	yes	SW, airwave	LR
8/4/2001	B4	B1	100	Mala	15:00	18:00	0.05	0.20	yes	SW, airwave	tomo
8/4/2001	B4	B1	100	Sensors	9:00	23:00	0.25	0.25	yes	SW, airwave	tomo
8/5/2001	B4	B2	250	Mala	8:45	14:00	0.05	0.20	yes	SW, airwave	tomo
8/5/2001	B4	B1	250	Mala	7:45	8:45	0.10	0.10	yes	SW, airwave	LR
8/5/2001	B4	B2	100	Mala	14:40	15:15	0.10	0.10	yes	SW, airwave	LR
8/5/2001	B4	B1	100	Mala	15:15	20:30	0.05	0.20	yes	SW, airwave	tomo
8/6/2001	B4	B1	250	Mala	8:30	8:45	0.10	0.10	yes	SW, airwave	LR
8/6/2001	B4	B2	250	Mala	8:45	14:00	0.05	0.20	yes	SW, airwave	tomo
8/6/2001	B4	B2	100	Mala	14:15	15:00	0.10	0.10	yes	SW, airwave	LR
8/6/2001	B4	B1	100	Mala	15:00	19:30	0.05	0.20	yes	SW, airwave	tomo
8/7/2001	B4	B1	250	Mala	8:40	9:00	0.10	0.10	yes	SW, airwave	LR
8/7/2001	B4	B2	250	Mala	9:00	13:40	0.05	0.20	yes	SW, airwave	tomo
8/7/2001	B4	B2	100	Mala	14:30	15:00	0.10	0.10	yes	SW, airwave	LR
8/7/2001	B4	B1	100	Mala	15:00	20:30	0.05	0.20	yes	SW, airwave	tomo
8/7/2001	B5	B2	100	Sensors	17:15	19:15	0.25	0.25	yes	SW, airwave	LR, monitoring
8/8/2001	B4	B1	250	Mala	8:40	8:55	0.10	0.10	yes	SW, airwave	LR
8/8/2001	B4	B2	250	Mala	8:55	14:45	0.05	0.20	yes	SW, airwave	tomo
8/8/2001	B4	B2	100	Mala	15:00	15:15	0.10	0.10	yes	SW, airwave	LR
8/8/2001	B4	B1	100	Mala	15:15	20:15	0.05	0.20	yes	SW, airwave	tomo

Appendix 5. Schedule of cross-hole radar measurements during the TTLT. (continued)

Date	Tx well	Rx well	Freq (MHz)	System	Start time	End time	Tx step size (m)	Rx step size (m)	Packers installed	Calibration	Survey type
8/9/2001	B4	B1	250	Mala	9:10	9:25	0.10	0.10	yes	SW, airwave	LR
8/9/2001	B4	B2	250	Mala	9:30	13:40	0.05	0.20	yes	SW, airwave	tomo
8/9/2001	B4	B2	100	Mala	15:00	15:15	0.10	0.10	yes	SW, airwave	LR
8/9/2001	B4	B1	100	Mala	15:15	19:00	0.05	0.20	yes	SW, airwave	tomo
8/9/2001	B5	B1	200	Sensors	10:45	14:45	0.00	0.00	yes	SW, airwave	monitoring
8/9/2001	C3	B2	100	Sensors	16:45	20:15	0.25	0.25	yes	airwave	tomo
8/10/2001	B4	B1	250	Mala	8:15	8:30	0.10	0.10	yes	SW, airwave	LR
8/10/2001	B4	B2	250	Mala	8:40	9:00	0.05	0.20	yes	SW, airwave	LR
8/10/2001	B4	B2	100	Mala	16:15	16:30	0.10	0.10	yes	SW, airwave	LR
8/10/2001	B4	B1	100	Mala	16:30	20:00	0.05	0.20	yes	SW, airwave	tomo
8/10/2001	B3	B6	200	Sensors	10:50	11:05	0.25	0.25	yes	SW	LR
8/10/2001	B3	B6	100	Sensors	11:25	18:00	0.25	1.00/0.25/0.125	yes (B3 no)	SW, airwave	tomo
8/10/2001	B5	B1	200	Sensors	18:00	23:59	0.00	0.00	yes	airwave	monitoring
8/11/2001	B4	B1	250	Mala	8:10	8:25	0.10	0.10	yes	SW, airwave	LR
8/11/2001	B4	B2	250	Mala	8:30	15:00	0.05	0.20	yes	SW, airwave	tomo
8/11/2001	B4	B2	100	Mala	15:45	16:00	0.10	0.10	yes	SW, airwave	LR
8/11/2001	B4	B1	100	Mala	16:15	20:00	0.05	0.20	yes	SW, airwave	tomo
8/12/2001	B4	B1	250	Mala	8:15	8:30	0.10	0.10	yes	SW, airwave	LR
8/12/2001	B4	B2	250	Mala	8:45	13:30	0.05	0.20	yes	SW, airwave	tomo
8/12/2001	B4	B2	100	Mala	14:50	15:00	0.10	0.10	yes	SW, airwave	LR
8/12/2001	B4	B1	100	Mala	22:00	1:15	0.05	0.20	yes	SW, airwave	tomo
8/13/2001	B4	B2	250	Mala	10:20	13:55	0.05	0.20	yes	SW, airwave	tomo
8/13/2001	B4	B1	100	Mala	14:45	18:30	0.05	0.20	yes	SW, airwave	tomo
8/13/2001	B5	B1	200	Sensors	1:46	7:21	0.00	0.00	yes	none	monitoring
8/13/2001	B3	B6	100	Sensors	8:40	13:30	0.25	1.00/0.25/0.125	yes (B3 no)	SW, airwave	tomo

Appendix 5. Schedule of cross-hole radar measurements during the TTLT. (continued)

Date	Tx well	Rx well	Freq (MHz)	System	Start time	End time	Tx step size (m)	Rx step size (m)	Packers installed	Calibration	Survey type
8/14/2001	B4	B2	250	Mala	8:40	13:00	0.05	0.20	yes	SW, airwave	tomo
8/14/2001	B4	B1	250	Mala	13:00	13:15	0.10	0.10	yes	SW, airwave	LR
8/14/2001	B4	B2	100	Mala	14:00	14:15	0.10	0.10	yes	SW, airwave	LR
8/14/2001	B4	B1	100	Mala	14:15	18:15	0.05	0.20	yes	SW, airwave	tomo
8/14/2001	B4	B2	100	Mala	18:20	18:40	0.10	0.10	yes	SW, airwave	LR
8/15/2001	B4	B2	250	Mala	8:30	14:00	0.05	0.20	yes	SW, airwave	tomo
8/15/2001	B4	B1	250	Mala	14:10	14:25	0.10	0.10	yes	SW, airwave	LR
8/15/2001	B4	B2	100	Mala	14:45	15:00	0.10	0.10	yes	SW, airwave	LR
8/15/2001	B4	B1	100	Mala	15:15	18:40	0.05	0.20	yes	SW, airwave	tomo
8/15/2001	B4	B2	100	Mala	18:40	19:00	0.10	0.10	yes	SW, airwave	LR
8/15/2001	B3	B6	100	Sensors	8:00	13:20	0.25	1.00/0.25/0.125	yes (B3 no)	SW, airwave	tomo
8/16/2001	B4	B1	250	Mala	8:30	8:45	0.10	0.10	yes	SW, airwave	LR
8/16/2001	B4	B2	250	Mala	9:00	12:50	0.05	0.20	yes	SW, airwave	tomo
8/16/2001	B4	B1	100	Mala	13:00	13:30	0.10	0.10	yes	SW, airwave	LR
8/17/2001	B4	B2	100	Mala	7:45	8:00	0.10	0.10	yes	SW, airwave	LR
8/17/2001	B4	B1	100	Mala	8:15	14:00	0.05	0.20	yes	SW, airwave	tomo
10/5/2001	B3	B6	100	Sensors	11:45	17:00	0.25	1.00/0.25/0.125	yes (B3 no)	SW, airwave	tomo
6/19/2002	B3	B6	100	Sensors	10:30	17:20	0.25	1.00/0.25/0.125	yes	SW, airwave	tomo

Appendix 6. TTLT Restart chronology: June 14-19, 2002

Month/Day	Military Time	Event
6/14	1100	install 6 x 1 m log-through systems in B1, B2, B4, B5, B6
	1100	install 20 x .25 m packer and port system in A1
	1520	measure depth to water in wells with e-tape
6/15	1035	measure depth to water in wells with e-tape
	1100	install fiber-optic transducers (see Table 4, Figure 25)
	1635	river stage at 1.50 ft
6/16	000	start background measurements with fiber-optic transducers
	0900	river stage at 1.50 ft
	0930	measure depth to water in wells with e-tape
	1100	install straddle packer in B3
	1300	install transducers in C wells, B3, and river
	1815	start filling tank
	1900	stop filling tank
	1930	start practice injection at ~28.2 gpm
	2010	stop injection test after 1000 gal on totalizer flowmeter
	2020	connect packers in B2 to compressed gas and charge
	2200	start filling tank from C2
	2245	stop filling tank
6/17	1015	tank water temperature is 60 ^{o}F
	1115	reconfigure Bus channels
	1127	tank water temperature is 61 ^{o}F
	1145	tank water temperature is 62 ^{o}F
	1200	tank water temperature is 62 ^{o}F
	1219	pull straddle packer from B3 to change foot valve
	1230	tank water temperature is 62 ^{o}F
	1257	tank water temperature is 62 ^{o}F
	1259	start priming
	1330	start injecting at ~29.5 gpm into target zone in B3
	1335	tank water temperature is 63 ^{o}F
	1346	adjust pumping rate to ~30.5 gpm
	1403	stop injecting after 33 min (9942 gal on totalizer flowmeter)
	1438	start pumping from B6 at ~5 gpm
	1952	note pressure leaks at A1 and B1
	2000	stop pumping at B6
	2240	decrease pressure to packers to 20 psi, note decrease in leak at A1
	2247	start pumping from B6 at ~22 gpm

Appendix 6. TTLT Restart chronology: June 14-19, 2002 (continued)

Month/Day	Military Time	Event
6/18	0451	stop pumping from B6
	0900	remove hose from C2 with some return flow
	1050	remove straddle packer from B3
	1100	start and stop pumping (lost prime) from B6
	1138	start pumping from B6 at ~22 gpm
	1202	stop pumping from B6
	1230	raining
	1415	peristaltic pumps: turn on and pump at 30 ml/min
	1423	start and stop pumping (lost prime) from B6
	1427	start pumping from B6 at 5 gpm
	1525	peristaltic pumps: turn down to 5 ml/min
	1726	stop pumping from B6
	1733	start pumping from B6 at ~26 gpm
	2145	measure depth to water in wells with e-tape, river stage at 1.47 ft
6/19	0630	measure depth to water in wells with e-tape, river stage at 1.47 ft
	0825	collect water quality samples (see Table 5)
	0910	stop pumping from peristaltic pumps
	0920	stop pumping from B6
	1130	measure depth to water in wells with e-tape
	1136	start radar tomography from B3-B6 for background
	1657	stop radar tomography